Fouling in Emulsion Polymerization Reactors

Jone Urrutia

Chemical Engineering Group
University of the Basque Country UPV/EHU
Donostia-San Sebastian
(2016)

Contents

Chapter 1. Introduction

1.1. Description of the problem

Emulsion polymerization became an important industrial process due to the need of synthesizing synthetic rubber during the World War II in order to replace the latex of natural rubber that was controlled by Japan. Emulsion polymerization is presently the predominant process for the commercial polymerization of vinyl acetate, chloroprene, acrylates and copolymerization of butadiene with styrene and acrylonitrile. It is also used for methacrylates, vinyl chloride, acrylamide, and some fluorinated ethylenes[1]. This wide range of the polymers finds applications as paints, adhesives, paper coatings, synthetic rubbers, toughened plastics, floor polishes, sealants, cement and concrete additives, and nonwoven tissues[2]. Global demand for emulsion polymers is forecast to advance 5.1 percent annually to 13.3 million metric tons (dry basis) in 2018[3]. One of the driving forces for this huge success is that emulsion polymerization uses water as reaction medium and the product is an aqueous polymer dispersion (latex). Therefore, no or negligible volatile organic compounds are released in the

production and use of these materials. Water-based paints, coatings, and adhesives are displacing solventborne formulations in virtually all parts of the world. In addition to the environmental advantages of the waterborne emulsions, the use of water as reaction medium also facilitates agitation, mass and heat transfer because of the low viscosity medium. Moreover, the high heat capacity of water allows a better temperature control. Emulsion polymerization offers many additional advantages over other polymerization methods[4]. Thus, it is possible to produce high molecular weight polymer at high reaction rates. In addition, the viscosity of the emulsion is independent of the molecular weight. Consequently, high solids content emulsions with low viscosity can be achieved in contrast to polymer solutions. The efficient mass transfer allows a good control of the polymer composition, molecular weights and architecture[5–14]. In situ formed polymer-polymer[15–17] and polymer-inorganic[18–22] waterbone hybrid dispersions are materials that cannot be produced otherwise. It is worth pointing out that although temperature control of emulsion polymerization is much easier than in other polymerization process, production is controlled by the heat removal rate.

A typical latex has a solids content of 50 wt% and an average particle size of about 120 nm. Simple calculations show that the surface area of the particles is about 2.5 x 10^4 m^2, namely the system is thermodynamically unstable. Kinetic stability is provided by emulsifiers (ionic and non-ionic[23]), but due to the problems created by the surfactants in the application (water sensitivity of the films, lower gloss and adhesion) their amount is limited.

A consequence of the limited amount of surfactants used in emulsion polymerization is that the process is frequently accompanied by the formation of deposits on the internal surfaces of the polymerization reactor (reactor wall, baffles, impeller). The formation of fouling on the

reactor wall reduces heat transfer, lowering production and may even affect product quality because broken-off deposit fragments may contaminate the product. Therefore, fouling must be cleaned periodically, which reduces productivity.

Surprisingly, although the process of emulsion has been used for decades and notwithstanding the industrial importance of the fouling, little attention has been paid in literature to this topic. There appear to be comparatively few references to this issue in the technical literature and a satisfactory solution of the problem has not been attained yet.

Because fouling is related to the colloidal stability of the latex, which in turn is affected by the emulsion polymerization process, the basics of the stability of colloids and a brief description of emulsion polymerization are given below.

1.2. Stability of polymer colloids

The product of an emulsion polymerization (latex) is a dispersion of submicron hydrophobic polymer particles in a continuous aqueous phase. Consequently, polymer colloids are thermodynamically unstable and the particles tend to aggregate to reduce the free energy of the system. Surfactants are used to kinetically stabilize the system.

Ionic surfactants provide electrostatic repulsion between particles and non-ionic surfactants provide steric repulsion stability. Stability is governed by the interplay between van der Waals attractive forces and repulsive forces.

For ionically stabilized systems, the electrical potential can be described by the Debye-Hückel equation[24]:

$$\Psi = \Psi_0 \frac{r}{x}\, exp\big(\kappa\,(r-x)\big) \qquad for\ \ \Psi_0 < 25\,mV \tag{1.1}$$

where Ψ_0 is the surface potential of the particle, *r* is the radius of the particle, *x* is the distance from the center of the particle and κ is the Debye-Hückel screening length referred to as the reciprocal double-layer thickness, given by:

$$\kappa = \sqrt{\frac{e^2\ \sum {z_{i0}}^2\ n_{i0}}{\varepsilon k_B T}} \tag{1.2}$$

where *e* and $\boldsymbol{\varepsilon}$ are the electron charge and permittivity of the liquid phase; z_{io} and n_{i0} is the valency and bulk concentration of ions of type i; k_B is the Boltzmann constant, and *T* the absolute temperature.

The surface potential of the particle (Ψ_0) is related to the surface charge density (σ_0) by the Grahame equation[25]:

$$\sigma_0 = \ (8 n_0 \varepsilon k_B T)^{1/2} \sinh\left(\frac{ze\Psi_0}{2k_B T}\right) \tag{1.3}$$

The potential energy for electrostatic repulsion between particles of the same size is:

$$U_{rep}(h) = \frac{32\pi d n_0 k_B T \emptyset^2}{\kappa^2}\, exp(-\kappa h) \tag{1.4}$$

where *d* is the diameter of the particles, n_0 the counter-ion concentration in the bulk of the aqueous phase, *h* the distance between particles and Φ is given by:

$$\emptyset = \tanh\left(\frac{ze\Psi_0}{4k_BT}\right) \tag{1.5}$$

The attractive potential between polymer particles is due to the van der Waals attraction forces that are always present and arise from transitory dipoles originated by the polarization of one molecule by the fluctuation in the charge distribution of the second. For spheres of the same material and size, the equation that describes the van der Waals energy is[26]:

$$U_W = -\frac{A_{eff}\, r}{12\ h} \tag{1.6}$$

where r is the particle radius, h the interparticle distance and A_{eff} the effective Hamaker constant that takes into account the properties of the particles and of the liquid phase.

Ionic repulsion and van der Waals attraction are combined in the DLVO theory developed by Derjaguin and Landau[27] and Verwey and Overbeek[28]. This theory describes quantitatively the total potential energy of interaction between charged particles in the liquid phase as a function of the distance between them. A typical result is shown in Figure 1.1 where the van der Waals potential dominates at small separations and decays rapidly to zero when the particles are far (Eq. 1.6). The stability of the polymer colloid is determined by the maximum height of the energy barrier, the higher Ψ_{max}, the higher the stability. Stability is mainly affected by the ionic strength and by the surface charge density (Eq. 1.3). Ionic strength increases with

the salt concentration and with the valence of the salt, being the last the main factor because it appears as second power (z_i^2) in Eq. 1.2.

Figure 1.1 shows that at larger interparticle distances, the interaction may present a secondary minimum where particles stay in a weakly flocculated state.

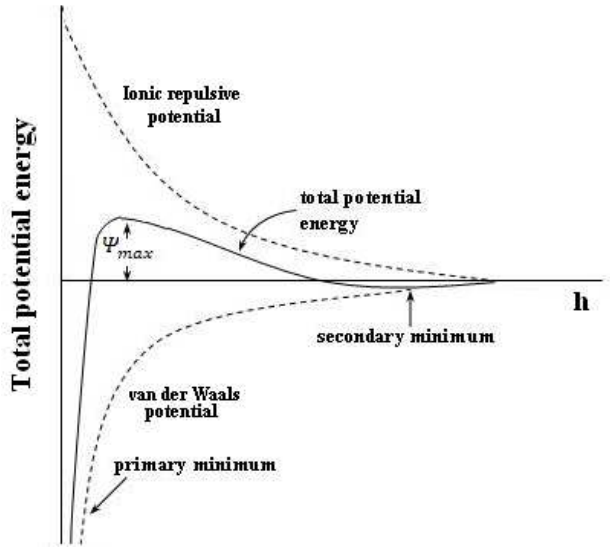

Figure 1. 1. Potential energy diagram as a function of the separation distance between two particles.

Another method of stabilizing latex particles is the steric stabilization[29–31] achieved by the use of non-ionic surfactants which adsorbed on the surface of the polymer particles form a hairy layer of solvated polymer that can physically prevent particle coagulation. The thickness of the hairy layers (δ) has to be thick enough to cover the region in which the van der Waals attractive forces are important. When the hairy layers of the approaching particles come into contact, the concentration of polymer (hairs) in the overlapping region increases, leading to an increase of osmotic pressure. To maintain osmotic equilibrium, the water molecules will tend to decrease the local concentration of hairs, which results in separation of the particles.

Figure 1. 2 presents the potential diagram for a combination of ionic and non-ionic surfactants. Steric stabilization may eliminate the primary minimum shown in Figure 1.1.

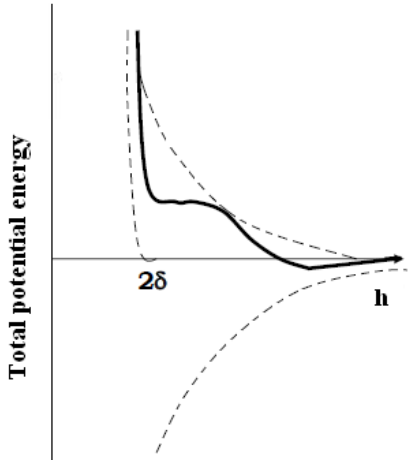

Figure 1. 2. Potential energy diagram as a function of the separation distance between two particles taking into account the van der Waals attraction and the ionic and steric repulsion.

With all the said above, destabilization of polymer colloids (i.e. coagulum formation) will occur when the particles have enough energy to overcome the energy barrier (Ψ_{max}). The energy of the particles is due to both Brownian motion (thermal energy) and agitation.

1.3. Emulsion polymerization[32–34]

Typically, commercial implementation of emulsion polymerization is carried out in stirred tank reactors operated semicontinuously for a better control of the heat generation and of the polymer characteristics, although batch and continuous operations are also used. Besides, conventional free radical polymerization is the process used to manufacture almost all commercial emulsion polymers.

In the simplest emulsion polymerization formulation, the recipe typically includes as basic ingredients: water, relative hydrophobic monomer(s), surfactant(s) (also known as emulsifier) and free radical initiator; although small amounts of functional monomers, chain transfer agents, buffers, acids, bases, etc. can also be used. Therefore, at the beginning of a batch emulsion polymerization reaction, the mixture of monomers is usually dispersed in the water medium as a mixture of emulsified monomer droplets and surfactant micelles swollen with monomer too, since in most formulations, the amount of surfactant exceeds that needed to completely cover the monomer droplets and saturate the aqueous phase (Figure 1.3 a)). The polymerization is commonly started by the addition of water-soluble initiators (both thermal and redox) although oil-soluble initiators may also be used. When a water-soluble initiator such as

potassium persulfate is added to the monomer dispersion within a certain temperature range (typically 50-90°C), it generates free radicals and as these radicals are often too hydrophilic to directly enter the organic phase, they react with the monomer dissolved in the aqueous phase and forms oligoradicals. The growth rate of the oligoradicals is generally slow because of the low concentration of monomer in the aqueous phase. After adding some monomer units, the oligoradicals become hydrophobic enough to be able to enter the micelles (entry into the monomer droplets is not likely because their total surface area is about three orders of magnitude smaller than that of the micelles). Because of the high concentration of monomer in the micelle, the oligoradical that has entered the monomer swollen micelle grows fast, forming a polymer chain. The new species formed upon entry of a radical into a micelle is considered to be a polymer particle. The process of formation of polymer particles by entry of radicals into micelles is called heterogeneous nucleation[35]. The oligoradicals that do not enter into micelles will continue growing in the aqueous phase, and upon reaching some critical length they become too hydrophobic and precipitate. The precipitated polymer chain is stabilized by the surfactant present in the aqueous phase and monomer diffuses into the new polymer particle. The process of formation of polymer particles by precipitation of oligoradicals is called homogeneous nucleation[36].

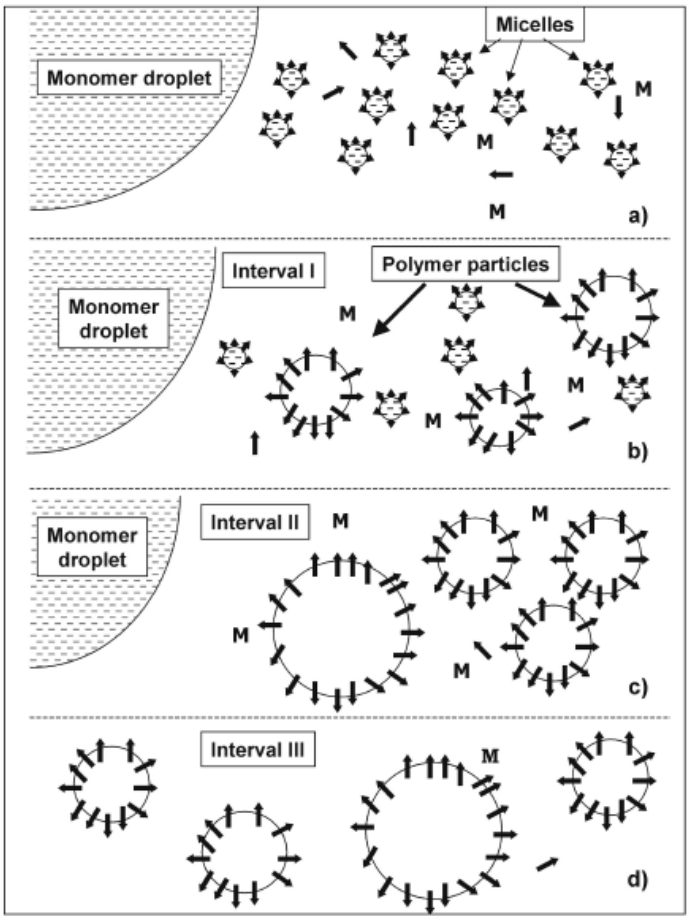

Figure 1. 3. Intervals in the batch emulsion polymerization[34].

Both homogeneous and heterogeneous nucleation may be operative in a given system but irrespective of the mechanism of particle nucleation, the newly formed particles are very

small and suffer a tremendous increase in surface area upon particle growth. It is arguable that the surfactant molecules may diffuse fast enough to adsorb on the surface of these fast-growing particles, stabilizing them. If the surfactant molecules do not diffuse rapidly enough to stabilize the surface of the fastly growing particles, they coagulate. This combined process is sometimes called coagulative nucleation[37].

During nucleation, monomer droplets, monomer swollen micelles, and monomer swollen polymer particles coexist in the reactor (Figure 1.3 b)). Polymer particles compete efficiently for radicals, and hence monomer is consumed by polymerization inside the polymer particles which become the main polymerization loci. The monomer that is consumed by free radical polymerization in the polymer particles is replaced by monomer that diffuses from the monomer droplets through the aqueous phase. Therefore, the size of the particles increases and that of the monomer droplets decreases. The number of micelles decreases because they become polymer particles upon entry of a radical and also because they are destroyed to provide surfactant to stabilize the increasing surface area of the growing polymer particles. After some time, all the micelles disappear. This is considered to be the end of the nucleation; only limited formation of new particles may occur after this point because heterogeneous nucleation is not possible and there is no free surfactant available in the system to stabilize the particles formed by homogeneous nucleation. The stage of the batch emulsion polymerization in which particle nucleation occurs is called Interval I. At the end of Interval I, which typically occurs at a monomer conversion of about 5–10% (depending on the surfactant/monomer ratio), 10^{17}–10^{18} particles per liter are formed. Unless coagulation occurs, the number of particles remains constant during the rest of the process.

In Interval II, the system is composed of monomer droplets and polymer particles (Figure 1.3 c)). The monomer consumed by polymerization in the polymer particles is replaced by monomer that diffuses from the monomer droplets through the aqueous phase. The mass-transfer rate of monomers with water solubility equal or greater than that of styrene (0.045 g/100 g of water) is substantially higher than the polymerization rate, and hence monomer partitions between the different phases of the system according to the thermodynamic equilibrium. Therefore, in the presence of monomer droplets, the concentration of the monomer in the polymer particles reaches a maximum value. This saturation value arises from the energy (interfacial tension) needed to increase the surface area of the polymer particles upon swelling. Consequently, the monomer concentration in the polymer particles is roughly constant during Interval II. The transport of monomers with water solubility lower than that of the styrene from monomer droplets to polymer particles may be diffusionally limited.

Because of the polymerization and monomer transport, the polymer particles grow in size, and after some time the monomer droplets disappear. This marks the end of Interval II. The monomer conversion at which Interval II ends depends on the capability of the polymer particle to be swollen by monomer. The higher the maximum swelling, the earlier the monomer droplets disappear. In general, the more water-soluble the monomer, the higher the maximum swelling, and hence the lower the monomer conversion at the end of Interval II. Thus, the transition from Interval II to Interval III occurs at about 40% conversion for styrene and at about 15% conversion for vinyl acetate. This means that most monomer polymerizes in Interval III (Figure 1.3 d)). In this interval, monomer concentration in the polymer particles decreases

continuously. The final product is a waterborne, concentrated (50–60 wt % solids) dispersion of tiny (80–500 nm in diameter) polymer particles called latex.

In a semicontinuous reactor in which monomers, surfactant, initiator, and water may be continuously fed into the reactor, emulsion polymerization does not follow the sequence of events described above. Thus, slow monomer feed and fast surfactant feed may lead to a system composed of polymer particles and micelles (Figure 1.3 a)). The system will contain only monomer-swollen polymer particles if both monomer and surfactant are fed slowly (Figure 1.3 b)). On the other hand, a fast monomer feed and a low surfactant feed will lead to a system containing monomer droplets and polymer particles (Figure 1.3 c)).

Besides, the explained above considers an ab initio emulsion polymerization (unseeded polymerization process), where no reaction loci are initially present and the particle nucleation proceed in a significant period during the early stage of the reaction. But in industry is normal to use seeded emulsion polymerization process where reaction loci are present in the initial system. The loci are formed by a separate reaction and thus, the particle nucleation stage of the reaction is eliminated by use of a pre-formed latex that is introduced to the reaction mixture at the beginning. There must be enough seed particles to avoid new particles being subsequently nucleated. If the particle number is sufficiently high (typically, $\geq 10^{16}$ particles per liter is satisfactory), then the seed particles efficiently capture free-radical species from the aqueous phase and all primary particles that form by homogeneous nucleation (second stage of the emulsion polymerization)[4]. The seeded process provides many advantages in the

production of latex particles as uniformity and excellent size monodispersity and also high production yields.

Despite the apparently relative simplicity of the emulsion polymerization process, the rate of formation and growth of polymer particles involves many mechanistic events (see Figure 1.4) that makes the understanding really difficult[38]. As explained above, radicals formed in the aqueous phase from water-soluble initiators, react with the monomer dissolved in the aqueous phase forming oligoradicals. These oligoradicals may i) enter into the polymer particles, ii) enter into the micelles (heterogeneous nucleation), iii) propagate in the aqueous phase until they become insoluble and precipitate forming new polymer particles (homogeneous nucleation), and iv) terminate with other radicals in the aqueous phase. The likelihood of each of these events depends on the particular conditions of the system (e.g., number of polymer particles, emulsifier concentration, initiator concentration, monomer type and concentration, etc). Within the polymer particles, polymerization follows the same mechanisms as in bulk free radical polymerization. These mechanisms involve chain transfer to small molecules (e.g., monomers and chain transfer agents), that yield small radicals. These small radicals may exit the polymer particles diffusing into the aqueous phase. Figure 1.4 illustrates the case in which monomer radicals are the exiting species. But basically, emulsion polymerization involves the propagation reaction of free radicals with monomer molecules in a very large number of discrete polymer particles (10^{16}–10^{18} dm^{-3}) dispersed in the continuous aqueous phase[39].

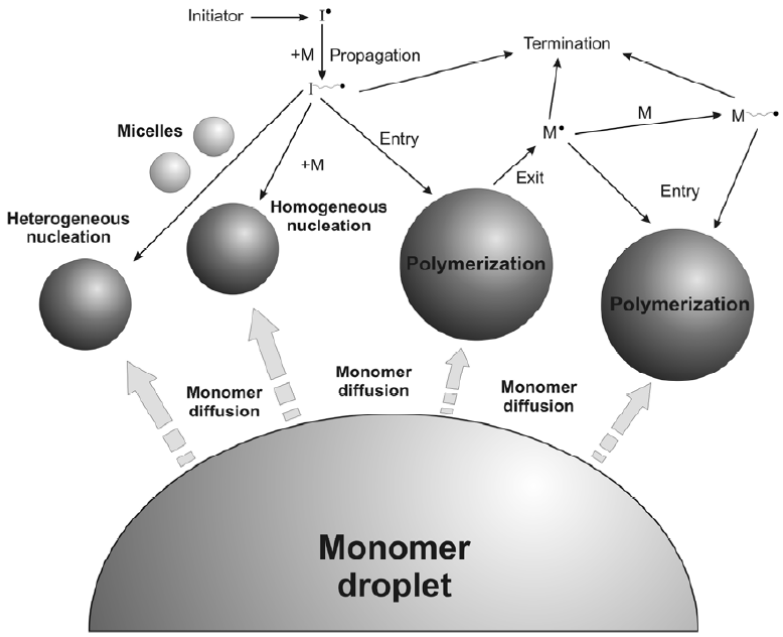

Figure 1. 4. Scheme of kinetic events taking place in a typical emulsion polymerization reaction[32].

1.4. Literature review

Fouling is the accumulation of unwanted material on solid surfaces and it can be often observed in heat exchanger surfaces[40], piping, flow channels, turbines, membranes[41],

injection/spray nozzles, and reactors. In emulsion polymerization, the terms fouling and coagulation are not clearly separated. Actually, the first author reviewing the fouling issue in emulsion polymerization reactor was Vanderhoff[42] and he used the term coagulum for all the polymer recovered in a form other than stable latex. Therefore, in this work coagulum encompassed the polymer aggregates formed in the latex by aggregation of particles and polymer build-up on the internal surfaces (reactor walls, cooling coils, baffles, thermometer wells, and agitator(s)). *In this PhD Thesis,* **fouling** *refers to the polymer deposited on the internal surfaces and* **coagulum** *refers to the polymer aggregates formed in the latex.* According to Vanderhoff both colloidal destabilization of latex particles and formation of polymer by polymerization processes other than emulsion polymerization (bulk polymerization within the monomer droplets or within a separate monomer layer; surface polymerization on the reactor surfaces, or polymerization of monomer in the vapor space) can contribute to fouling and coagulum.

In order to coagulate, the polymer particles should collide between them overcoming the electrostatic/steric stabilization. The movement of the particles may be caused by Brownian motion (called perikinetic coagulation)[43,44], as well as by agitation (called shear, mechanical or orthokinetic coagulation)[44–46].

Surface coagulation is a special case of coagulation in which colloidal particles adsorb on the air-water interface and coagulate there. Renewal of the air-latex interface by means of agitation reduces surface coagulation because the adsorbed particles do not have time to coagulate. Heller et al.[47–52] observed that surface coagulation rates can be more important than the coagulation rates in the liquid phase if a large air-water interface is present. The reasons

provided were that electrolyte concentration is higher at the interface and that there is an asymmetry of the particle double layer at the interface and a lower dielectric constant.

Some works can be found in literature dealing with coagulation in stirred tank reactors. Lowry et al.[53,54] studied the coagulation of a 35% solids content latex and proposed that the coagulation rate was proportional to the agitation per unit volume (see Section 1.5.2). Matejicek et al.[55] studied the dependence of the amount of coagulum on the agitation intensity for a 52% solids content latex during the emulsion polymerization reaction of styrene/butyl acrylate/acrylic acid system. They reported that coagulum was minimum for a power input of 80 W/m^3. Lower agitation rates resulted in bad homogenization of the ingredients that increased coagulum. Higher agitation rates led to a higher shear coagulation.

Kiparissides et al.[56] reported coagulum formation during the emulsion polymerization of vinyl acetate in a continuous stirred tank reactor (CSTR). In these reactors, large variations of the number of particles occur due to intermittent nucleations, which causes strong variations on the surfactant coverage of the particles because the concentration of surfactant is constant. When coverage is low, coagulation occurs in the bulk of the latex that later gives fouling. Coagulation increased with the initiator concentration (because of the higher ionic strength).

Chern and Chen[57] found that coagulum and fouling increased with both agitation and ionic strength. In the absence of surfactant[58] coagulum was a chaotic process. Zubitur and Asua[59] reported that coagulum and fouling occurred at low agitation rates (100 rpm) due to the formation and polymerization for a monomer layer in the reactor. No proof for shear induced coagulation was found in the range of agitation rates studied (≤ 220 rpm). Bianco et al[60] found

that polymerization of the monomers in the droplets led to coagulum formation in the copolymerization of tribromostyrene (a fire resistant monomer) and styrene. The reason was that tribromostyrene can suffer thermal polymerization at low temperatures (30°C)[61,62].

Fouling caused by polymerization at the internal surfaces of the reactor is important in poly(vinyl chloride) (PVC) production. The exact cause of the fouling is not completely understood but appears to occur in two steps: the first is the adsorption and subsequent polymerization of vinyl chloride monomer on the wall. The second is the deposition of PVC formed in the bulk of the reactor onto the previously formed deposit layer.

Solutions proposed involve the use of glass-coated reactors, reactor internals with smooth surfaces, and particular types of stainless steel inert lining aiming at reducing the adsorption of the vinyl chloride monomer. Polymer buildup can also be reduced by correct choice of initiator, suspending agent, and pH of aqueous phase, or agitation optimization.

It is worth pointing out that as about 90% of the production of PVC is made in suspension polymerization, prevention methods are focused on this process and efficiency of these methods is greatly reduced in emulsion polymerization[63]. In addition, efficiency of these methods is dependent on the type of the monomers.

Another way of reducing fouling in the polymerization of vinyl chloride is by using antifouling agents, which are radical inhibitors that can adsorb on the walls of the reactor.

AkzoNobel[64] manufactures a product for preventing reactor fouling and polymer build-up which trade under the names Noxol® and Everplus. They claim that they reduce fouling in

suspension PVC and in the production of styrenic and acrylic (co)polymers. INEOS[65] has a product called Evicas that is used to prevent fouling in the production of PVC homopolymer and copolymers as well as in paste/ emulsion manufacturing processes.

Fouling of emulsion polymerization reactors is often mentioned in emulsion polymerization books[66–74] where the topic is treated in a qualitative way. These qualitative ideas can be summarized as follows:

- Fouling decreases as colloidal stability of the latex increases. A latex is stable while the repulsion potential created by the surfactant (plus initiator fragments and functional monomers) cannot be overcome by the energy provided by the Brownian motion and the agitation (a discussion of colloidal stability is given in Section 1.2).

- As the particles undergo many changes during the process (nucleation and growth) that affect the concentration the stabilizaing moieties at the particle surface, particle stabilization is strongly affected by way in which the polymerization is conducted.

- Agitation, which is needed for mixing and heat removal, may affect fouling by providing the particles with the energy needed to stick to the internal surfaces of the reactor. In this regard, the flow patterns in the reactor are critical.

- The nature and texture of the internal surfaces of the reactor are believed to affect fouling. Low energy (e.g., reactors with fluoropolymer coatings) and smooth surfaces reduce fouling.

- The air-latex interface promotes the formation of polymer aggregates (surface coagulation) and fouling (due to wetting-drying of the internal surfaces of the reactor caused by changes of the liquid level in agitated vessels).

- Local increases of the ionic strenght (e.g. if the initiator is fed in a non-well agitated region) increases coagulum (particularly in the case of ionically stabilized latexes).

- Fouling and coagulum formation is specially critical in continuous systems because they lead to the interruption of the operation.

Several spproaches have been proposed to reduce or eliminate the coagulum/fouling by modifying the polymerization formulation and technique[75]: (i) the use of a seeded system instead of a unseeded system; (ii) addition of emulsifier at the appropriate conversion; (iii) rigorous temperature control that avoids temperature increases often decreases the amount of coagulum formed (particularly for the systems stabilized with non-ionic surfactants that can present a cloud point[76]); (iv) varying the mode of monomer addition, e.g., adding the monomer continuously instead of at the beginning of the reaction; and (v) adjusting the agitation rate to the level just sufficient to maintain good heat transfer and mixing.

Modification of the reactor design has also been proposed: (i) use of a semicontinuous process instead of a batch process; (ii) substitution of a different reactor configuration, a stirred tank reactor used for continuous polymerization may give less coagulum than a tubular reactor that suffers clogging; (iii) modification of the agitator and baffle system to ensure uniformity throughout the reactor and complete but mild mixing of the ingredients and (iv) different mode

of addition of ingredients, e.g., addition of monomer below the surface of the latex rather than by dropping it through the vapor space to the upper surface of the latex.

1.5. Mechanisms for fouling formation

The mechanisms for fouling formation are summarized in Figure 1. 5. Fouling can be formed by i) adsorption of latex particles on the internal surfaces followed by wet sintering of the particles; ii) coagulation of particles in the bulk of the latex and adsorption/adhesion of the coagulum to the internal surfaces; iii) adsorption of polymer to the internal surfaces, followed by absorption of monomer and radicals whose polymerization leads to a polymer film; and iv) adsorption of (oligo)radicals to the internal surfaces and subsequent polymerization at the surface.

Formation of polymer aggregates by polymerization in large droplets and monomer layers (both resulting from poor mixing) as well as by surface coagulation may also contribute to fouling formation.

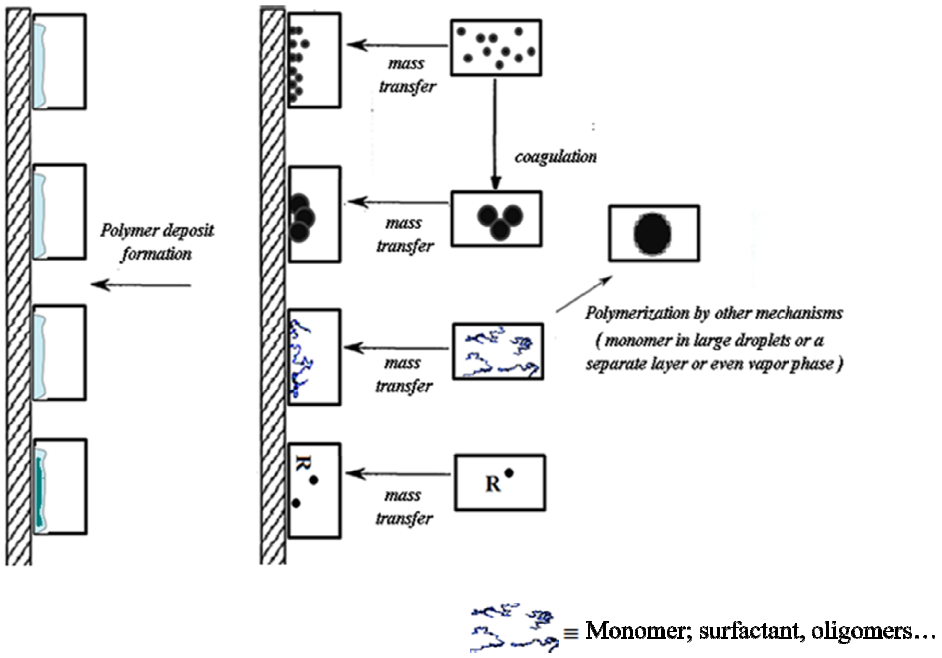

Figure 1. 5. Scheme of the mechanisms for fouling formation.

1.5.1. Adsorption of particles on surfaces

Deposition (physical adsorption) is the process whereby colloidal particles are transported to a surface where they become attached. Deposition of colloidal particles on surfaces from flowing suspensions is of great importance in many technological processes[77]. In some applications such as waste water filtration, painting and coating, deposition is promoted; in others, deposition is not desired (microelectronic manufacture, membrane filtration,

biofouling of artificial organs); and finally in others (as in the deinking of waste papers) is the detachment of colloidal particles which is desired. In fouling science, the deposition of solid particles on solid surfaces is known as *particulate fouling*.

Deposition has several features in common with coagulation and can be considered as an extreme case of particle-particle coagulation in which one of the particles has an infinite dimension[78]. An important difference is that the characteristics of the surface are different from that of the polymer particles and hence the interaction may be completely different from that between latex particles.

Due to its technological significance, research on particulate fouling has received plenty of interest and excellent reviews and books on the subject are available[77,79–83]. The following discussion on the factors controlling particulate fouling is largely based on these references.

The particulate fouling process can be divided into three steps: i) the transport of particles over macroscopic distances from the liquid phase to the vicinity of the solid-liquid interface; ii) the interaction regime when particles approach the solid surface at distances comparable with their dimensions and where the particle-surface interaction forces appear; and iii) the formation of the deposit which is a compromise between the deposition and the removal. In each of these steps, particle–fluid interactions (hydrodynamics), particle–particle interactions (especially at high particle concentration and high surface coverage) and particle–surface interactions are involved.

For a concentrated latex, transport of particles is not expected to be the rate determining step of particulate fouling. Therefore, attention is focused on other steps that will be discussed together.

At the early stages of particulate fouling (i.e. at low surface coverage), particle-surface interaction is prevailing and this interaction can be described in terms of DLVO theory for the interaction of a sphere with a flat surface. Under these conditions, electrostatic interaction is the main factor. Depending on the sign of the charge on both particles and the surface; repulsive or attractive situations are possible.

At higher coverages, particle-particle interactions come into play and the evolution of the adsorption depends on the sign and relative values of the particle-surface and particle-particle interactions. For attractive particle-surface interactions, particle adsorption rate decreases with coverage due to the repulsion between particles. If the particles are well stabilized, this leads to a monolayer that limits coverage. For particles that are not that well stabilized, multilayers can be formed. For repulsive particle-surface interactions, which is the situation sought in practice, adsorption occurs when the energy (thermal, hydrodynamic) of the particles overcomes the maximum of the repulsion potential in the DLVO plot. The evolution of the coverage depends on the relative values of the particle-surface and particle-particle interactions. Formation of polymer patches occur when $U_{p-p} < U_{p-s}$, whereas monolayers of limited coverage are formed when $U_{p-s} < U_{p-p}$.

Increasing of the ionic strength reduces the interaction between charged surfaces and leads to higher adsorption for repulsive potentials and lower adsorption for attractive potentials.

Hydrodynamic strongly affects the mechanisms discusses above. On one part, it may lead to higher adsorption/coagulation by providing the particles with energy to overcome the repulsive potentials. On the other hand, it may remove adsorbed particles. It is worth pointing out that due to the complex flow patterns in an agitated reactor, the effect of hydrodynamics changes from point to point in the reactor.

Emulsion polymerization is commonly carried out at a temperature that exceeds the T_g of the polymer formed. This difference is even higher if the T_g of the monomer-swollen polymer particles is considered. This means that under reaction conditions, the material forming the particles is sticky and coalescence of the adsorbed particles forming a continuous difficult to detach film is expected. This film may absorb monomer, that if radicals reach the film, will cause a rapid grow of the fouling.

1.5.2. Coagulation of particles in the latex and adhesion of the coagulum to internal surfaces

In the absence of agitation, the (perikinetic) coagulation rate of particles in the latex is

$$\frac{dN_p}{dt} = -kN_p^2 \tag{1.7}$$

where N_p is the concentration of polymer particles and

$$k = \frac{8k_BT}{3\eta W'} \tag{1.8}$$

where k_B is the Boltzmann constant, T the temperature, $\boldsymbol{\eta}$ is the viscosity and W' is the Fuchs stability factor given by[84]:

$$W' \approx \frac{1}{2\kappa R}\exp\left(\frac{\Psi_{max}}{k_BT}\right) \tag{1.9}$$

It can be seen that coagulation rate increases as the maximum of the interaction potential (Ψ_{max}) decreases and as κ (Eq. 1.2) increases (which occurs when the ionic strength increases).

In agitated vessels, equation 1.7 can be used, but the orthokinetic rate coefficient is[53,54]

$$k \div \frac{\left(P/V\right)^{1/2}}{W'} \tag{1.10}$$

where P is the agitation power and V the volume of the reactor.

Due to the large size of the coagulated aggregates, their transport to the surface of the reactor depends on the flow patterns.

1.5.3. Adsorption of polymer and oligomers to the internal surfaces

During emulsion polymerization amphiphilic polymer chains and oligomers are present in the aqueous phase. These materials may adsorb on surfaces following the classical adsorption mechanisms. Due to the huge surface area of the polymer particles as compared to the area of the reactor, the probability of adsorption on the internal surfaces of the reactor is very low. However, if it occurs, the consequences may be serious as fouling may grow fast due to polymerization. The use of fouling inhibitors discussed in Section 1.4. aims at avoiding this reaction.

1.6. Objectives and outline of the Thesis

This PhD Thesis is an attempt to shed some light on the fundamental mechanisms that control fouling formation in emulsion polymerization reactors. As it has been discussed in Section 1.3, emulsion polymerization is a multiphase complex process that involves particle nucleation and coagulation; numerous chemical reactions (propagation, chain transfer, termination) with several monomers; and mass transfer of radicals, monomer and surfactants. On the other hand, the scarce literature available that was reviewed in Section 1.4 shows that many of these processes directly or indirectly influence reactor fouling. Because the study of the fundamental mechanisms of fouling in the presence of all these processes seems to be an almost impossible task, in this work the strategy outlined in Figure 1.6 was used.

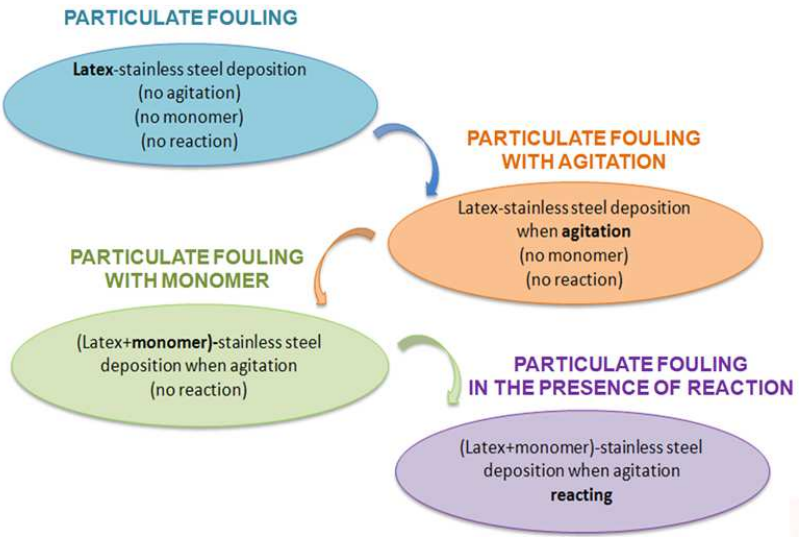

Figure 1. 6. Strategy designed for the study of the reactor fouling.

Firstly, the interaction between polymer particles and solid surfaces was studied under perikinetic conditions (Brownian motion), namely without agitation, monomers and reactions. Secondly, the interaction between polymer particles and solids surfaces was studied under orthokinetic conditions (under agitation) but with the absence of monomer and reactions. Thirdly, the effect of swelling the particles with monomer on fouling was investigated under agitation, but without reaction. Finally, fouling of the reactor during the seeded emulsion polymerization (namely, in the absence of particle nucleation) was investigated.

The thesis is organized in six chapters, of which the first one is devoted to the introduction and motivation of the work.

In **Chapter 2**, the selection of the latex-solid surface system and the experimental setups developed for the study of the particulate fouling in emulsion polymerization are presented.

Chapter 3 analyzes particulate fouling in the absence of agitation, monomer and reaction, namely, how the polymer particles interact with the internal surfaces under orthokinetic conditions (Brownian motion). A study of the effect of polymer composition, exposure time, solids content and temperature is carried out. In addition, the effect of the cleaning procedure of the reactor on particulate fouling is also reported.

In **Chapter 4** agitation is introduced to the study. Here firstly a theoretical background is presented and the effect of the polymer composition, agitation time, solids content and temperature is investigated with neither monomer nor reaction.

In **Chapter 5**, fouling under reaction conditions is studied.

In **Chapter 6**, the most relevant conclusions of this thesis are summarized.

1.7. References

(1) Odian, G. *Principles of Polymerization, 4th*; Wiley: New Jersey, 2004.

(2) Yamak, H. B. Emulsion Polymerization: Effects of Polymerization Variables on the Properties of Vinyl Acetate Based Emulsion Polymers. In *Polymer Science*; Yılmaz, F., Ed.; InTech: Croatia, 2013; pp 35–72.

(3) Freedonia, G. *World Emulsion Polymers Market*; 2012.

(4) Yamak, H. B. Emulsion Polymerization: Effects of Polymerization Variables on the Properties of Vinyl Acetate Based Emulsion Polymers. In *Emulsion Polymerization*; 2013; pp 35–73.

(5) Arzamendi, G.; Asua, J. M. Monomer Addition Policies for Copolymer Composition Control in Semicontinuous Emulsion Copolymerization. *J. Appl. Polym. Sci.* **1989**, *38* (11), 2019–2036.

(6) Arzamendi, G.; Asua, J. M. Modeling Gelation and Sol Molecular Weight Distribution in Emulsion Polymerization. *Macromolecules* **1995**, *28* (vii), 7479–7490.

(7) Plessis, C.; Arzamendi, G.; Leiza, J. R.; Schoonbrood, A. S.; Charmot, D.; Asua, J. M. Seeded Semibatch Emulsion Polymerization of N-Butyl Acrylate. Kinetics and Structural Properties. *Macromolecules* **2000**, *33*, 5041–5047.

(8) Plessis, C.; Arzamendi, G.; Leiza, J. R.; Schoonbrood, A. S.; Charmot, D.; Asua, J. M. Seeded Semibatch Emulsion Polymerization of Butyl Acrylate: Effect of the Chain-Transfer Agent on the Kinetics and Structural Properties. *J. Polym. Sci. Part A Polym. Chem.* **2001**, *39* (7), 1106–1119.

(9) Ilundain, P.; Alvarez, D.; Da Cunha, L.; Salazar, R.; Barandiaran, M. J.; Asua, J. M. Modification of the Microstructure of Emulsion Polymers. *J. Polym. Sci. Part A Polym. Chem.* **2003**, *41* (23), 3744–3749.

(10) Elizalde, O.; Aramendia, E.; Illundain, P.; Salazar, R.; Alvarez, D.; Grade, J.; Blease, T.; Barandiaran, M. J.; Leiza, J. R.; de la Cal, J. C.; et al. Knowledge-Based Development of Emulsion Polymerization Processes for Tailoring of Polymer Latex Properties. *Prog. Colloid Polym. Sci.* **2004**, *124*, 1–6.

(11) Sayer, C.; Arzamendi, G.; Asua, J. M.; Lima, E. L.; Pinto, J. C. Dynamic Optimization of Semicontinuous Emulsion Copolymerization Reactions: Composition and Molecular Weight Distribution. *Comput. Aided Chem. Eng.* **2000**, *8* (C), 457–462.

(12) Echevarria, A.; Leiza, J. R.; de la Cal, J. C.; Asua, J. M. Molecular-Weight Distribution Control in Emulsion Polymerization. *AIChE J.* **1998**, *44* (7), 1667–1679.

(13) González, I.; Asua, J. M.; Leiza, J. R. The Role of Methyl Methacrylate on Branching and Gel Formation in the Emulsion Copolymerization of BA/MMA. *Polymer (Guildf).* **2007**, *48* (9), 2542–2547.

(14) Vicente, M.; Leiza, J. R.; Asua, J. M. Control of Microstructural Properties in Emulsion Polymerization Systems. *Macromol. Symp.* **2002**, *182*, 291–303.

(15) Herrera, V.; Pirri, R.; Asua, J. M.; Leiza, J. R. Morphology Control in Polystyrene/poly(methyl Methacrylate) Composite Latex Particles. *J. Polym. Sci. Part A Polym. Chem.* **2007**, *45* (12), 2484–2493.

(16) Lopez, A.; Degrandi-Contraires, E.; Canetta, E.; Creton, C.; Keddie, J. L.; Asua, J. M. Waterborne Polyurethane-Acrylic Hybrid Nanoparticles by Miniemulsion Polymerization: Applications in Pressure-Sensitive Adhesives. *Langmuir* **2011**, *27* (7), 3878–3888.

(17) Paulis, M.; Asua, J. M. Knowledge-Based Production of Waterborne Hybrid Polymer Materials. *Macromol. React. Eng.* **2016**, *10*, 8–21.

(18) Peruzzo, P. J.; Bonnefond, A.; Reyes, Y.; Fernández, M.; Fare, J.; Ronne, E.; Paulis, M.; Leiza, J. R. Beneficial in-Situ Incorporation of Nanoclay to Waterborne PVAc/PVOH Dispersion Adhesives for Wood Applications. *Int. J. Adhes. Adhes.* **2014**, *48*, 295–302.

(19) Asua, J. M. Mapping the Morphology of Polymer-Inorganic Nanocomposites Synthesized by Miniemulsion Polymerization. *Macromol. Chem. Phys.* **2014**, *215* (5), 458–464.

(20) González-Matheus, K.; Leal, G. P.; Tollan, C.; Asua, J. M. High Solids Pickering Miniemulsion Polymerization. *Polymer (Guildf).* **2013**, *54* (23), 6314–6320.

(21) Paulis, M.; Leiza, J. Polymer/clay Nanocomposites through Emulsion and Suspension Polymerization. In *Advances in Polymer Nanocomposite Technology*; Mittal, V., Ed.; Nova Science Publishers, Inc.: New York, 2009; pp 53–100.

(22) Aguirre, M.; Paulis, M.; Leiza, J. R. Particle Nucleation and Growth in Seeded

Semibatch Miniemulsion Polymerization of Hybrid CeO2/acrylic Latexes. *Polym.* **2014**, *55* (3), 752–761.

(23) Anderson, C. D.; Daniels, E. S. Emulsion Polymerisation and Latex Applications. *Rapra Rev. Reports 160* **2003**, *14* (3), 3144.

(24) Hiemenz, P. C. *Principles of Colloid and Surface Chemistry, 2nd Ed.;* Marcel Dekker, Inc.: New York, 1986.

(25) Grahame, D. C. The Electrical Double Layer and the Theory of Electrocapillarity. *Chem. Rev.* **1947**, *41*, 441–501.

(26) Hamaker, H. C. The London – van Der Waals Attraction between Spherical Particles. *Physica* **1937**, *4* (10), 1058–1072.

(27) Derjaguin, B.; Landau, L. Theory of the Stability of Strongly Charged Lyophobic Sols and of the Adhesion of Strongly Charged Particles in Solutions of Electrolytes. *Acta Phys. Chem. URSS* **1941**, *14*, 633.

(28) Verwey, E. J. W.; Overbeek, J. T. G. *Theory of the Stability of Lyophobic Colloids*; Elsevier: Amsterdam, 1948.

(29) Napper, D. H. *Polymeric Stabilization of Coloidal Dispersion*; Academic Press: London, 1983.

(30) Napper, D.H. and Netschey, A. Studies of the Steric Stabilization of Colloidal Particles. *J. Colloid Interface Sci.* **1971**, *37* (1), 528–535.

(31) Cowell, C. and Vincent, B. Flocculation Kinetics and Equilibria in Sterically Stabilized Dispersions. *J. Colloid Interface Sci.* **1983**, *95* (2), 573–582.

(32) Barandiaran, M. J.; de la Cal, J. C.; Asua, J. M. Emulsion Polymerization. In *Polymer Reaction Engineering*; Asua, J. M., Ed.; Blackwell Publishing Ltd: Oxford, UK, 2007; pp 233–272.

(33) Tomovska, R.; de la Cal, J. C.; Asua, J. M. Reactions in Heterogeneous Media. In *Monitoring Polymerization Reactions: From Fundamentals to Applications*; Reed, W. F., Alb, A. M., Eds.; Wiley: Hoboken, New Jersey, 2014; pp 59–77.

(34) de la Cal, J. C.; Leiza, J. R.; Asua, J. M.; Butté, A.; Storti, G.; Morbidelli, M. Emulsion Polymerization. In *Handbook of Polymer Reaction Engineering*; Meyer, T., Keurentjes,

J., Eds.; Wiley, 2005; pp 249–322.

(35) Harkins, W. A General Theory of the Mechanism of Emulsion Polymerization 1. *J. Am. Chem. Soc.* **1947**, *69* (6), 1428–1444.

(36) Priest, W. . Particle Growth in the Aqueous Polymerization of Vinyl Acetate. *J. Phys. Chem.* **1952**, *56*, 1077–1082.

(37) Feeney, P. J.; Napper, D. H.; Gilbert, R. . Coagulative Nucleation and Particle Size Distributions in Emulsion Polymerization. *Macromolecules* **1984**, *17* (12), 2520–2529.

(38) Asua, J. M. *Polymer Reaction Engineering*; Asua, J., Ed.; Wiley-Blackwell, 2007.

(39) Chern, C. S. Emulsion Polymerization Mechanisms and Kinetics. *Prog. Polym. Sci.* **2006**, *31* (5), 443–486.

(40) Bott, T. R. *Fouling of Heat Exchangers*; Elsevier: Amsterdam, 1995.

(41) Li, H. C. V. *Membrane Technology: A Practical Guide to Membrane Technology and Applications in Food and Bioprocessing*; Cui, Z.F. and Muralidhara, H. S., Ed.; Elsevier: Amsterdam, 2010.

(42) Vanderhoff, J. W. The Formation of Coagulum in Emulsion Polymerization. In *Emulsion Polymers and Emulsion Polymerization*; Bassett, David R. Hamielec, A. E., Ed.; American Chemical Society, 1981; pp 199–208.

(43) von Smoluchowski, M. Drei Vortrage Uber Diffusion, Brownsche Bewegung Und Koagulation von Kolloidteilchen. *Phys. Zeit.* **1916**, *17*, 557–585.

(44) von Smoluchowski, M. Versuch Eine Mathematischen Theorie Der Koagulationskinetik Kolloidaler Losungen. *Z. Phys. Chem* **1917**, *92*, 129–168.

(45) Tuorila, P. Über Orthokinetische Und Perikinetische Koagulation. *Kolloidchem. Beihefte* **1927**, *24*, 1–122.

(46) Müller, H. Zur Allgemeinen Theorie Der Raschen Koagulation. *Kolloidchem. Beihefte* **1928**, *27*, 223.

(47) Heller, W.; Peters, J. Mechanical and Surface Coagulation: I. Surface Coagulation of α-FeOOH Sols. *J. Colloid Interface Sci.* **1970**, *32* (4), 592–605.

(48) Peters, J. and Heller, W. Mechanical and Surface Coagulation II. Coagulation by Stirring of α-FeOOH-Sols. *J. Colloid Interface Sci.* **1970**, *33* (4), 578–585.

(49) Heller, W.; De Lauder, W. Mechanical and Surface Coagulation III. Promotion of Mechanical Coagulation by Addition of Destabilizing Electrolyte. *J. Colloid Interface Sci.* **1970**, *35* (1), 60–65.

(50) Heller, W.; Peters, J. Mechanical and SurFace Coagulation IV. Prevention of Mechanical Coagulation by Surface-Active Additives. *J. Colloid Interface Sci.* **1970**, *35* (2), 300–307.

(51) De Lauder, W. B. and Heller, W. Mechanical and Surface Coagulation V. The Role of the Solid-Liquid Interface and of Turbulence in Mechanical Coagulation. *J. Colloid Interface Sci.* **1971**, *35* (2), 308–313.

(52) Diop, S.; Heller, W.; Kalousdian, S. Mechanical and Surface Coagulation: VI. Differential Surface Coagulation in Two-Component Colloidal Solutions. *J. Colloid Interface Sci.* **1979**, *70* (2), 328–337.

(53) Lowry, V.; El-Aasser, M. S.; Vanderhoff, J. W.; Klein, A. Mechanical Coagulation in Emulsion Polymerizations. *J. Appl. Polym. Sci.* **1984**, *29* (12), 3925–3935.

(54) Lowry, V.; El-Aasser, M. S.; Vanderhoff, J. W.; Klein, A.; Silebi, C. A. Kinetics of Agitation-Induced Coagulation of High-Solid Latexes. *J. Colloid Interf. Sci.* **1986**, *112* (2), 521–529.

(55) Matejicek, A.; Pivonkova, A.; Kaska, J.; Formánek, L. Influence of Agitation on the Creation of Coagulum during the Emulsion Polymerization of the System Styrene-Butylacrylate-Acrylic Acid. *J. Appl. Polym. Sci.* **1988**, *35*, 583–591.

(56) Kiparissides, C.; Macgregor, J . F.; Hamielec, A. E. Continuous Emulsion Polymerization of Vinyl Acetate. Part I: Experimental Studies. *Can. J. Chem. Eng.* **1980**, *58*, 48–55.

(57) Chern, C. S.; Chen, Y. C. Stability of the Polymerizable Surfactant Stabilized Latex Particles during Semibatch Emulsion Polymerization. *Colloid Polym. Sci.* **1997**, *275*, 124–130.

(58) Chern, C.S. and Lin, C. H. Semibatch Surfactant Free Emulsion Polymerization of Butyl Acrylate. *Polym. J.* **1995**, *27*, 1094–1103.

(59) Zubitur, M.; Asua, J. M. Factors Affecting Kinetics and Coagulum Formation during the

Emulsion Copolymerization of Styrene/butyl Acrylate. *Polymer (Guildf).* **2001**, *42* (14), 5979–5985.

(60) Bianco, H.; Cohen, Y.; Narkis, M. Coagulum Formation and Elimination in Emulsion Copolymerization of Tribromostyrene with Styrene. *Polym. Adv. Technol.* **1996**, *7* (10), 809–812.

(61) Cubbon, R. C. P.; Smith, J. D. B. The Properties of Nuclear Brominated Styrenes I—The Synthesis and Polymerization of Dibromostyrene and Tribromostyrene. *Polymer (Guildf).* **1969**, No. 10, 479–487.

(62) Cubbon, R. C. P.; Smith, J. D. B. The Properties of Nuclear Brominated Styrenes II—The Copolymerization of Dibromostyrene and 2,4,5-Tribromostyrene with Styrene. *Polymer (Guildf).* **1969**, *10*, 489–493.

(63) Hajime Kitamura, T. S. Method for the Polymerization of Vinyl Chloride. US4105838 A, 1978.

(64) http://www.akzonobel.com/polymer/our_products/noxol_everplus_antifouling_agents/.

(65) http://www.ineos.com/products?bu=ineos+technologies&m=pvc+additives.

(66) Asua, J. M. *Polymeric Dispersions: Principles and Applications*, NATO ASI S.; Kluwer Academic Publishers, 1997.

(67) Enrique Saldivar-Guerra, E. V.-L. *Handbook of Polymer Synthesis, Characterization, and Processing*; Wiley: New Jersey, 2013.

(68) Erbil, Y. H. *Vinyl Acetate Emulsion Polymerization and Copolymerization with Acrylic Monomers*; CRC Press: Boca Raton, 2000.

(69) Ferdinand Rodriguez, Claude Cohen, Christopher K. Ober, L. A. *Principles of Polymer Systems, Sixth Edition*; CRC Press: Boca Raton, 2014.

(70) Fitch, R. M. *Polymer Colloids II*; Plenum Press, Springer: New York, 1980.

(71) McGreavy, C. *Polymer Reactor Engineering*; Springer Science+Business Media, 1994.

(72) Thoenes, D. *Chemical Reactor Development: From Laboratory Synthesis to Industrial Production*; Springer Science+Business Media: Dordrecht, 1998.

(73) Blackley, D. C. *Polymer Latices: Science and Technology Volume 2: Types of Lattices. Chapter 10: Synthetic Lattices: General Principles of Production*; Springer: The Netherlands, 1997.

(74) Okubo, M. *Polymer Particles*; Springer: The Netherlands, 2005.

(75) Poehlein, G.W.; Ottewill, R.H. and Goodwin, J. W. *Science and Technology of Polymer Colloids: Preparation and Reaction Engineering*, Volume I.; Nijhoff, 1983.

(76) Thompson, L.; Pryde, D. N. Weak Aggregation of Non-Ionic Surfactant Stabilised Dispersions. *J. Chem. Soc. Faraday Trans. 1* **1981**, *77*, 2405–2415.

(77) Adamczyk, Z. *Particles at Interfaces: Interactions, Deposition, Structure*; Elsevier Ltd.: The Netherlands, 2006.

(78) Elimelech, M.; Gregory, J.; Jia, X.; Williams, R. A. *Particle Deposition and Aggregation: Measurement, Modelling and Simulation*; Elsevier Ltd: Oxford, 1995.

(79) Henry, C.; Minier, J.-P.; Lefèvre, G. Towards a Description of Particulate Fouling: From Single Particle Deposition to Clogging. *Adv. Colloid Interface Sci.* **2012**, *185-186*, 34–76.

(80) Bowling, R. A. A Theorical Review of Particle Adhesion. In *Particles on Surfaces 1. Detection, Adhesion and Removal.*; Plenum Press: New York, 1988.

(81) Visser, J. Adhesion and Removal of Particles I and II. In *Fouling Science and technology*; Kluwer Academic Publishers: Dordrecht, 1988.

(82) Oliviera, D. R. Physico-Chemical Aspects of Adhesion. In *Biofilms – Science and Technology*; Kluwer Academic Publishers: Dordrecht, 1992.

(83) Van De Ven, T. G. M. The Capture of Colloidal Particles on Surfaces and in Porous Material: Basic Principles. *Colloids Surfaces A Physicochem. Eng. Asp.* **1998**, *138*, 207–216.

(84) Fuchs, V. N. Uber Die Stabilitat Und Aufladung Der Aerosole. *Phys. Chemie* **1934**, 736–743.

Chapter 2. Particulate fouling study strategy: selection of the model system and development of the setups

2.1. Introduction

In this Thesis, the interaction between polymer particles and solids surfaces was studied under both perikinetic and orthokinetic conditions in the absence of monomer and reactions and under (orthokinetic conditions) in the presence of reaction. The interaction was expected to depend on latex and surface characteristics. A judicious choice of the type and number of latexes and surfaces should be made in order to keep the problem manageable. In what follows, the selection of the case study is discussed and the experimental setups described.

2.2. Selection of the case study

2.2.1.Latex selection

According to Freedonia Group[1], acrylics will remain the largest and fastest growing emulsion polymer product type through 2016, accounting for nearly 40 percent of the world market. Demand for acrylics will benefit from rapid growth in the paint and coatings markets, where acrylic polymers are valued for their durability and wide range of applications. In addition, they will also be extensively used in adhesives. For these reasons, a butyl acrylate methyl methacrylate latex was chosen for this study and the copolymer composition was varied to include both coatings and adhesives applications.

Commercial-like 50 wt% solids content latexes were synthesized by batch and semicontinuous emulsion copolymerization of butyl acrylate and methyl methacrylate (BA, MMA). Table 2.1 summarizes the latexes synthesized. A 50/50 wt/wt monomer ratio was used for coating formulations and a 90/10 wt/wt BA/MMA for the adhesives. In addition, 1wt% of methacrylic acid (MA) was used in some formulations. Technical monomers (i.e. containing inhibitors) were used and stabilization was provided by both anionic and non ionic surfactants. Methyl methacrylate (MMA, Quimidroga), butyl acrylate (BA, Quimidroga) and methacrylic acid (MAA, Quimidroga) were used as supplied. Potassium persulfate (KPS, Fluka) and sodium metabisulfite (MBS, Sigma-Aldrich) were used as redox initiators. The surfactants were Dowfax 2A1 (Dow Chemical) and Disponil A3065 (BASF). Dowfax 2A1 is an alkyldiphenyloxide disulfonate (branched 12-carbon hydrophobe) (Figure 2.1). Disponil A surfactants are non-ionic

surfactants based on mixtures of ethoxylated linear fatty alcohols (Figure 2.2). Disponil A 3065 is a modified ethoxylated fattyalcohols POE 30. Deionized water has been used throughout the work. To increase the pH of the latexes to 8 a 25 wt% solution of ammonia (Fluka) was used.

Table 2. 1. Latexes used in this study.

		Weight fraction of the monomers		
Name	**Process**	**BA**	**MMA**	**MAA**
50/50 batch	Batch	50	50	-
50/50 semi	Semicontinuous	50	50	-
90/10 batch	Batch	90	10	-
50/50/MAA	Semicontinuous	49.5	49.5	1
90/10/MAA	Semicontinuous	89.1	9.9	1

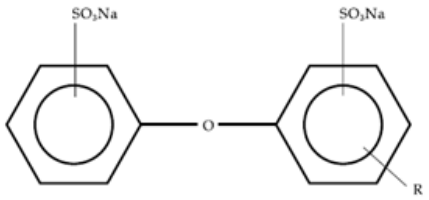

Figure 2. 1. Structural formula of Dowfax2A type surfactants.

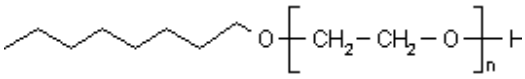

Figure 2. 2. Structural formula of Disponil A type surfactants.

50 wt% solids content (meth)acrylic latexes were synthesized by batch and semicontinuous seeded emulsion polymerization and the formulations of both seeds and latexes are given in Tables 2.2 and 2.3. 20 wt% solids content (meth)acrylic seeds were synthesized in batch in a 2L reactor equipped with reflux condenser, stirrer and nitrogen inlet at 70 ºC, injecting the aqueous KPS solution when the temperature was reached and letting to react overnight. Seeded batch polymerizations were carried out charging all the monomer with the seed in the same 2L glass reactor. The redox pair was fed in two streams for 2 hours and then, the system was kept 1 hour in batch. The reaction temperature was maintained constant at 70 ºC by controlling the temperature of the fluid in the jacket by means of a thermostatic bath. Seeded semicontinuous polymerizations were carried out in 1 L reactor equipped with reflux condenser, stirrer and nitrogen inlet. The seed, 35 wt% of the total water and the buffer (when used), were initially charged in the reactor and kept under nitrogen atmosphere while heating to 70 °C. The aqueous solution of KPS was injected as a shoot when the reaction temperature was reached. The preemulsion with the monomers, surfactants and water was added to the reactor using a flow rate of 2 g/min during 4 hours. Then, the system was kept 1 hour in batch.

Table 2. 2. Formulations used to prepare the seeds.

SEED	BA	MMA	KPS	NaHCO3	Dowfax 2A	Disponil A 3065	Water
50/50 batch (1) latexes	10	10	0.15	0.05	0.49	0.28	79.03
50/50 batch (2), 50/50 semi and 50/50 MAA latexes	10	10	0.15	0.05	0.43	0.28	79.10
90/10 latexes	18	2	0.15	0.05	0.43	0.28	79.10

Table 2. 3. Formulations used to prepare the latexes.

LATEX	Polymer in seed	BA	MMA	MAA	NH_3	KPS	MBS	$NaHCO_3$	Dowfax 2A	Disponil A 3065	Total water
50/50 batch (1)	5.7	22.1	22.1	-	-	0.2	0.2	0.1	0.54	0.6	48.4
50/50 batch (2)	5.7	22.1	22.1	-	-	0.2	0.2	0.1	0.47	0.6	48.5
50/50 semi	5.7	22.1	22.1	-	-	0.4	-	0.1	0.47	0.6	48.4
90/10 batch	5.7	39.9	4.4	-	-	0.2	0.2	0.1	0.47	0.6	48.5
50/50 MAA	5.7	21.9	21.9	0.4	0.1	0.4	-	-	0.47	0.6	48.4
90/10 MAA	5.7	39.5	4.4	0.4	0.1	0.4	-	-	0.47	0.6	48.4

2.2.2.Solid surface selection

Emulsion polymerization is a highly corrosive environment, particularly in the presence of persulfate initiators. Glass-lined reactors are resistant to corrosion but the cost is very high. Stainless steel 316L is the most often used material for the polymerization reactors vessel and has been used for this work.

A practical problem in the study of the reactor fouling is the measurement of the polymer adhered to the internal surfaces in particular to the reactor wall. Gravimetry is difficult to use because the weight of the fouling is low as compared to that of the reactor and hence the polymer should be removed from the reactor wall. In this work, this problem was overcome by determining the polymer deposited on removable baffles (substrates).

2.3. Development of the experimental setups

2.3.1.Setup for the study of particulate fouling without agitation

Chapter 3 is devoted to the study of particulate fouling in the absence of agitation, monomer and reaction, that is, how the latex particles interact with stainless steel without fluid motion. For that purpose an experimental setup where the stainless steel substrates were able to be in contact with the latexes has been developed.

The stainless steel substrates were held in the middle of 100 ml glass bottles containing 40 g of a completely converted latex by the use of flexible silicon septums attached to the caps (Figure 2.3 a)). The bottles were placed in a thermal bath (Figure 2.3 b)) and kept at a constant temperature for a given time. In order to remove the non-deposited latex from each substrate, the whole system withouth the cap was directly immersed in a beaker filled with 2 liters of deionized water at room temperature (Figure 2.4). The reason for such a procedure was that it was found that the amount of polymer on the substrate strongly depended on the way that the substrate was treated after its immersion in the latex. Thus, direct removal of the substrate from the latex at a temperature above the ambient one, followed by an inmediate immersion in deionized water, led to a higher amount of attached polymer, than cooling the latex and then extracting and rinsing the substrate (see Chapter 3). The washed substrates were allowed to dry and the particulate fouling was measured gravimetrically.

a)  b) 

Figure 2. 3. a) Stainless steel substrate held in the bottle. b) Bottles with substrates in contact with latex in the thermal bath.

Figure 2. 4. Sequence of steps for removing the non deposited latex after the experiment.

2.3.2.Setup for the study of particulate fouling with agitation

The experiments were carried out in a 1 L jacketed cylindrical glass reactor. A reactor lid with four holders for placing stainless steel baffles was designed (Figure 2.5). An Ekato Mig impeller of 7.5 cm diameter (Figure 2.6), which provides a wide range of mixing and shear was selected for the agitated experiments. In Figure 2.7, the final configuration is shown, where the stainless steel substrates held paralel to the glass reactor surronding the impeller rotation field mimicking in this way the stainless steel internal vessel.

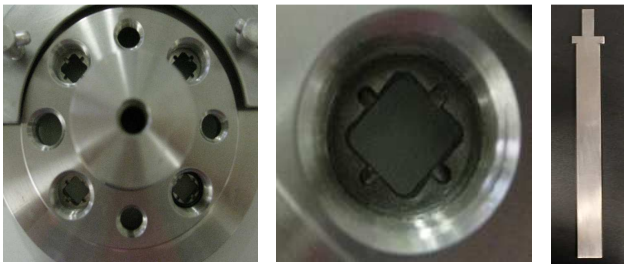

Figure 2. 5. Reactor lid designed, zoom of a substrate holder and stainless steel substrate.

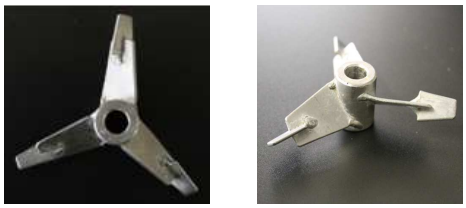

Figure 2. 6. Ekato Mig impeller bottom (left picture) and side (right picture) view.

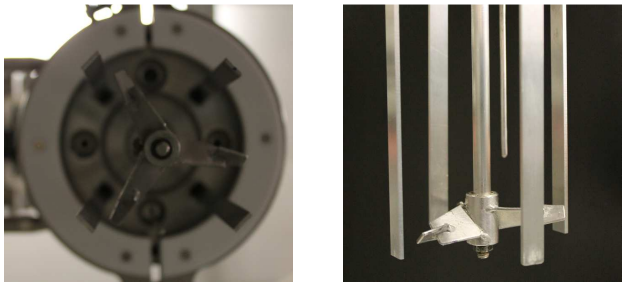

Figure 2. 7. Bottom and side view of the agitated system setup.

Figure 2.8 illustrates the way in which the agitated system impacts the substrates. The impeller has two perpendicular sections of blades (angle = 45 º) and as a clockwise agitation was used, the inner blade pushed the fluid downward and the outer blade pumped the fluid upward to enhance the liquid circulation. In addition, the agitator created an outwards radial flow and a rotating flow. This makes the system to impact preferentially the front and left sides of the zone of the baffles that was in front of the impeller.

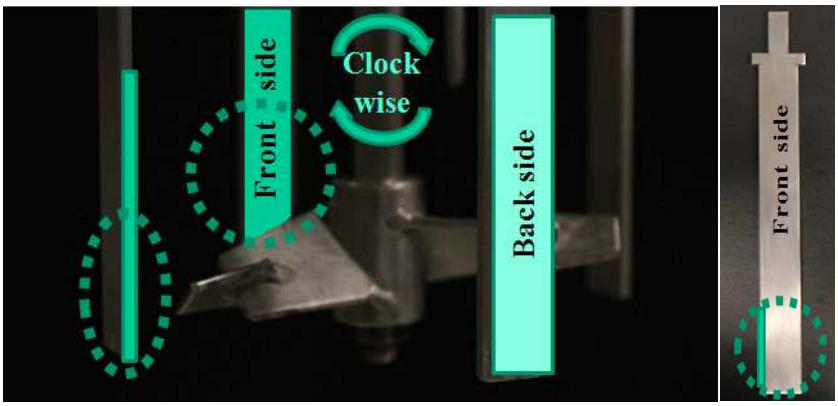

Figure 2. 8. Preferential zones marked (approximated) where the latex will impact the substrates pushed by the impeller.

This setup has been used in Chapters 4 and 5 for quantifying the particulate fouling under agitation. The particulate fouling on the removable substrates was measured gravimetrically.

2.4. References

(1) Freedonia, G. *World Emulsion Polymers Market*; 2012.

Chapter 3. Particulate fouling without agitation: latex-substrate interaction

3.1. Introduction

In the absence of agitation, particulate fouling is ruled by the transport of polymer particles to the solid-latex interphase and the interaction of the particles with the solid substrates. A schematic representation of this process is presented in Figure 3.1 where δ_a is the thickness of the diffusion boundary layer, and N_p the concentration of polymer particles.

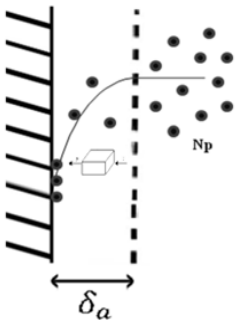

Figure 3. 1. Schematics of diffusion boundary layer of thickness δ_a.

The microscopic mass balance in the boundary layer is:

$$\frac{\partial N_p}{\partial t} + \nabla . \vec{J} = 0 \quad (\text{particles/m}^3.\text{s}) \tag{3.1}$$

where the first term accounts for the accumulation of particles per unit volume and the second for the neat entry rate. $\vec{J}$ is the flux (particles/ m^2.s) given by,

$$\vec{J} = -D \nabla N_p + u_i N_p + u_j N_p \tag{3.2}$$

where *D* is the particle diffusion coefficient of the particles (m^2/s), u_i is the particle terminal velocity due to particle-surface interactions and u_j is the velocity due to convective flow.

Let us assume that the convection effects can be neglected (u_j =0), so there is stagnant flow through the boundary layer. Substitution of Eq. 3.2 in Eq 3.1 leads to:

$$\frac{\partial N_p}{\partial t} = D \nabla^2 N_p - \nabla . \left(u_i N_p\right) \tag{3.3}$$

The terminal velocity due to particle-surface interactions is,

$$u_i = \frac{F}{\Phi_{drag}} \tag{3.4}$$

where *F* is the force acting on the particle and Φ_{drag} the viscous drag that for an spherical particle of radius *R* can be approximated by,

$$\Phi_{drag} = 6\pi R\eta \tag{3.5}$$

where η is the viscosity of the continuous phase.

The force is given by the gradient of the particle-surface interaction potential, *U*:

$$F = -\nabla \mathrm{U}(x) \tag{3.6}$$

For spherical particles, the diffusion coefficient is related to the friction coefficient according to the Stokes-Einstein equation:

$$D = \frac{k_B T}{6\pi R\eta} \tag{3.7}$$

where k_B is the Boltzmann's constant and *T* is the absolute temperature.

Substituting Eq. 3.4 and 3.6 into Eq. 3.3, one gets

$$\frac{\partial N_p}{\partial t} = D\,\nabla^2 N_p - \nabla.\left(\frac{\nabla U}{6\pi R\eta}\,N_p\right) \tag{3.8}$$

Under steady state conditions, in the absence of reaction (no source of new particles) $\left(\frac{dN_p}{dt} = 0\right)$, Eq. 3.8 reduces to:

$$0 = D\,\frac{d^2 N_p}{dx^2} + \frac{d\left(\frac{\nabla U N_p}{6\pi R\eta}\right)}{dx} \tag{3.9}$$

Integration of Eq. 3.9 gives:

$$D\ \frac{dN_p}{dx} + \frac{\nabla U}{6\pi R\eta}\ N_p = \mathrm{C}_1 = \vec{J} \tag{3.10}$$

Combination of Eqs 3.6 and 3.10 leads to:

$$D\left(\frac{dN_p}{dx} + \frac{\nabla U}{k_B T}\right) = \vec{J} \tag{3.11}$$

that can be rearranged as:

$$\frac{dN_p}{dx} + \frac{dU}{dx}\ \frac{N_p}{k_B T}\ = \frac{\vec{J}}{D} = \mathrm{C}_2 \tag{3.12}$$

In order to integrate Eq. 3.12, let us consider the following equation:

$$\frac{d\left(N_p exp\left(\frac{U}{k_B T}\right)\right)}{dx} = \frac{N_p}{k_B T}\ exp\left(\frac{U}{k_B T}\right)\frac{dU}{dx} + exp\left(\frac{U}{k_B T}\right)\frac{dN_p}{dx} \tag{3.13}$$

Multiplying Eq. 3.12 by $exp\left(\frac{U}{k_B T}\right)$ one gets:

$$exp\left(\frac{U}{k_B T}\right)\frac{dN_p}{dx} + \frac{N_p}{k_B T}\ exp\left(\frac{U}{k_B T}\right)\frac{dU}{dx} = \mathrm{C}_2 exp\left(\frac{U}{k_B T}\right) \tag{3.14}$$

Combination of Eqs 3.13 and 3.14 results in

$$\frac{d\left(N_p exp\left(\frac{U}{k_B T}\right)\right)}{dx} = \mathrm{C}_2 exp\left(\frac{U}{k_B T}\right) \tag{3.15}$$

Integrating of Eq. 3.15 one gets,

$$\int_{U=0 \rightarrow N_p=N_p}^{U \rightarrow N_{p_1}} d\left(N_p exp\left(\frac{U}{k_B T}\right)\right) = \int_{\delta_a}^{x} \mathrm{C}_2 exp\left(\frac{U}{k_B T}\right) dx \tag{3.16}$$

$$N_{p_1} exp\left(\frac{U}{k_B T}\right) - N_p = \mathrm{C}_2 \int_{\delta_a}^{x} exp\left(\frac{U}{k_B T}\right) dx \tag{3.17}$$

It was assumed that at the surface of the solid (x=0) the particles are deposited on the surface, and hence they disappear from the suspension (irreversible adsorption). Therefore, $N_{p_1} = 0$ at x = 0, and Eq. 3.17 reduces to:

$$-N_p = \mathrm{C}_2 \int_{\delta_a}^{0} exp\left(\frac{U}{k_B T}\right) dx \tag{3.18}$$

Therefore,

$$\mathrm{C}_2 = \frac{\vec{J}}{D} = \frac{N_p}{\int_0^{\delta_a} exp\left(\frac{U}{k_B T}\right) dx} \tag{3.19}$$

Consequently, the flux is:

$$\vec{J} = \frac{DN_p}{\int_0^{\delta_a} exp\left(\frac{U}{k_B T}\right) dx} \quad \left(\frac{part}{m^2 s}\right) \tag{3.20}$$

It can be noticed that this equation is similar to the one developed by Fuchs[1] when he studied the particle-particle coagulation:

$$\vec{J} = \frac{D\varphi}{\int_{2R}^{\infty} \frac{1}{x^2} exp\left(\frac{U}{k_B T}\right) dx} \tag{3.21}$$

where *x* is the particle-particle distance, φ the volume fraction of particles and *U* the particle-particle interaction potential.

It is interesting to observe that in the limit of a negligible particle-surface interaction (U=0), the stationary flux reduces to the Fick's first law:

$$J = \frac{D}{\delta_a} N_p \tag{3.22}$$

Although the agitation is not considered in this chapter, it is worth pointing out that the effect of the agitation is: i) to reduce the value of δ_a and ii) to increase the value of D because of the turbulence in the boundary layer.

The properties of the polymer particles and substrate are accounted for by means of the particle-surface interaction potential U. Equation 3.20 shows that the higher U the lower the fouling. The first condition for a repulsive potential is that particles and surface have the same charge. Charges of opposite sign lead to attractive potentials. In this regard, it has to be pointed out that the surface charge of the stainless steel changes from positive at low pH to negative for pH>4.3 (Figure 3.2).

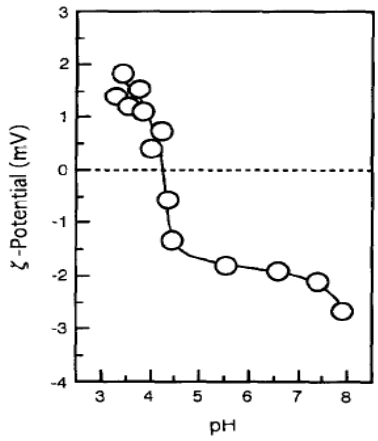

Figure 3. 2. The ζ- potential of stainless steel particles as function of pH[2].

Assuming charges of the same sign, U increases as the ionic strength of the continuous medium decreases and as the surface charge density of both particles and solid surface increase.

The interaction between the solid surface and the polymer particles evolves during the fouling process because the particles deposited on the surface modify the characteristics of the surface. A limiting case of this modification is the pseudo equilibrium conditions, namely when fouling reaches a constant value because the flux J approaches zero.

3.2. Latexes used in the study

The synthesis of the latexes used in this chapter is reported in Chapter 2. The ratio of the main monomers methyl methacrylate and butyl acrylate was adjusted for both coating (BA/MMA = 50/50 wt/wt) and adhesive (BA/MMA = 90/10 wt/wt) applications. Stability was provided by a blend of ionic (Dowfax 2A1) and non ionic (Disponil A3065) surfactants. Regarding the 50/50 composition synthesized by batch process, different proportions of Dowfax 2A1 were used for obtaining latexes with the same composition but different stability (50/50 batch (1) and 50/50 batch (2)). Besides, in some cases 1% of methacrylic acid (MMA) was used. This monomer is used to improve both stability and adhesion to substrates. In the context of the present study, its contribution to stability is the main factor. Both batch and semibatch polymerizations were employed. High conversions were achieved and the solids content was around 50 wt%. The particle size was close to 180 nm for all latexes. The pH of the final latexes was acidic (pH=2) due to the use of potassium persulfate (KPS) as initiator. In the formulations including MAA, ammonium was added to keep a basic pH (pH=8) that maintained the MMA deprotonated ($pK_a \approx 4.5$). Except for the latex 50/50 batch, the glass

transition temperatures (T_g) were in agreement with the copolymer composition. The exception of the 50/50 batch is due to the fact that a MMA-rich polymer was formed at the beginning of the polymerization because of its higher reactivity ratio (r_{BA}=0.13; r_{MMA}=0.92)[3], and although only this T_g for this copolymer was observed in the differential scanning calorimeter, a low T_g softer polymer was also present. The zeta potential of the latexes was in the range of 52-54 mV in the absence of MAA, and about 61 mV with MAA. Similar values of the surface tension were obtained for all latexes, indicating that the adsorption equilibrium of the surfactants was not significantly varied for the copolymer content.

Table 3. 1. Characteristics of the latexes.

LATEX	Particle size (nm)	Solids content (%)	Conversion (%)	pH	Tg exp (°C)	ζ (mV)	Surface tension (mN/m)
50/50 batch (1)	167	50-51	98-100	2	41 (*)	-55	47
50/50 batch (2)	175	50-51	98-100	2	43 (*)	-52	46
50/50 semi	185	50-51	97-99	2	16	-58	44
90/10 batch	177	50-51	97-98	2	-38	-54	46
50/50/MAA	175	50	97	8	15	-62	46
90/10/MAA	183	49	93-95	8	-39	-61	43

(*)Although only this T_g was observed, a softer polymer was present.

As the stability of the latex was expected to affect fouling formation, the salt and mechanical stability of the latexes were measured (Table 3.2 and Table 3.3). From these data the following ranking of relative stabilities was obtained: 90/10 batch < 50/50 batch (2) < 50/50 batch (1) < 50/50 semi < 50/50/MAA < 90/10/MAA, which roughly follows the order of the ζ - potential.

Figure 3.3 presents the rheological curves for the different latexes. It can be seen that although they showed differences at low shear rates, they had the same behavior for shear rates greater than 1 s^{-1}.

Table 3. 2. Salt stability of the latexes. The cells written with % symbol indicate the coagulum percentage if present.

		NaCl		$CaCl_2$				
	Initial size	**0.5**	**1**	**0.05**	**0.1**	**0.25**	**0.5**	**1**
50/50 batch (1)	167	173	171	170	176	< 1 %	< 1 %	< 1 %
50/50 batch (2)	175	182	186	189	182	< 1 %	< 1 %	2%
50/50 semi	185	187	188	182	< 1 %	< 1 %	< 1 %	9%
90/10 batch	177	6%	21%	8%	16%	22%	23%	25%
50/50 MAA	175	171	204 (5µm)	171	170	171	168	246 (5 µm)
90/10 MAA	183	178	173	175	175	173	173	185

Table 3. 3. Mechanical stability of the latexes.

LATEX	Destabilization time (seconds)
50/50 batch (1)	-
50/50 batch (2)	23
50/50 semi	35
90/10 batch	15
50/50 MAA	44
90/10 MAA	More than 120

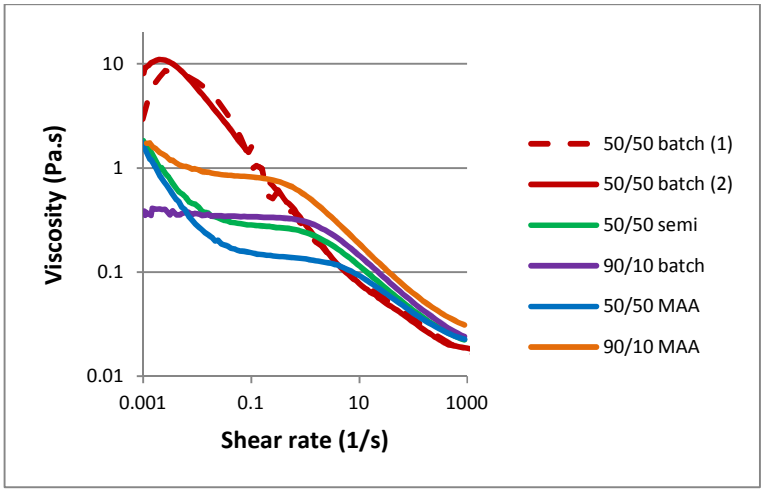

Figure 3. 3. Viscosity vs. shear rate.

3.3. Determination of the particulate fouling under perikinetic conditions

Chapter 2 details the set-up built for the study of particulate fouling. A necessary condition for this study is the availability of a robust and accurate method to measure the fouling. Preliminary experiments showed that this method is far from simple.

The experimental setup that was developed to monitor the fouling under perikinetic conditions (Brownian motion) consists in 100 ml bottles in which stainless steel substrates were place in the middle. These substrates were removed from the system after being in contact with the latex for a certain period of time. The substrate was then rinsed with water and the amount of fouling determined by gravimetry.

Although the procedure is rather straightforward, it was found that the amount of coagulum depended on the way in which the substrate was treated after being in contact with the latex. Figure 3.4 shows the fouling measured on a stainless steel 316 substrate that had been in contact with latex 50/50 batch (2) for 2 hours at 70 °C when i) the substrate was removed from the latex held a few seconds in the air, and then rinsed with deionized water; ii) the substrate was removed from the latex and rinsed with water as soon as possible and iii) in order to avoid contact with air the whole system was immersed in 2L of deionized water that was at room temperature, and the substrate was not exposed to air until quite dilution was reached by adding fresh water to the beaker. Each of these procedures was repeated five times.

Figure 3.4 shows that the amount of fouling increased as the time in contact with air increased. The effect can be observed visually.

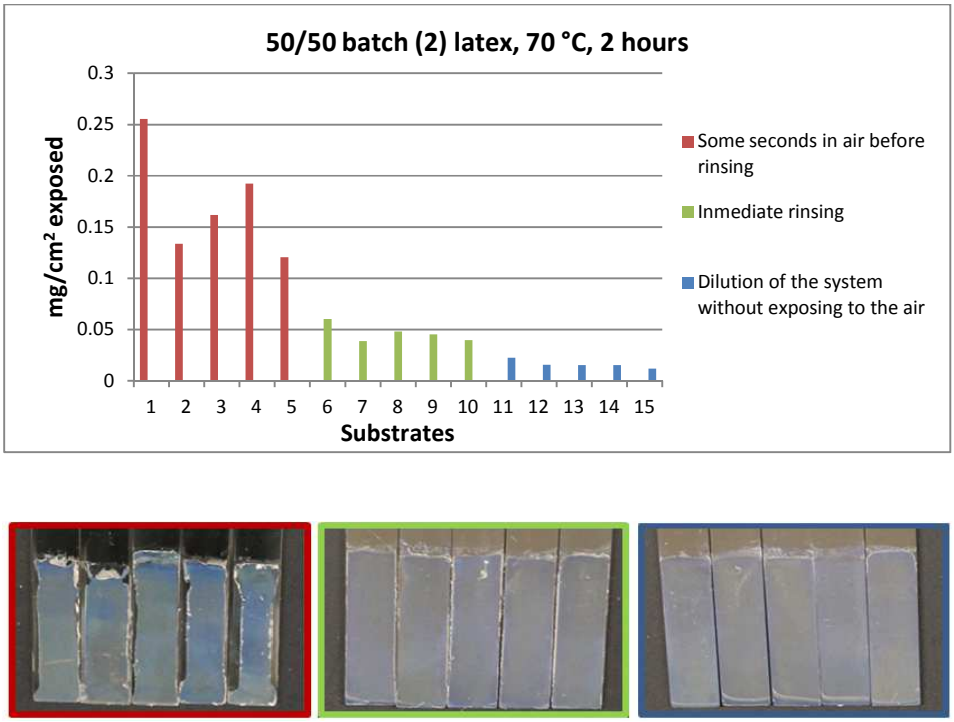

Figure 3. 4. Effect of the measuring method on the amount of fouling.

The same procedures were applied to other latexes obtaining the same trends for all of them as shown in Figure 3.5 (the effect of the different latexes is discussed in Section 3.4.4).

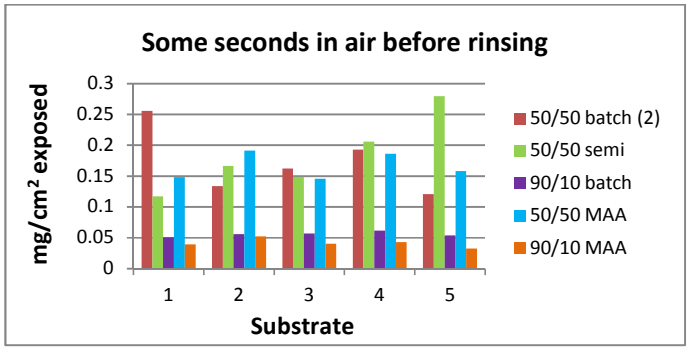

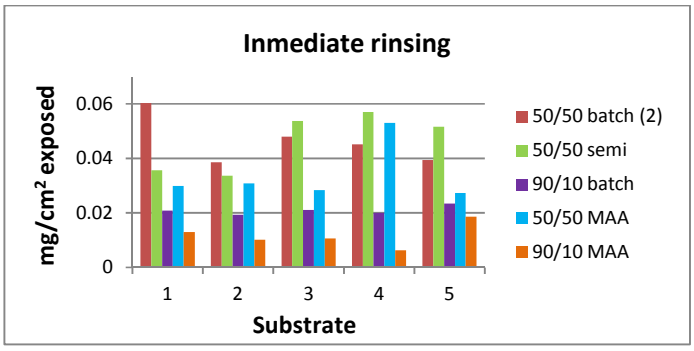

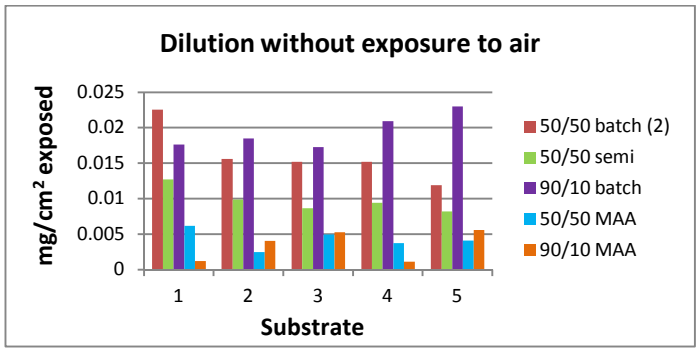

Figure 3. 5. Effect of the contact time with air on fouling for different latexes.

The results presented above suggest that the differences in the fouling observed were due to water evaporation which depends on both the time of contact with air and the temperature. Therefore, one experiment using the 50/50 batch (2) latex was carried out in which after 2 h at 70 °C, the whole bottle was cooled down to 25 °C and then the substrate removed, kept in contact with air for some seconds before rinsing. Figure 3.6 shows that this procedure gave a much lower amount of fouling than when the substrate was collected at 70 °C, but still higher than the case in which there was no contact with air.

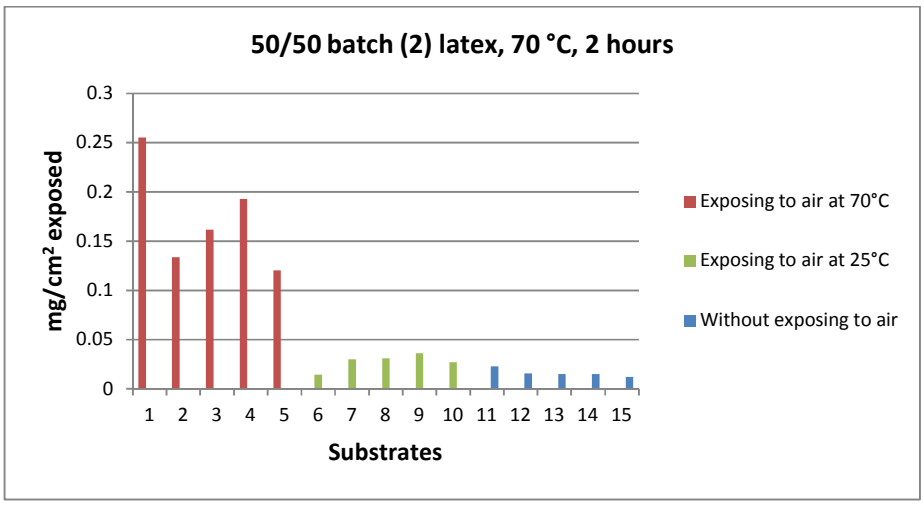

Figure 3. 6. Effect of cooling down the system before removing the substrates from the bottle.

Water evaporation may increase the solids content of the latex in the film, which in turn increases the probability of formation of coagulum that can later attach to the substrate. However, the amount of water that can evaporate in the short period of time elapsed from the moment in which the substrate was removed until it was rinsed, does not seem enough to create a substantial increase in the solids content.

On the other hand, water evaporation may create a temperature profile in the latex film. The evaporation of only 5% of the water will result in an average decrease of about 18 °C in the film creating a temperature profile across the latex film. Heat transfer from the film to air further contributes to this profile. Temperature gradients are known to contribute to the mass transport of colloids by means of the thermodiffusion also known as Ludwig-Soret effect[4,5]. This phenomenon affects to dissolved molecules such as methanol[6] as well as charged[7] and uncharged[8] colloids.

For binary mixtures, the flux of colloids is, *J*, is

$$J = -\rho D \nabla w - \rho w\,(1-w) D_T \nabla T \qquad (3.23)$$

where $\boldsymbol{\rho}$ is the mass density of the homogeneous mixture, *D* is the diffusion coefficient, *w* is the weight fraction of component 1, and D_T is the thermal diffusion coefficient. Therefore, the first term accounts for the Fick's diffusion and the second describes the Ludwig-Soret effect. The term *w(1-w)* is introduced because Ludwig-Soret effect does not occur in pure fluids. The Fickian diffusion leads to homogenization of the concentration whereas the Ludwig-Soret effect leads to mass separation. The Soret coefficient is

$$S_T = \frac{D_T}{D} \tag{3.24}$$

and can be positive or negative depending on the sign of D_T, which is positive when the colloid moves towards the lower temperature and negative when it travels in the direction of the hot points.

For dilute colloids S_T is positive for temperatures higher than a critical temperature which is in the range of 20-25 °C and negative below this limit[7]. On the other hand, S_T decreases with the concentration of the colloid and may even switch the sign from positive to negative[8]. Similar results have been reported for solutions of molecules[6].

The critical temperature at which the sign of S_T changes increases with the solids content. Thus, at 20 wt% solids, the critical temperature is about 40°C whereas for 40 wt% solids is 50 °C[8]. This means that for the current system (50 wt% solids), the critical temperature should be above 50 °C, that is in the range of temperatures in which the evaporation of water and heat transfer to the surroundings may bring the outer part of the latex films. Under these conditions, particles will move towards the hotter stainless substrate, which will increase fouling.

The results discussed above show that in order to avoid artifacts in the measurement of particulate fouling under perikinetic conditions, contact with air prior rinsing should be avoided. Therefore, the results presented below were obtained under these conditions.

An important practical consequence of the results presented in this section is that the latex film remaining on the walls after the emptying of the reactor may cause additional fouling if a temperature profile is generated.

3.4. Results and discussion

3.4.1.Kinetics of particulate fouling

A typical industrial emulsion polymerization lasts 2-4 hours due to the heat removal limitations of the industrial reactors. Therefore, it is of interest to know the characteristic time of particulate fouling, because if it is longer than 2-4 hours, it will be of no significance in an industrial process.

The kinetics of particulate fouling was measured by placing the bottle with substrate and the latex into a thermal bath already heated to the chosen temperature. This was considered to be time zero. It was checked that about 15 minutes were necessary for the latex to reach 70 °C.

The fouling at 30 min, 2 and 4 hours and 2 days for the 50/50 batch (1) latex was measured. Figure 3.7 presents the results obtained in three replicate experiments. It can be seen that data were affected by some scattering. In this regard, it should be pointed out that

the latex used in each experiment cannot be reused since in the procedure used, the bottle is immersed in deionized water and then the latex diluted. Therefore, some of the variations observed in the particulate fouling were due to batch to batch variations in the different 50/50 batch (1) latexes used. Figure 3.7 shows that a limiting value of fouling was reached in a time shorter than 30 min. This indicates that the kinetics of fouling was fast as compared with the process time for an industrial emulsion polymerization. In addition, the limiting value indicates that above a certain value, particle attachment to the surface is hindered.

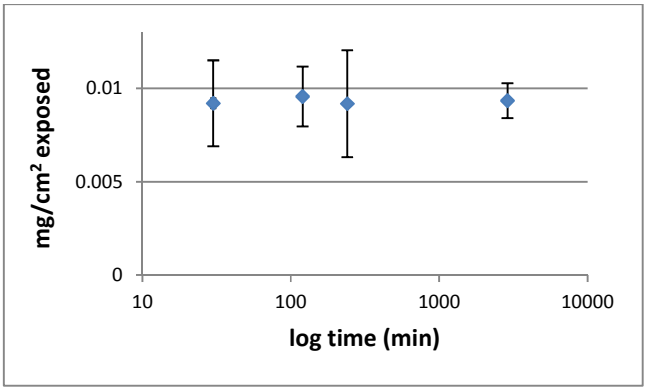

Figure 3. 7. Kinetics of particulate fouling with the 50/50 batch (1) latex, 50% SC on 316L stainless steel substrates at 70 °C presented as the average value of the three replicates.

A quick calculation shows that the weight of a monolayer of particles with diameter of 180 nm in a simple cubic arrangement is about 10^{-2} mg/cm^2 (assuming a density of 1.1 kg/L).

Comparison of this value with Figure 3.7 shows that the attachment of the particles to the surface stopped at about 80% of the single layer coverage. These results can be explained as follows. The polymer particles were negatively charged because they contained sulfonate groups from the Dowfax 2A1 (Figure 2.1) and sulfate groups from the KPS. On the other hand, at the latex pH (pH=2), the surface of the stainless steel was positively charged (Figure 3.2). Therefore, fast attachment of the particles to the substrate occurred. The attachment modified the surface of the substrate changing its charge from positive to negative, and when the surface is well covered by polymer particles (about 80% of the single layer coverage) attachment of more particles was prevented by electrostatic repulsion. In this context, it is worth pointing out that because the temperature of the experiment was much higher than the T_g of the polymer, most likely the particles attached to the surface coagulate between them forming polymer patches on the substrate.

In order to gain more information about the limiting coverage, another experiment was carried out by diluting the latex to 29 wt% solids. The fouling measured after 2 h at 70 °C is presented in Figure 3.8. It can be seen that the amount of fouling decreased to about half of that measured for 50% solids suggesting an equilibrium between the concentration of particles in the latex and the amount attached. This also indicates that the surface charge density on the stainless steel is relatively low and can be counteracted by a relatively modest amount of particles. Once the surface becomes neutral attachment of particles is a regular adsorption process. A high surface charge density on the stainless steel will promote the continuous attachment of the negatively charged particles even at low solids content.

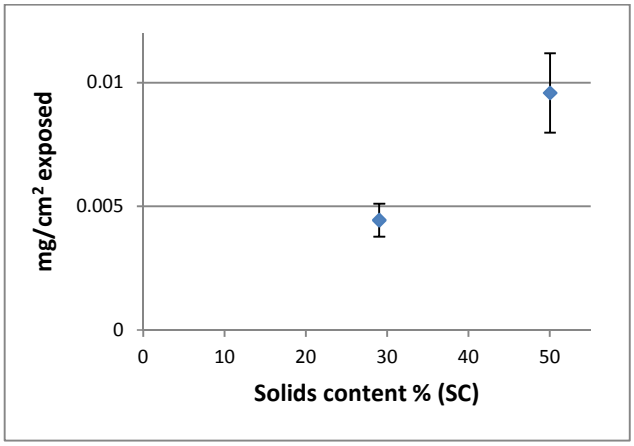

Figure 3. 8. Effect of the solids content on the particulate fouling at 70°C and 2 hours.

3.4.2.Effect of temperature

Even though 70 °C is a typical industrial reaction condition, others can be used. Thus lower temperatures are employed for redox initiators, and in post-polymerization higher temperatures are often required. Therefore, it is important to study the effect of temperature on fouling. Figure 3.9 shows that fouling slightly increases with temperature. A possible reason is that the extension of the hydrophilic moiety of the non ionic surfactant (Figure 2.2) in water decreases with temperature. This has two effects that can affect fouling. On one part, the stability of the latex decreases with temperature and on the other, the particles can be packed more closely on the surface of the substrate.

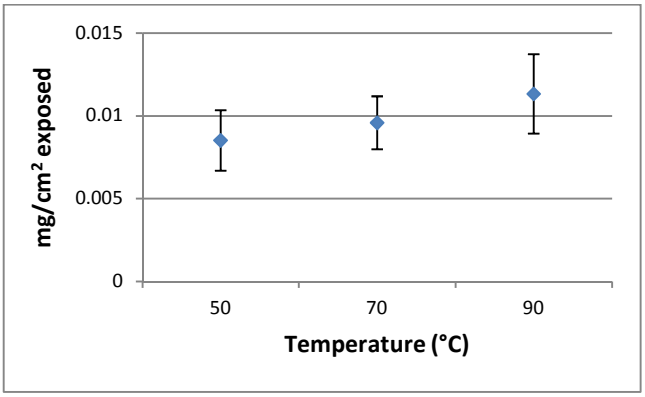

Figure 3. 9. Particulate fouling of the 50/50 batch (1) latex 50% SC over stainless steel substrates during 2hours at different temperatures.

3.4.3.Effect of the charge of the substrate

The isoelectric point of the stainless steel is pH=4.3[2]. This means that at the pH of the latex (pH=2) was positively charged, leading to an electrostatic attraction with the anionically stabilized polymer particles. In order to check the influence of the charge of the substrate, fouling was measured at pH=9 (obtained by adding ammonia to the latex). Figure 3.10 shows that in experiments carried out at 70 °C with 2 h of contact, the fouling observed with the 50/50 batch (1) latex was reduced to less than half when the pH was varied from 2 to 9. It is also noticeable that some fouling was observed at pH=9 even though the substrate was negatively charged, which may be due to the low **ζ** -potential of the stainless steel (**ζ** -potential = -10/20 mV at pH=9)[9].

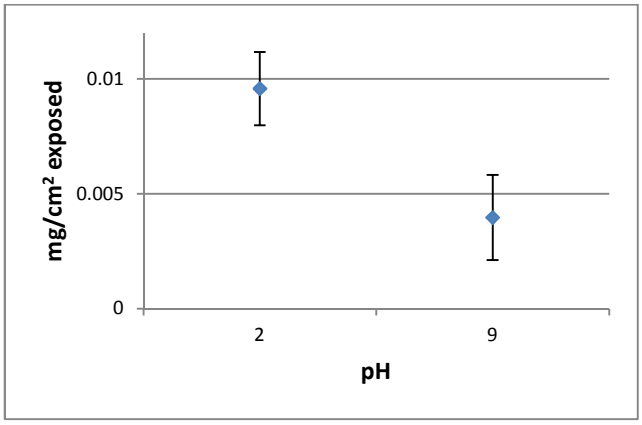

Figure 3. 10. Effect of the surface charge on particulate fouling. 70 °C, 2 h of contact, 50/50 batch (1) latex.

3.4.4.Effect of the latex stability

Figure 3.11 presents the effect of the type of latex on the amount of fouling. The latexes are organized in an arbitrary stability scale based on the stability tests presented in Tables 3.2 and 3.3. It can be seen that particulate fouling decreased as the stability of the latex increased. In terms of the equation 3.20, this simply shows that fouling increases as the particle-particle (covered surface) repulsive interaction potential decreases. For the least stable latex (90/10 batch) the amount of fouling accounts for the formation of 2-3 layers of particles on the substrate. On the other hand, no clear effect of the T_g of the polymer on fouling was observed.

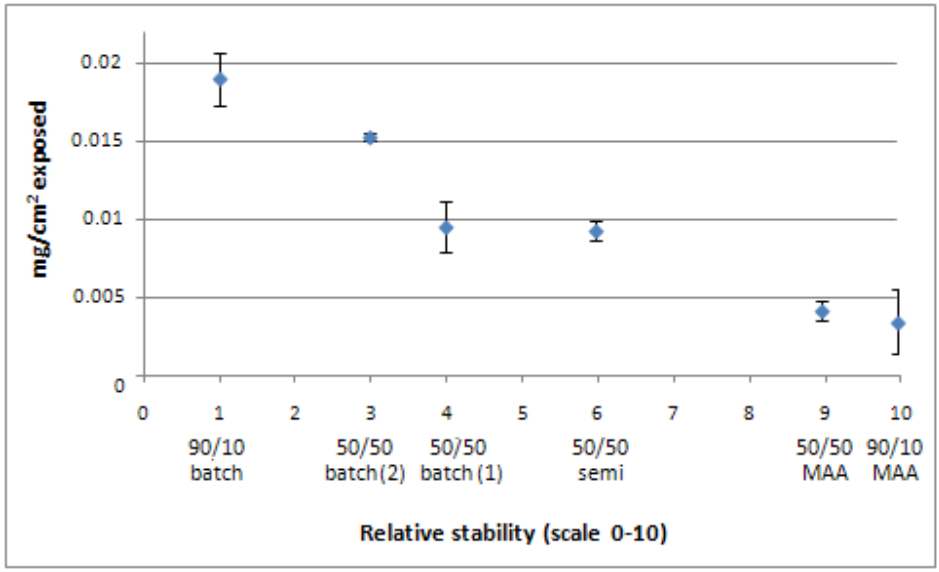

Figure 3. 11. Effect of the latex stability on particulate fouling.

3.5. Conclusions

In this chapter, fouling formation in the absence of agitation was studied using six different latexes of different composition and stability. The latexes were stabilized by a mixture of anionic and non-ionic surfactants. Some additional anionic stabilization was provided by sulfate groups from the initiator (KPS). Besides, in some cases 1% of methacrylic acid (MMA)

was used for further stabilization. Stainless steel 316 plates were used as substrate and the fouling was determined gravimetrically after removing the plates from the latex where they were immersed at controlled temperature for a given period of time.

It was found that the way in which the non-attached latex was removed from the substrate strongly affected the observed fouling. Even a few seconds of contact with air increased the amount of fouling. This effect was attributed to thermodiffusion, namely the transport of colloids due to differences in temperature. In contact with air a temperature gradient was established between the air-latex interface and the latex-substrate interface due to water evaporation and convection. For the solids content of the latex an inverse thermodiffusion (colloids moving from cold to hot areas) is expected and this caused a flow of latex particles towards the substrate, and consequently more fouling. It was found that this problem was overcome by immersing the whole system in deionized water.

The fouling was at least qualitatively well described by equation 3.20 that predicts that the rate of fouling is proportional to the number of particles in the system and inversely proportional to the particle-surface repulsive interaction potential. Attractive potentials accelerate fouling. After the reaction, the pH of the latexes was pH=2, due to the effect of the initiator used (KPS). At this pH the stainless steel is positively charged and fouling is favored by electrostatic attraction. The process is fast reaching a limiting amount of fouling that corresponded to a surface partially covered by a monolayer of latex particles. The change in the overall charge of the surface from positive to negative due to the attachment of anionic particles, created an increasing electrostatic repulsion potential that prevented the attachment

of more particles. This equilibrium depended on the solids content of the latex, and fouling decreased as solids content decreased.

Fouling was also decreased when the particle-surface repulsive potential was increased making the surface anionic by increasing the pH above the isoelectric point of the stainless steel. Temperature slightly increased fouling, likely due to the lower stability of the non-ionic surfactant. The stability of the latex was a major factor determining fouling, which strongly decreased as latex stability increased. The reason is that for the more stable latexes, the strong repulsive potential between the particles attached to the substrate and those dispersed basically stops the flow of particles towards the surface of the substrate.

3.6. References

(1) Fuchs, V. N. Uber Die Stabilitat Und Aufladung Der Aerosole. *Phys. Chemie* **1934**, 736–743.

(2) Fukuzaki, S.; Urano, H.; Nagata, K. Adsorption of Protein onto Stainless-Steel Surfaces. *J. Ferment. Bioeng.* **1995**, *80* (1), 6–11.

(3) Brandrup, J.; Immergut, E. H. *Polymer Handbook, 3rd Ed.*; John Wiley: New York, 1989.

(4) Ludwig, C. Diffusion Zwischen Ungleich Erwwärmten Orten Gleich Zusammengestzter Lösungen. *Sitz. Ber. Akad. Wiss. Wien. Math.-naturw. Kl* **1856**, *20*, 539.

(5) Soret, C. Sur L'état D'équilibre Que Prend Au Point de Vue de Sa Concentration Une Dissolution Saline Primitivement Homohéne Dont Deux Par- Ties Sont Portées à Des Températures Différentes. *Arch. Sci. Phys. Nat.* **1879**, *2*, 48–61.

(6) Maeda, K.; Shinyashiki, N.; Yagihara, S.; Wiegand, S.; Kita, R. How Does Thermodiffusion of Aqueous Solutions Depend on Concentration and Hydrophobicity? *Eur. Phys. J. E* **2014**, *37* (10), 94–99.

(7) Putnam, S. A.; Cahill, D. G.; Wong, G. C. L.; Putnam, S. A.; Cahill, D. G.; Wong, G. C. L. Temperature Dependence of Thermodiffusion in Aqueous Suspensions of Charged Nanoparticles Temperature Dependence of Thermodiffusion in Aqueous Suspensions of Charged Nanoparticles. *Langmuir* **2007**, No. 23, 9221–9228.

(8) Ning, H.; Buitenhuis, J.; Dhont, J. K. G.; Wiegand, S. Thermal Diffusion Behavior of Hard-Sphere Suspensions. *J. Chem. Phys.* **2006**, *125*, 204911.

(9) Boulangé-Petermann, L.; Doren, A.; Baroux, B.; Bellon-Fontaine, M. N. Zeta Potential Measurements on Passive Metals.pdf. *J. Colloid Interface Sci.* **1995**, *171*, 179–186.

Chapter 4. Particulate fouling with agitation

4.1. Introduction

In Chapter 3, the fouling of stainless steel surfaces in the absence of agitation was investigated. It was found that, at least qualitatively, fouling is well described by Eq. 3.20

$$\vec{J} = \frac{DN_p}{\int_0^{\delta_a} exp\left(\frac{U}{k_B T}\right) dx} \quad \left(\frac{part}{m^2 s}\right) \tag{3.20}$$

where D is the diffusion coefficient, N_p the concentration of polymer particles and U the particle-surface interaction potential.

In this chapter, fouling under orthokinetic conditions (with agitation) is investigated. In an agitated reactor, the energy provided by the agitator increases the frequency and the energy of the collisions between the particles and the substrate. For particle-particle coagulation under laminar flow, Smoluchowski predicted that the rate of coagulation is[1]

$$\frac{dN_p}{dt} = -\frac{16}{3}\dot{\gamma}\, R^3 N_p^2 \tag{4.1}$$

where $\dot{\gamma}$ is the shear rate and *R* the radius of the polymer particle. Obviously, stability should be incorporated in Eq. 4.1 to account for the particle-particle interactions.

Following the method outlined in Chapter 3, the use of these concepts for surface fouling leads to

$$J \div \frac{\dot{\gamma}_s R^3 N_p}{\int_0^{\delta_a} exp\left(\frac{U}{k_B T}\right) dx} \div \frac{\dot{\gamma}_s \varphi_s}{\int_0^{\delta_a} exp\left(\frac{U}{k_B T}\right) dx} \tag{4.2}$$

where $\dot{\gamma}_s$ is the local shear rate and φ_s the solids content. The local shear rate is proportional to the square root of the local power per unit volume P_v

$$\dot{\gamma}_s = \left(\frac{P_v}{\eta}\right)^{1/2} \tag{4.3}$$

where $\boldsymbol{\eta}$ is the viscosity of the latex.

The flow patterns in an agitated reactor are very complex and the local shear rates can vary tremendously from one part to other of the reactor. Therefore, a heterogeneous distribution of fouling is expected.

The flow created by the agitator may remove fouling from the internal surfaces of the reactor. It is worth pointing out that as the temperature of the process is much higher than the T_g of the polymer, the particles attached to the substrate likely coagulate between them forming an aggregate of polymer. These aggregates may be removed by the flow.

4.2. Experimental part

Fouling was studied in the 1L glass reactor presented in Figure 4.1. The system included four removable stainless steel baffles that were used to measure fouling gravimetrically. The baffles were distributed around the agitator as shown in Figure 4.2. The latexes used in this study and their characteristic are presented in Table 4.1. In a typical experiment, the reactor was charged with 650 g of latex and heated to the temperature of the experiment under agitation. The moment in which this temperature was reached was considered to be time zero. Then, the baffles were removed at given times and the fouling determined gravimetrically.

Figure 4.3 shows that two types of fouling could be clearly distinguished in the baffles. Fouling formed at the air-film interface presumably by many wetting and drying process due to the effect of the agitation. This will be called *interfacial fouling*. Fouling created in the areas that are always submerged in the latex, which is referred to as *wet fouling*. In a lab scale reactor because of the high ratio between the air-latex interfacial area and the reactor volume, the interfacial fouling accounts for a significant fraction of fouling, which is not the case for large scale commercial reactors.

Figure 4. 1. Reactor used to study orthokinetic fouling.

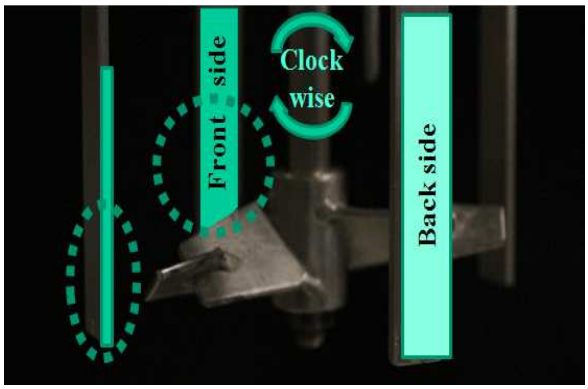

Figure 4. 2. Position of the agitator and baffles.

Table 4. 1. Latexes used in the study of orthokinetic fouling.

LATEX	Particle size (nm)	Solids content (%)	pH	Tg exp (°C)	ζ (mV)	Surface tension (mN/m)
50/50 batch (1)	167	50-51	2	41 (*)	-55	47
50/50 batch (2)	175	50-51	2	43 (*)	-52	46
50/50 semi	185	50-51	2	16	-58	44
90/10 batch	177	50-51	2	-38	-54	46
50/50/MAA	175	50	8	15	-62	46
90/10/MAA	183	49	8	-39	-61	43

(*)Although only this T_g was observed, a softer polymer was present.

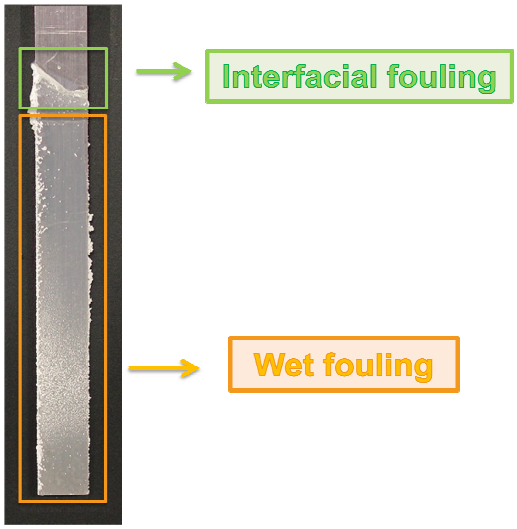

Figure 4. 3. Types of fouling.

The effect of the agitation rate (0,100, 300, 400 y 500 rpm) was initially screened by using the 50/50 batch (2) latex for 2 h at 70 °C. After each run, the latex was filtered through a nylon screen with a mesh size of 80 μm and the final particle size was measured. The results are summarized in Table 4.2. It can be seen that no coagulum was detected filtering the latex through the 80 μm mesh for agitation rates lower than 500 rpm. At 500 rpm a small amount of filtered coagulum (0.2%) was observed. However, the main problem at 500 rpm was the high amount of foam that might be the cause of the small amount of coagulum because no effect of the agitation on the particle size was observed in the range of agitation rates studied.

At agitation rates lower than 400 rpm a coagulum was formed at the air-latex interface. Figure 4.4. and Table 4.2 show that this coagulum increased as agitation rate decreased.

It is remarkable that substantial surface coagulation was observed with no agitation, and this was not observed in Chapter 3 were the experiments were conducted in the absence of agitation. The reason may be that the experiments in Chapter 3 were carried out in a basically isothermal closed vessel whereas in the present case, as the reactor lid was at a lower temperature than the latex, water evaporates from the latex and condensed on the lid. This led to an increase in the concentration of polymer particles at the air-film interface that eventually coagulated between them yielding the polymer film that can be observed in Figure 4.4.

Table 4. 2. Effect of the agitation rate on particle size, and filtered and surface coagulum.

rpm	Filtered coagulum (%)	Particle size change	% Surface coagulum	Observations
0	0	No	4	Coagulum in the air/latex interface
100	0	No	3	Some coagulum in the air/latex interface
300	0	No	0.2	Some coagulum in the perimeter (air/latex/ reactor wall)
400	0	No	0	Some foam. Little surface coagulum in the perimeter
500	0.2	No	0	Plenty of foam. No surface coagulum

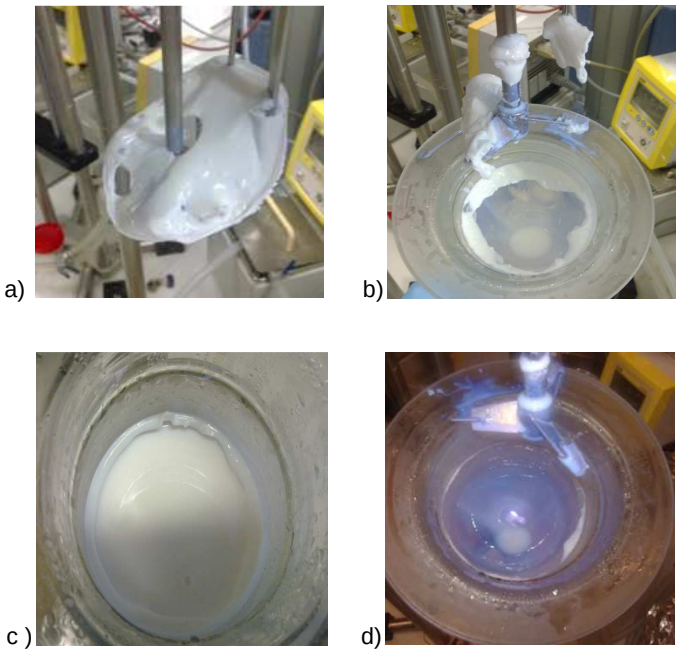

Figure 4. 4. Picture of the air-latex interface when: a) 0 rpm; b) 100 rpm; c) 300 rpm and d) 400 rpm.

This is different from the mechanism proposed by Heller et al.[2–7] and others[8,9] that assumed that surface coagulation involves the adsorption of polymer particles at the air-latex interface as a first step, which is followed by coagulation between the adsorbed particles. If this were the mechanism for the present system, surface coagulum would have been observed in Chapter 3, but this was not the case.

Because surface coagulum was formed below 400 rpm and foam above, an agitation rate of 400 rpm was used in this chapter.

In Chapter 3, it was shown that the way in which the baffles were rinsed to remove the liquid latex had a strong effect on the perikinetic particulate fouling due to thermodiffusion. Exposing the baffle to air before rinsing led to an increase of the fouling. Due to the characteristics of the reactor used in this chapter, it was not possible to avoid the exposure of the baffles to air. Fortunately, the amount of fouling due to agitation was much higher than the orthokinetic fouling (Figure 4.5), and hence the results of the orthokinetic fouling determined in this chapter were not significantly affected by thermodiffusion. Nevertheless, in order to minimize its effect, the reactor was cooled to 25 °C before removing the baffles. Figure 4.5 also shows that under agitation, fouling distributes heterogeneously in the baffles. Therefore, the results are presented in terms of amounts of wet and interfacial coagulum. The data presented are the average value of the four baffles.

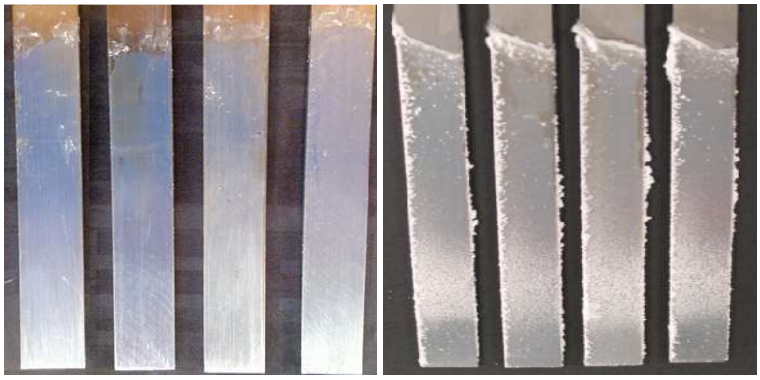

Figure 4. 5. Comparison between perikinetic (left) and orthokinetic (400 rpm, right) fouling after 2 hours and 70 °C with latex 50/50 batch (2).

4.3. Results and discussion

4.3.1.Fouling kinetics under agitation

The kinetics of the particulate fouling on stainless steel baffles under agitation was studied at 70 °C and 400 rpm for the 50 wt% solids 50/50 batch (1) and 50/50 batch (2) latexes. The colloidal stability of these latexes is different, the 50/50 batch (2) being the least stable.

Figure 4.6 shows the pictures of the front side of the four baffles at different times for the two latexes. It can be seen that the amount of fouling was greater for the less stable latex

(50/50 batch (2)), that this amount increased with time and that it was heterogeneously distributed in the baffles.

Figure 4.7 shows the averaged amount of fouling in the four baffles. It can be seen that the amount of wet fouling (fouling formed on the surface of the baffles that was immersed in the latex) continuously increased with time and showed an acceleration, which was particularly clear for the less stable latex (50/50 batch (2)). It can also be seen that the amount of fouling was lower for the more stable latex. The continuous increase of the amount of fouling indicates that the energy provided by the agitation was able to overcome the repulsion of the negatively charged particles attached to the baffles. This was easier for the less stable latex. In addition, the heterogeneous distribution of the fouling shows the effect of the local flow in different parts of the reactor.

Figure 4.7 also shows that the interfacial fouling (fouling created at the air-latex interface by consecutive wetting and drying processes) also increased with time but the kinetics was not well defined and the amount of fouling was not related to the stability of the latex, which was due to the fact that fouling was produced by wetting and drying and under these circumstances, the colloidal stability of the latex does not play any role (an exception to this may be the case of redispersable latexes, which are stabilized with PVOH).

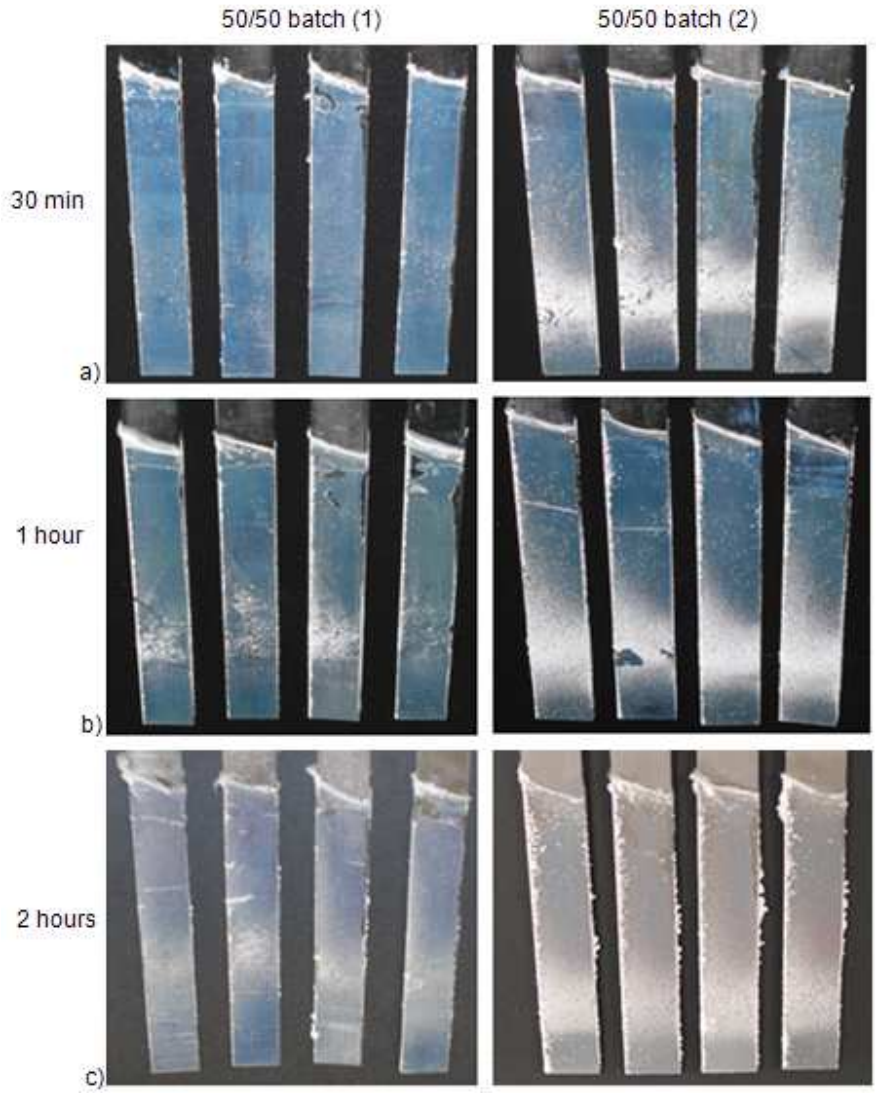

Figure 4. 6. Pictures of the front side of the baffles. a) 30 min, b) 1 hour and c) 2 hours. Left pictures corresponds to 50/50 batch (1) latex and right pictures to 50/50 batch (2).

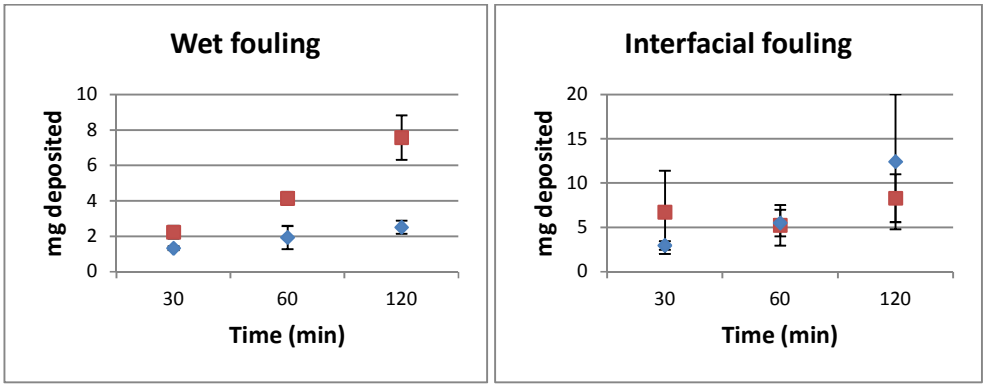

Figure 4. 7. Kinetics of wet and interfacial fouling. Diamonds correspond to the more stable latex (50/50 batch (1)) and squares correspond to the less stable one (50/50 batch (2)).

Even though the results presented in Figure 4.7 are the average of the four baffles, the heterogenous distribution of fouling in each baffle may cast doubts about the reproducibility of the measurements. Therefore, three replicate experiments were carried out, in which the fouling after 2 h at 70 °C and 400 rpm were measured for the two latexes. Figure 4.8 presents the amount of fouling measured for the two latexes in the three replicate experiments and Figures 4.9 and 4.10 present the front and back sides of the substrates for the 50/50 batch (1) and 50/50 batch (2) latexes. Each point in Figure 4.8 is the average of the 4 baffles. It can be seen that even though the error bars were significant, the reproducibility of the data of wet fouling was adequate. On the other hand, the variability of the measurements of interfacial fouling was much higher. Fortunately, as discussed above, the significance of the interfacial fouling (fouling created by the continuous wetting and drying of the internal surfaces of the

reactor at the air-latex interface) is limited because for the lab reactor used in this work the amount of this fouling is magnified by the high air-latex interfacial area/reactor volume ratio. This ratio is much smaller in commercial reactors. Therefore, although the data of interfacial fouling is given for completeness, the discussion will be mainly centered on the wet fouling.

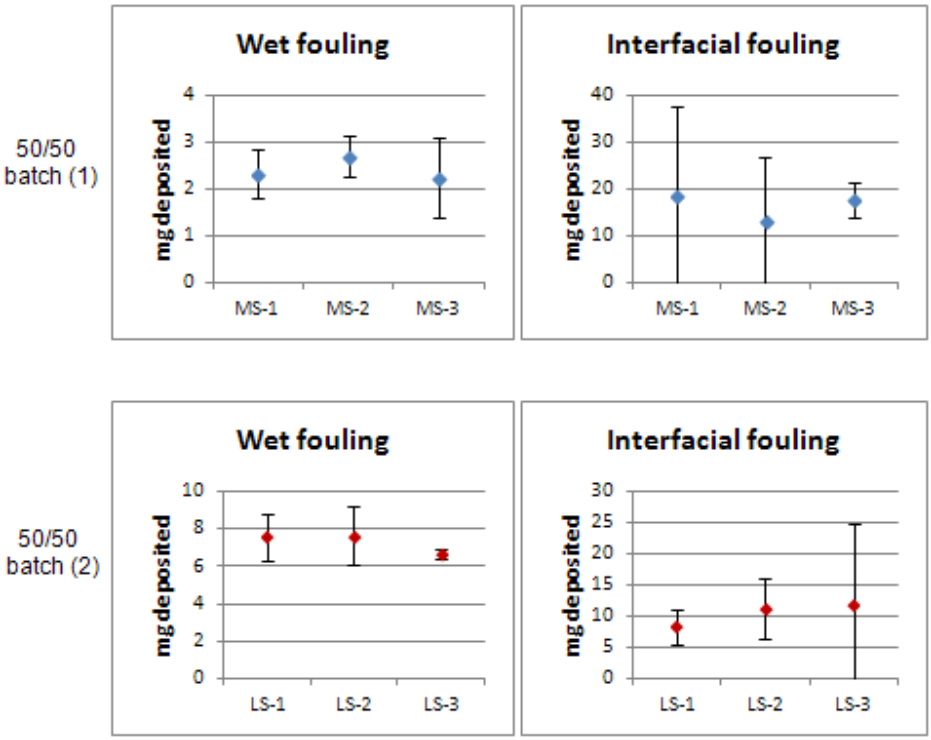

Figure 4. 8. Wet and interfacial average fouling for the 50/50 batch (1) latex (upper figures) and 50/50 batch (2) latex (lower figures) in the three replicate experiments.

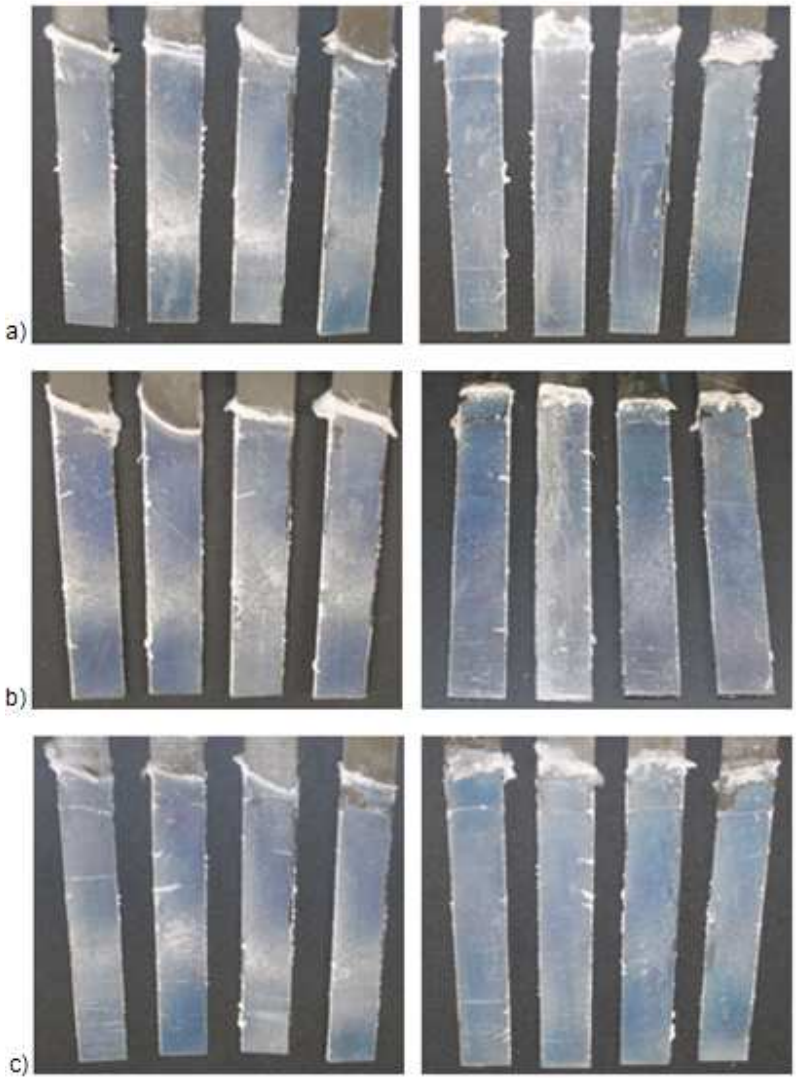

Figure 4. 9. Pictures of the front (left) and back (right pictures) sides of the fouled substrates in the three repeated experiments 50/50 batch (1) latex (more stable). 2 h at 70 °C and 400 rpm.

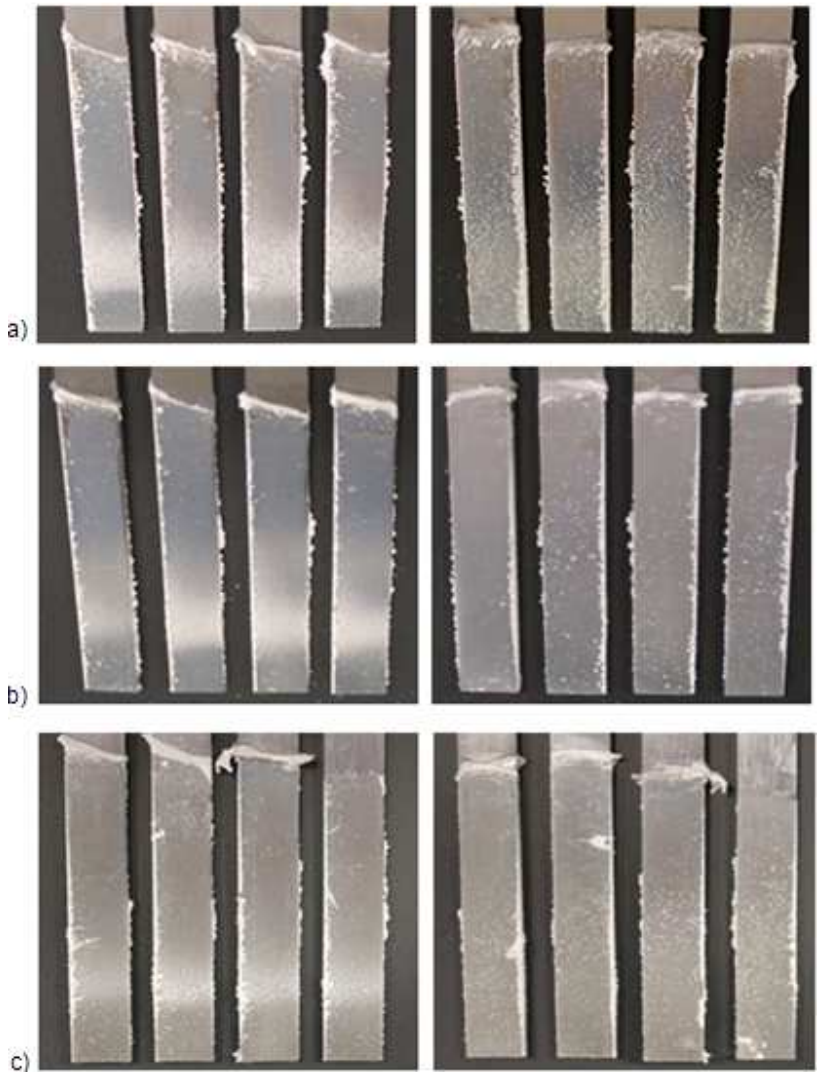

Figure 4. 10. Pictures of the front (left) and back (right pictures) sides of the fouled substrates in the three repeated experiments 50/50 batch (2) latex (less stable). 2 h at 70 °C and 400 rpm.

4.3.2.Effect of solids content

Theory predicts that wet fouling on a surface is proportional to $\varphi_s \left(\frac{P_v}{\eta}\right)^{1/2}$ (Eqs 4.2 and 4.3), where φ_s is the solids content, P_v the local power per unit volume and $\boldsymbol{\eta}$ is the viscosity of the latex. The estimated Reynolds number at the tip of the agitator was about Re=2000, which corresponds to a turbulent flow. Under this conditions, the agitation power is almost independent of Re[10]

$$P \div N^3 D^5 \, Re^{-\alpha} \tag{4.4}$$

where *N* is the agitation rate (s^{-1}), *D* the diameter of the reactor and $0<\boldsymbol{\alpha}<<1$.

For a given system (defined values of D and reactor volume) and a constant agitation rate, $P_v \div \eta^{\alpha}$, and hence the wet fouling is expected to be proportional to $\varphi_s \, \eta^{\alpha-1/2} \approx \varphi_s \, \eta^{1/2}$. As $\boldsymbol{\eta}$ increases with φ_s, the wet fouling is expected to be proportional to φ_s^{β} with β<1.

Figure 4.11 shows that this is not the case for the experiments carried out at 70 °C and 400 rpm for 2 h as the experimental value of β was greater than 1. On the other hand, the increase was more acute for the least stable latex (50/50 batch (2)) due to the lower value of U in Eq. 4.2. The interfacial fouling also showed a severe increase in the amount of fouling as the solids content increases, but this is only due to the fact that aggregation of particles by drying is delayed for low solids contents. Figure 4.12 shows that the effect of solids content on fouling can be observed visually.

A possible reason is that the Reynolds number was calculated at the tip of the agitator. Near the baffles a much lower value of Re is expected because the velocity of the liquid was lower and the viscosity higher (latexes are pseudoplastics). Under laminar regime

$$P \div \eta N^2 D^3 \tag{4.5}$$

which results in a wet fouling proportional to φ_s^{γ} with γ>10.

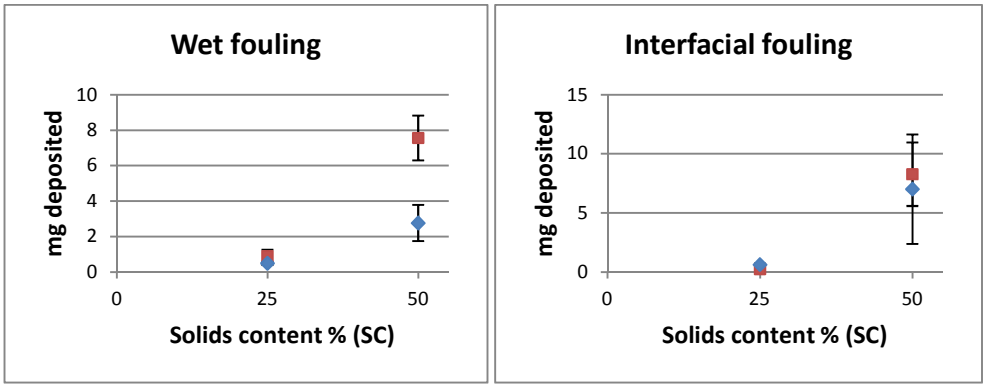

Figure 4. 11. Effect of the solids content on wet and interfacial fouling for latexes 50/50 batch (1) (diamonds) and 50/50 batch (2) (squares). 70 °C, 2 h, 400 rpm.

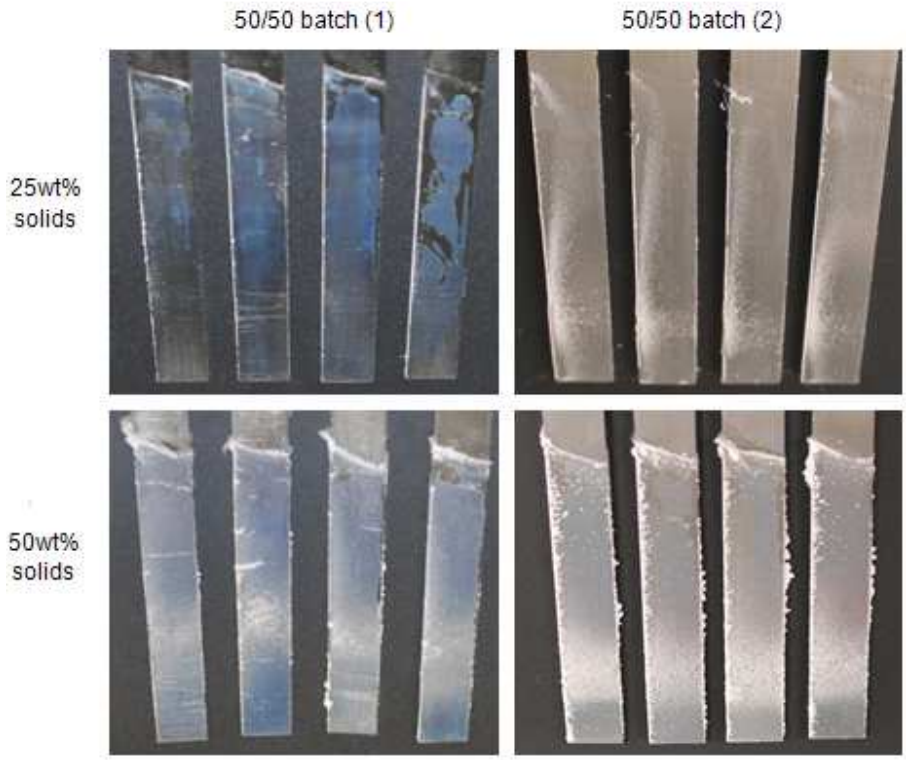

Figure 4. 12. Pictures of the front side of the baffles in the experiments carried out with 25wt% (upper figures) and 50wt% solids (lower figures) for 50/50 batch (1) (left) and 50/50 batch (2) (right) latexes. Experiments carried out at 70 °C and 400 rpm for 2 h.

4.3.3.Effect of temperature

Figure 4.13 presents the effect of the temperature on wet and interfacial fouling for 50/50 batch (1) and 50/50 batch (2) latexes. Fouling was measured after 2 h at 400 rpm using 50 wt% solids content latexes. Pictures of the baffles are shown in Figure 4.14. Figure 4.13 shows that wet fouling increases with temperature, possibly due to the combination of a lower repulsion between particles (Fuchs stability factor in the denominator of Eq. 4.2) and a softer polymer that makes particles more sticky. The amount of wet fouling was higher for 50/50 batch (2) latex because of its lower value of U (Eq. 4.2).

Interfacial fouling also increased with temperature, but in this case is due to the faster water evaporation. It can be seen that the stability of the latex did not have any effect on interfacial fouling.

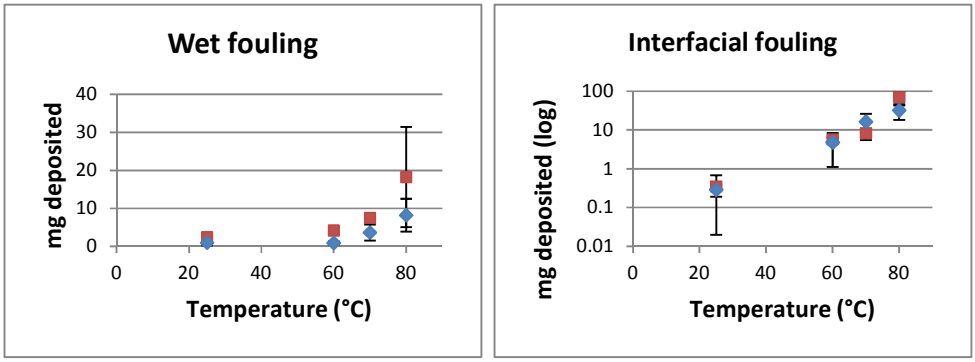

Figure 4. 13. Effect of temperature on wet and interfacial fouling for latexes 50/50 batch (1) (diamonds) and 50/50 batch (2) (squares). Experiments carried out out for 2 h at 400 rpm with 50 wt% solids content.

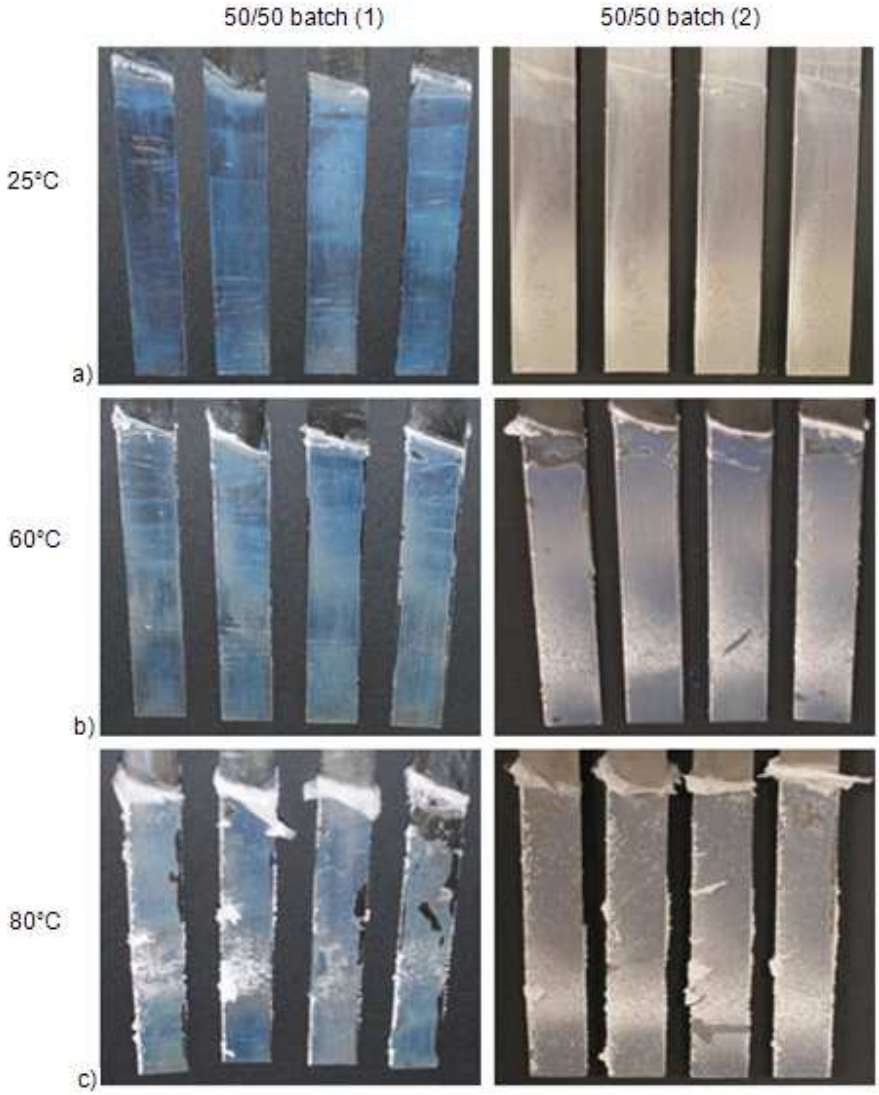

Figure 4. 14. Pictures of the front side of the baffles. a) 25°C, b) 60°C and c) 80°C. Experiments carried out for 2 h at 400 rpm using 50 wt% solids content latexes, 50/50 batch (1) (left) and 50/50 batch (2) (right).

4.3.4.Effect of the stability of the latex

Figure 4.15 presents the effect of the stability of the latex on the wet and interfacial fouling. The scale of relative stabilities presented in Chapter 3 (Figure 3.10) is used in Figure 4.15. Figure 4.16 includes the pictures of the baffles for three latexes: 90/10 batch (least stable), 50/50 MAA (intermediate stability) and 90/10 MAA (most stable). Experiments were carried out for 2 h at 70 °C and 400 rpm using 50 wt% solids content latexes. It can be seen that wet fouling decreased as stability increased due to the higher value of U in Eq. 4.2. On the other hand, scattered values of interfacial fouling were obtained for these experiments.

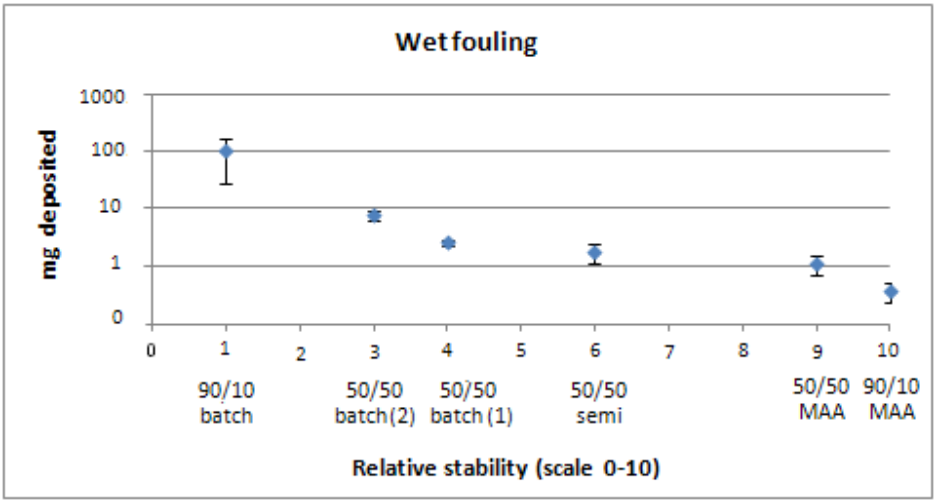

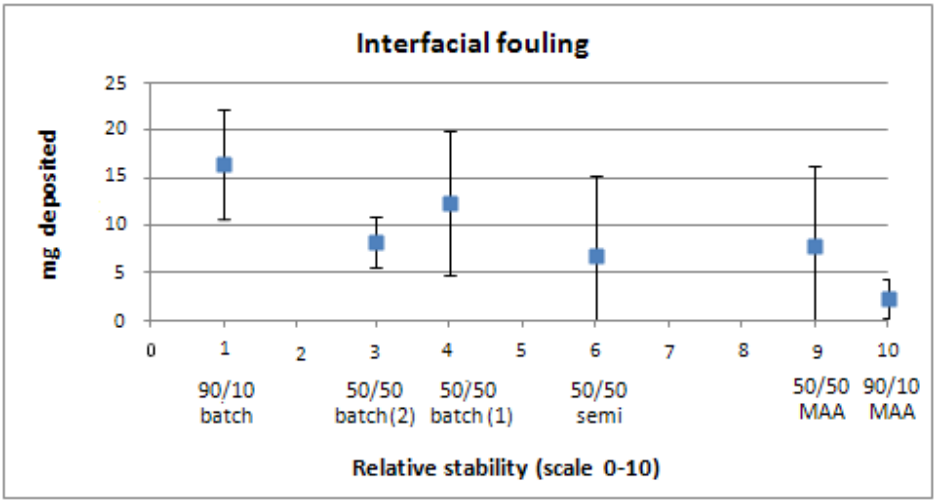

Figure 4. 15. Effect of the latex stability on wet and interfacial fouling. Experiments carried out for 2 h at 70 °C and 400 rpm using 50 wt% solids content latexes.

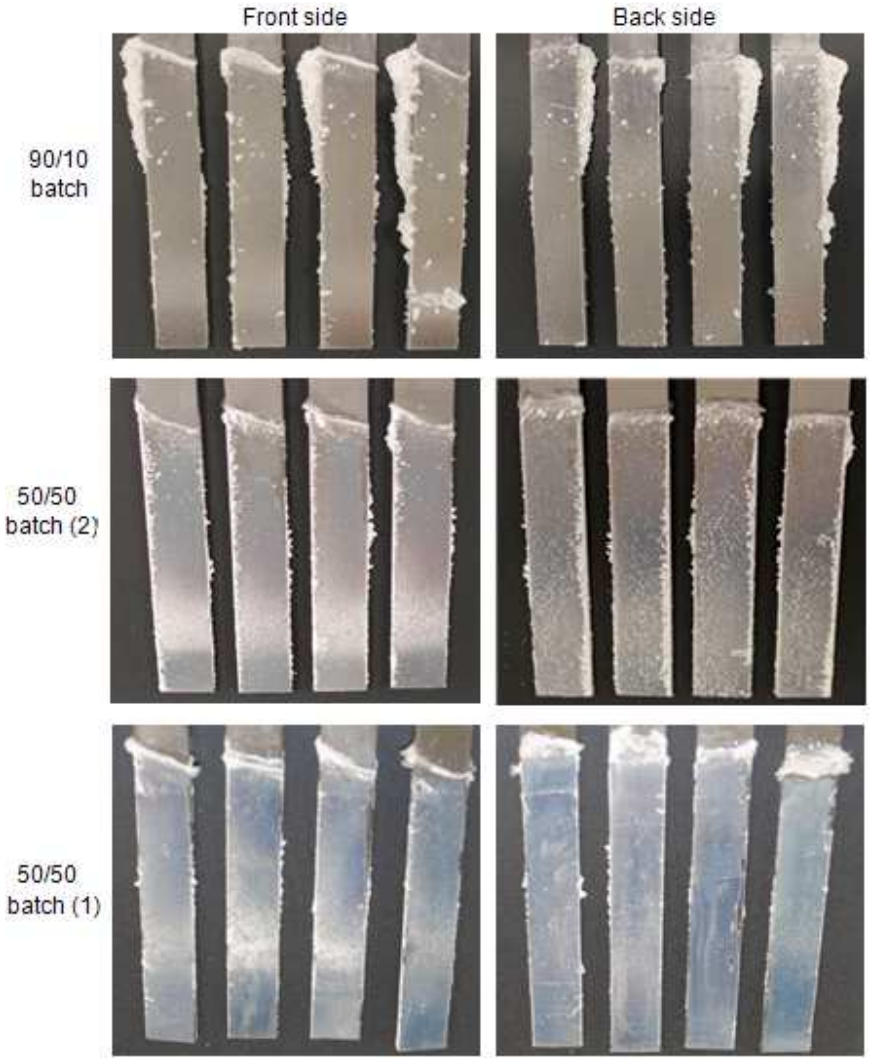
Front side
Back side
90/10
batch
50/50
batch (2)
50/50
batch (1)

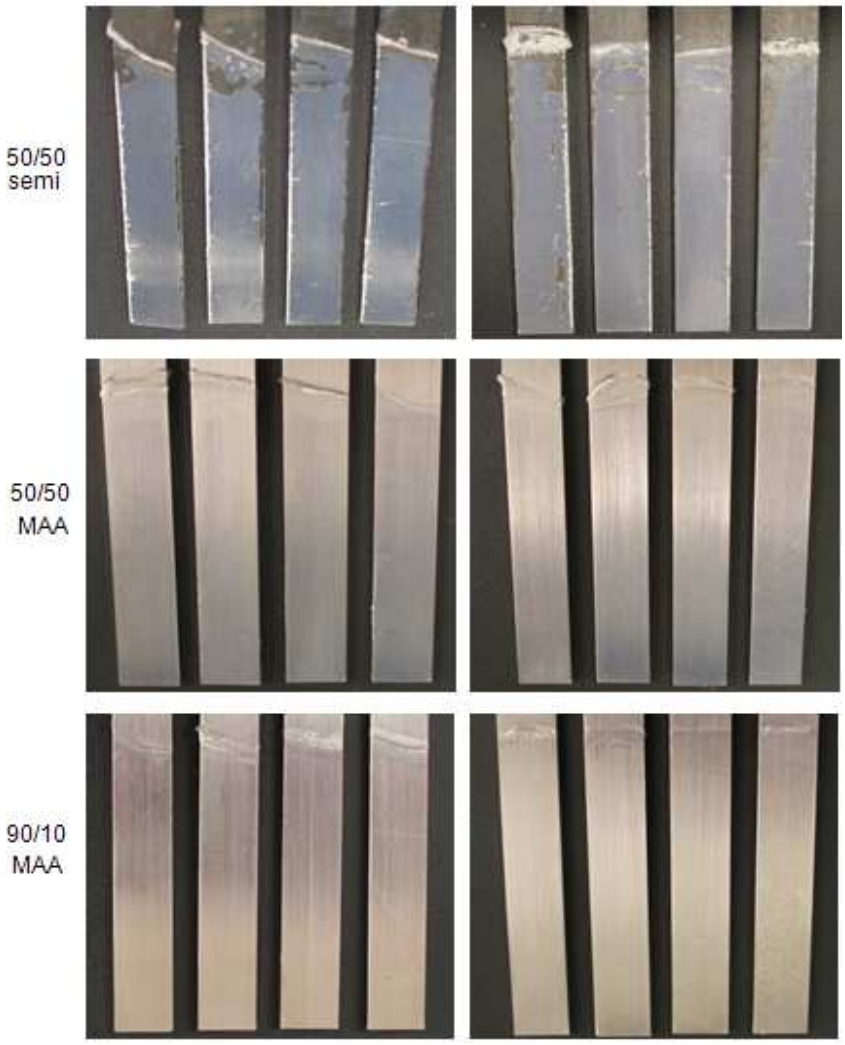

Figure 4. 16. Pictures showing the front side (left) and back side (right) of the baffles for the six latexes. Presented in order of stability being the upper one the least stable. Experiments carried out for 2 h at 70 °C and 400 rpm using 50 wt% solids content latexes.

4.3.5.Effect of the T_g of the polymer

In Section 4.3.3, it was proposed that the increase in the wet fouling with temperature might in part be due to the fact that temperature makes the polymer softer and hence more sticky. This hyphotesis is supported by some data in literature showing that polymers compositions with low T_g (e.g. adhesives) are prone to lead to fouling[11].

Unfortunately, the comparison between latexes synthesized in this work (e.g. BA/MMA 50/50 and 90/10 latexes) will not unveil the effect of the T_g because the differences in colloidal stability will hide the effect of T_g.

Therefore, in order to study the effect of the T_g, 50/50 batch (1) and 50/50 batch (2) latexes have been swollen with BA at different weight ratios (latex/BA: 96/4 and 92/8) adjusting the amounts of latex and BA to maintain a constant 50 wt% solids content. The BA monomer acts as a plasticizer decreasing the T_g of the latex particles. Table 4. 3 shows the theoretical T_gs of the mixtures. These calculations assume a value for the T_g of butyl acrylate taken as 2/3 of the crystal melting temperature and uses the Kelley-Bueche polymer/solvent equation[12]. The latexes after the addition of the corresponding amount of BA monomer, were magnetically stirred at room temperature during 30 minutes, and then, the mixtures were filtered and the coagulum recovered washed, dried and weighed. Table 4. 3 shows the data for the least stable latex (50/50 batch). It can be seen that although small amounts of coagula were measured, they can be considered negligible.

Table 4. 3. 50/50 batch latexes swollen with BA ratios, theoretical T_gs and coagula percent measured after 30 minutes of agitation. (*) Experimentally measured by DSC (it corresponds to the MMA rich polymer formed at the beginning of the polymerization).

	Theorical T_g (°C)		Coagulum %	
Latex/BA (%)	50/50 batch (1)	50/50 batch (2)	50/50 batch (1)	50/50 batch (2)
100	41 (*)	43 (*)	-	-
96/4	15	17	0.04	0.08
92/8	-7	-6	0.07	0.2

The reactor was filled with 650 g of the latex-monomer mixture (inhibitor also added to avoid possible polymerization under the experimental conditions) and it was agitated at 400 rpm and 70 °C during 2 hours. The wet and interfacial fouling obtained are compared with the values measured with 50/50 batch (1) and 50/50 batch (2) latexes (100/0) in Figure 4.17. The pictures of the front side of the baffles are given in Figure 4.18. For the most stable latex (50/50 batch(1)) an increase in fouling was observed as the polymer became softer due to the addition of BA. However, the opposite results were obtained for the 50/50 batch (2) latex. A possible reason is that the interfacial tension monomer/water is lower than that of the polymer/water[13], which will improve the stability of a poorly stabilized latex (50/50 batch (2)). The contribution of this effect to the stability of a well stabilized system (50/50 batch (1)) was not significant and in this case the effect of the T_g was apparent. Scattered data for interfacial fouling were obtained.

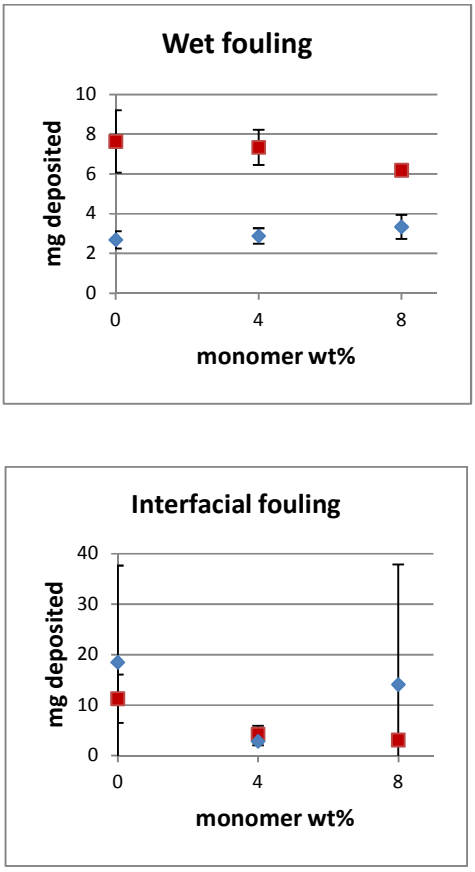

Figure 4. 17. Wet and interfacial fouling for the 50/50 batch (1) (diamonds) and 50/50 batch (2) (squares) latexes swollen with BA. 70 °C, 400 rpm, 2 h.

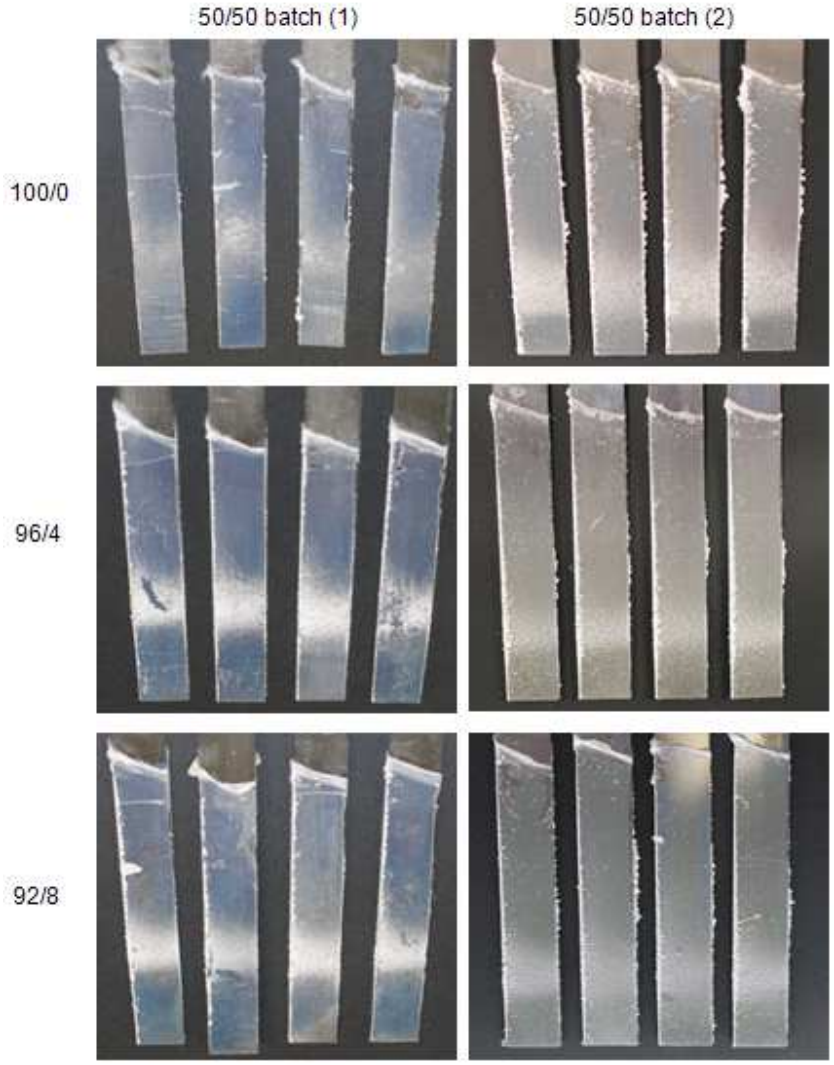

Figure 4. 18. Pictures of the front side of the baffles for the experiments with different BA concentrations. Left pictures 50/50 batch (1), right pictures 50/50 batch (2).

4.3.6.Effect of the flow patterns

The pictures of the baffles presented in the previous sections showed a very heterogeneous distribution of wet fouling in the baffles. This is further illustrated in Figure 4.19 where pictures of the front and back sides of baffles fouled with different latexes are shown. It can be seen that the wet fouling accumulated at some parts of the edges of the baffles and the front and back sides present different fouling patterns. Obviously, these differences are created by the flow patterns in the reactor. An example of the influence of the flow patterns is provided in Figure 4.20 that presents the pictures of the front (left) and back (right) sides of the baffles for a case in which the position of the agitator was moved. The arrows in the figure show the direction of the rotating flow.

a)  b) 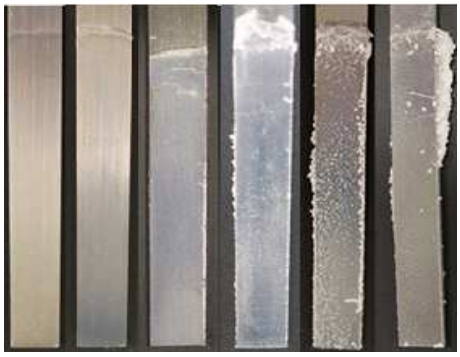

Figure 4. 19. Pictures of the front (left) and back (right) sides of baffles fouled with different latexes ordered from left to right by decreasing stability. 90/10/MAA, 50/50/MAA, 50/50 semi, 50/50 batch(2), 50/50 batch (1) and 90/10 batch.

Figure 4.20 shows that there was an accumulation of fouling in front of the agitation likely due to the radial flow created by the agitator. This accumulation did not appear in the back side of the baffles. On the other hand, there was accumulation of coagulum at the edges of the baffles, both on the edge facing the rotating flow and on the opposite edge. Interestingly, the coagulum at the edges is minimum at the height of the agitator (where the rotating velocity is expected to be maximum) and maximum in areas in which a lower rotating velocity is expected.

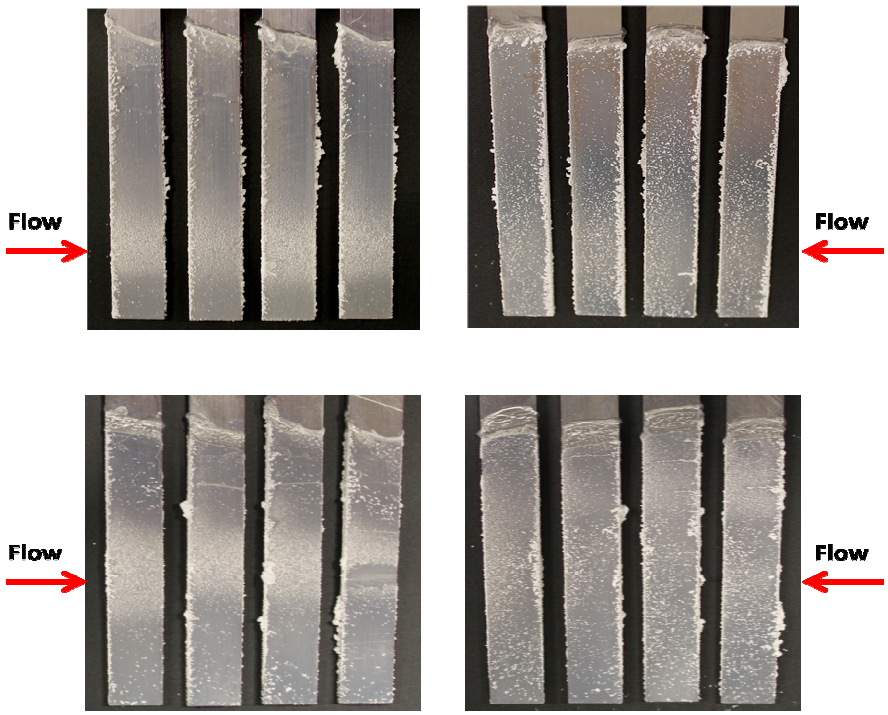

Figure 4. 20. Effect of the position of the reactor on the distribution of wet fouling in the baffles. 50/50 batch (2) latex, 2 h, 70°C, 400rpm. The arrows show the direction of the rotating flow.

Figure 4.21 shows the evolution of the wet fouling for a case in which the 50/50 batch (2) latex was used at 70 °C and 400 rpm. It can be seen that fouling appeared first in front of the agitator and at the upper part of the left edge of the baffle (the edge facing the rotating flow). Later, fouling appeared at the right edge, the amount of fouling on the left edge increased and the amount of fouling in front of the agitator seems to be rather constant. Almost no fouling was observed on the edges at the height of the agitator.

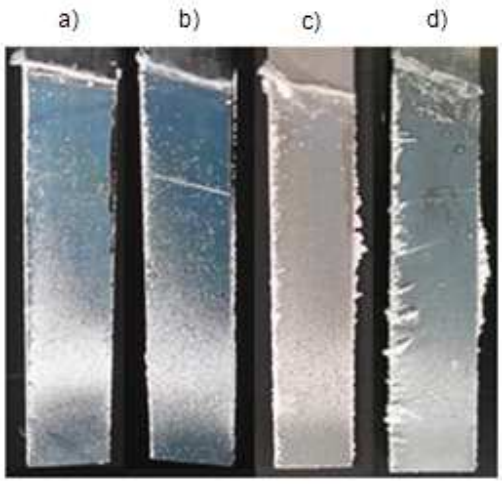

Figure 4. 21. Evolution of the wet fouling in the front side of the baffles for a 50/50 batch (2) latex at 70 °C and 400 rppm. The direction of the flow is from left to right. a) 30 min; b) 1 h; c) 2 h and d) 4 h.

In order to shed some light on these results, the flow patterns in the reactor were calculated using computational fluids dynamics (CFD). These calculations were carried out in collaboration with Dr. Alberto Peña (Nuclear Engineering and Fluid Mechanics Department, University of the Basque Country) using a STAR-CCM+ code. It was assumed that the Reynolds number was in the turbulent regime because the Navier-Stokes equations of motion converged more rapidly and this accelerate the calculations. For the same reason, a Newtonian fluid was considered.

Figure 4.22 presents the velocity distribution at different heights of the reactor referred to the position of the agitator. The figure for the height of the agitator (0 cm) shows that the maximum velocity is at the tip of outer blades of the agitator. These high velocity fronts impact the left edge of the baffles and then sweep the face which is in front of the agitator. On the right edge of the baffle, eddies are formed. Figure 4.22 shows that the velocities strongly decreased with the distance from the agitator height, although the flow patterns are similar. The decrease was more pronounced below than above of the agitator,due to the combined effect of the position of the agitator (placed closer to the bottom of the reactor than to the air-latex interface) and its geometry (the inner blades push the fluid downwards whereas the outer ones push the fluid upwards).

Combination of the information of the flow patterns provided by CFD calculations and the pictures of the wet fouling attached to the baffles allows making a hypothesis for the mechanisms of fouling formation. Just after the baffles are put in contact with the latex, the positively charged surface of the stainless steel is covered by negatively charged polymer particles by means of a perikinetic mechanism. From this moment on, the surface of the baffles

is negatively charged and a repulsive electrostatic potential between the baffle and the particles appears. Orthokinetic (shear induced) fouling starts in the areas of the baffles where the flow hits stronger, in particular in the front of the baffles at the height of the agitator and in the left edge of the baffles. In these zones, the energy provided by the flow is able to overcome the electrostatic repulsion. Fouling also occurs in other parts of the baffles at rates that depend on the energy of the fluid in these areas. The amount of fouling increases with time forming bigger clusters. Those of these clusters that are in regions where the fluid velocity is high, are subjected to a force that can remove them from the surface of the baffles. This process is illustrated in Figure 4.23. The result of this process is that the amount of coagulum is limited and reaches an asymptotic value in zones where the fluid velocity is high (e.g. in the front side and in the left edge of the baffles at the height of the agitator). On the other hand, in areas where the fluid velocity is moderate or low, big aggregates can survive and this leads to the formation of large clumps of polymer that can be observed at the upper part of the edges of the baffles.

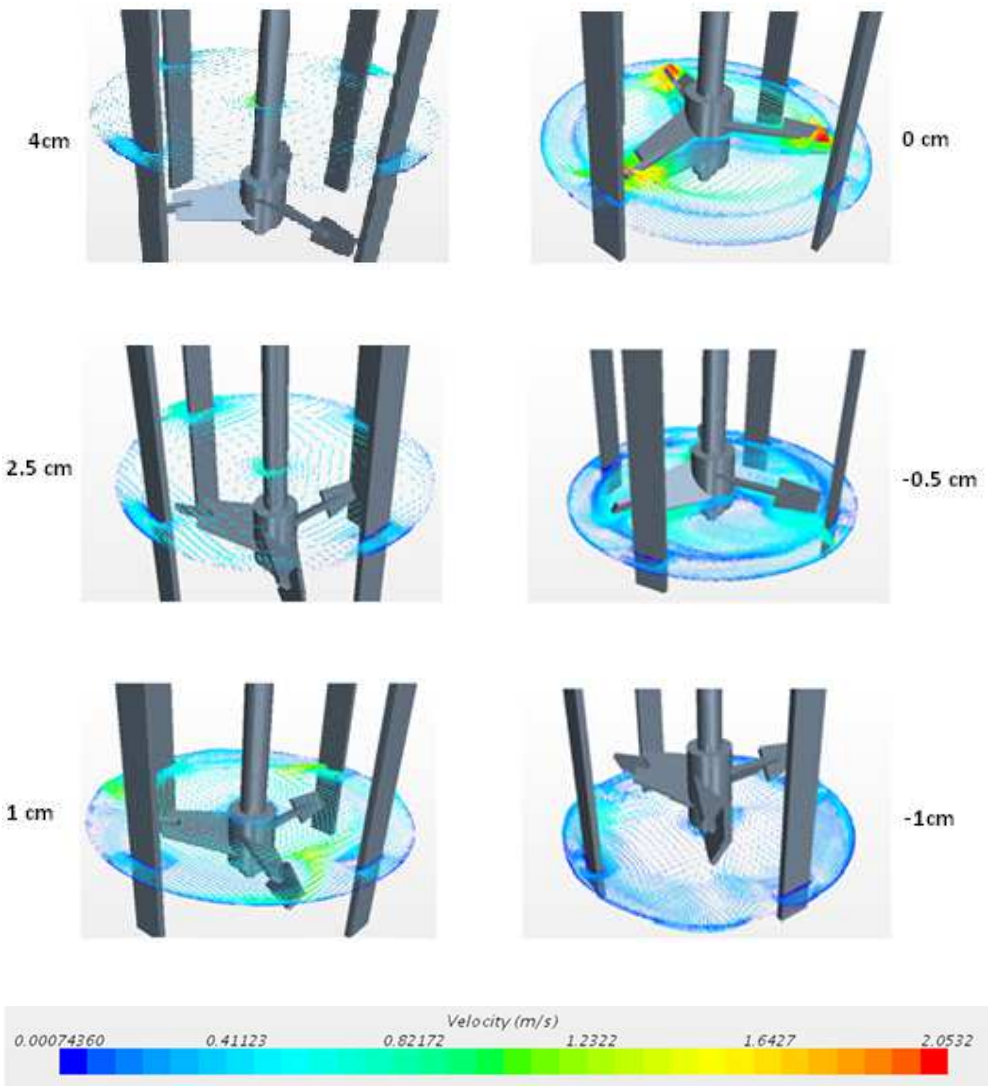

Figure 4. 22. Distributions of velocity at different height in the reactor referred to the position of the agitator calculated by CFD. Colors represent velocities and the arrows indicate direction of the flow in the horizontal plane.

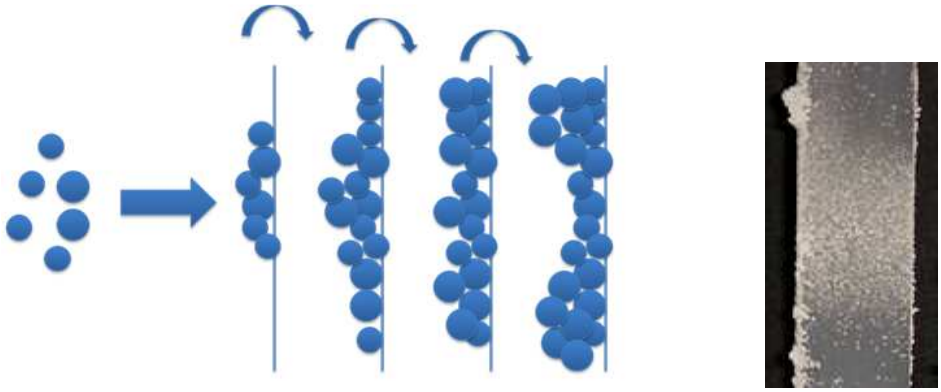

Figure 4. 23. Illustration of the mechanism for perikinetic fouling formation.

It is interesting that relatively large aggregates of fouling were formed at the right edges of the baffles, slightly above the agitator. In the right edges of the baffles, vortices are formed[14]. The energy of the vortices increases with the velocity of the fluid because for a smooth flat plate parallel to the stream the drag is proportional to the velocity of the fluid. Therefore, at the level of the agitator, the energy of the vortices may be too high and hence, the aggregates are removed. Slightly above the agitator, the vortices have enough energy to cause attachment of the polymer particles to the (fouled) baffle edge, but their energy was not enough to remove the aggregates. Above a certain height, the vortices do not have enough energy to form fouling and the left edges are relatively free of fouling.

The results discussed above were obtained with an Ekato MIG agitator, which generated characteristic flow patterns that in turn lead to formation of fouling in specific places.

The distribution of fouling will be different if another agitator is used. Figure 4.24 illustrates this point by comparing the fouling obtained with the Ekato MIG agitator with one obtained with a turbine impeller for the 50/50 batch (2) latex.

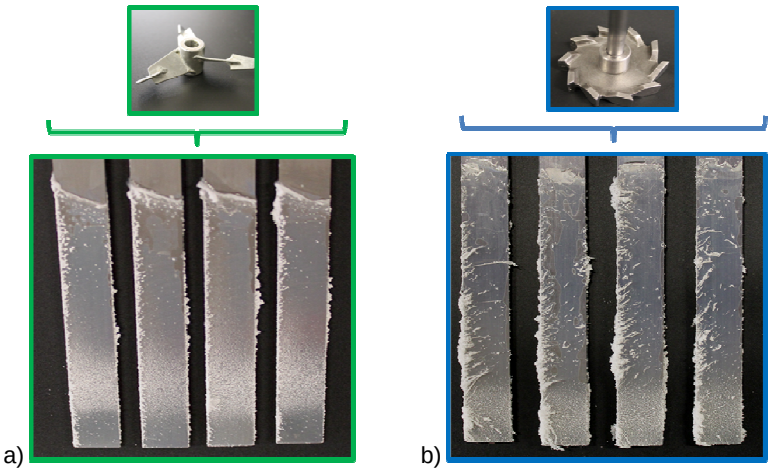

Figure 4. 24. Effect of the agitator type on the distribution of fouling. 2 h, 70 °C, 400 rpm. 50/50 batch (2) latex.

4.4. Conclusions

In this chapter, fouling under orhokinetic conditions, namely with agitation, was investigated. According to theory, fouling is proportional to the local shear rate and to the solids content and inversely proportional to the Fuchs stability factor.

For practical convenience, fouling was measured on 316 stainless steel baffles. 1L reactor equipped with an Ekato MIG agitator was used. Latexes with different colloidal stability were used in the study. Two types of fouling could be distinguished. Fouling formed at the air-latex interface due to continuous wetting-drying processes (interfacial fouling) and fouling formed in the areas that are always submerged in the latex (wet fouling). Because wet fouling is the most significant in large scale reactors, the study was centered in this type of fouling. Surface coagulation was observed for agitation rates up to 300 rpm. On the other hand, at 500 rpm a substantial amount of foam was formed. Therefore, the study was carried out at 400 rpm.

It was found that the amount of wet fouling increased with time, solids content and temperature, and it decreased as the colloidal stability of the latex increased. For the most stable latexes, fouling increased as the T_g of the polymer decreased. The flow patterns in the reactor determined the distribution of fouling in the baffles. Combination of computational fluid dynamics and experimental results showed that the observed fouling was the result of the interplay between attachment of polymer particles and removal of the polymer aggregates. In general, the bigger aggregates accumulated in areas where the flow rate was low.

4.5. References

(1) von Smoluchowski, M. Versuch Eine Mathematischen Theorie Der Koagulationskinetik Kolloidaler Losungen. *Z. Phys. Chem* **1917**, *92*, 129–168.

(2) Heller, W.; Peters, J. Mechanical and Surface Coagulation: I. Surface Coagulation of α-FeOOH Sols. *J. Colloid Interface Sci.* **1970**, *32* (4), 592–605.

(3) Peters, J. and Heller, W. Mechanical and Surface Coagulation II. Coagulation by Stirring of α-FeOOH-Sols. *J. Colloid Interface Sci.* **1970**, *33* (4), 578–585.

(4) Heller, W.; De Lauder, W. Mechanical and Surface Coagulation III. Promotion of Mechanical Coagulation by Addition of Destabilizing Electrolyte. *J. Colloid Interface Sci.* **1970**, *35* (1), 60–65.

(5) Heller, W.; Peters, J. Mechanical and SurFace Coagulation IV. Prevention of Mechanical Coagulation by Surface-Active Additives. *J. Colloid Interface Sci.* **1970**, *35* (2), 300–307.

(6) De Lauder, W. B. and Heller, W. Mechanical and Surface Coagulation V. The Role of the Solid-Liquid Interface and of Turbulence in Mechanical Coagulation. *J. Colloid Interface Sci.* **1971**, *35* (2), 308–313.

(7) Diop, S.; Heller, W.; Kalousdian, S. Mechanical and Surface Coagulation: VI. Differential Surface Coagulation in Two-Component Colloidal Solutions. *J. Colloid Interface Sci.* **1979**, *70* (2), 328–337.

(8) Williams, D. F.; Berg, J. C. The Aggregation of Colloidal Particles at the Air-Water Interface. *J. Colloid Interface Sci.* **1992**, *152*, 218–229.

(9) Chen, W.; Tan, S.; Huang, Z.; Ng, T.-K.; Ford, W. T.; Tong, P. Measured Long-Ranged Attractive Interaction between Charged Polystyrene Latex Spheres at a Water-Air Interface. *Phys. Rev. E* **2006**, *74* (2), 021406.

(10) Rushton, J. H.; Costich, E. W.; Everett, H. J. Power Characteristics of Mixing Impellers. I. *Chem. Eng. Prog* **1950**, *46*, 395–404.

(11) Slot, V. Der; Nabuurs, T.; Overbeek, G. C. US20080249242 A1 Aqueous Vinyl Graft Copolymer Compositions, 2008.

(12) López García, I.; Keddie, J. L.; Sferrazza, M. Some Insights into the Structural Relaxation of Spin-Cast, Glassy Polymer Thin Films. *Polym. J.* **2010**, *43* (2), 214–217.

(13) Dong, Y.; Sundberg, D. C. Estimation of Polymer/water Interfacial Tensions: Hydrophobic Homopolymer/water Interfaces. *J. Colloid Interface Sci.* **2003**, *258* (1), 97–101.

(14) Matsumoto, M. Vortex Shedding of Bluff Bodies: A Review. *J. Fluids Struct.* **1999**, *13*, 791–811.

Chapter 5. Particulate fouling under polymerization conditions

5.1. Introduction

Emulsion polymerization is a complex multiphase process involving nucleation and growth of colloidal polymer particles. The stability of these particles depends on the ratio surfactant amount/ surface area of the particles and on the availability of the surfactant which in turn depends on the interplay between adsorption, desorption and diffusion rates of the surfactant[1] to stabilize the area of the particles that is created by nucleation and growth.

The results in the previous chapters obtained using model systems show that fouling increases as latex stability decreases. Therefore, any event that reduces the colloidal stability of the latex will lead to higher fouling. Those skilled in the art know that some situations are prone to reduce stability of the latex. Some of these situations are:

i) adding all the surfactant at the beginning of the semicontinuous process. This will lead to the nucleation of many small polymer particles that upon growth will tremendously increase their surface area becoming unstable as the surfactant coverage decreases.

ii) Extensive secondary nucleation, mainly when using surfactants that do not desorb rapid enough from the existing particles, e.g. non-ionic surfactants[1] or solid particles in Pickering stabilized systems[2].

iii) Using surfmers that are too reactive in semicontinuous processes, because the early incorporation of the surfmer to the polymer leads to surfmer burying[3,4].

iv) Local increase of the ionic strenght by feeding initiator and/or buffer in a poorly agitated region.

v) Inhibitions leading to monomer accumulation in the reactor. This can cause thermal runaways that reduce the stability of the system (e.g. exceeding the cloud point of the non-ionic surfactant). Bulk polymerization of the monomer layer also leads to fouling.

The cases discussed above indicate that uncontrolled nucleation can promote fouling. Nucleation is the less controlled aspect of emulsion polymerization and in practice is avoided by using seeded emulsion polymerizations. This line is followed in this chapter, where seeded emulsion polymerizations are carried out. Local increase of the ionic strength at the

initiator/buffer feeding point and thermal runaways are avoided by using a well agitated lab scale reactor.

Therefore, in this chapter, latex 50/50 batch (1) described in Chapter 3 (Table 3.1) was used as seed. The reason of using this latex was that it was the relatively stable and hence the effect of the variables studied on fouling will be not masked by an intrinsic high fouling. First, the capability of the monomer swollen seeds to create fouling was studied. This was somehow indirectly studied in Section 4.3.5 when in order to vary the T_g of the polymer a small amount of butyl acrylate was added. Here, a BA/MMA monomer mixture was used and higher amounts of monomers in the polymer particles were used. In the second part of the chapter, the effect of the polymerization is investigated.

5.2. Experimental part

The amount of monomer was limited not to exceed the maximum swelling of the particles. In this way, polymerization in droplets and in monomer layers is avoided. The maximum swelling for BA in poly(BA) particles is 0.65 (monomer/ (monomer+polymer) vol/vol) and 0.73 for MMA in polymer particles[5]. In this chapter, a 50/50 wt/wt mixture of BA and MMA was used to swell BA/MMA copolymer particles. Therefore, these values are only indicative. The polymer/monomer weight ratio was limited to 60/40.

Different amounts of the 50/50 batch (1) latex were swollen with a mixture of BA/MMA (50/50 wt/wt) so that the total content of the organic phase was 50 wt %. 650 g of the monomer swollen latexes were placed in the reactor and agitated for 2 h at 400 rpm and 70 °C. Although technical monomers that contained some inhibitor were used, in the first part of the chapter, inhibitor (hydroquinone) was added to avoid any polymerization. In the second part, no inhibitor was added and KPS was fed as a shot. Also polymerizations initiated with the residual initiator from the synthesis of the 50/50 batch (1) latex were carried out. The fouling was measured on baffles as described in Chapters 3 and 4.

5.3. Results and discussion

5.3.1.Particulate fouling with monomer swollen latex

Figure 5.1 shows the effect of the monomer content on wet and interfacial fouling. In this plot, the data obtained in Chapter 4 for 2 and 4 wt% of BA were also included. It can be seen that the wet fouling increased with monomer concentration up to 20 wt%, and then it seemed to remain constant. However, the dispersion of the data for 40 wt% of monomer makes uncertain this value.

Figure 5.2 presents the pictures of the front (left) and back (right) sides of the baffles for monomer contents ranging from 0 to 40 wt%. It can be seen that the distribution of fouling followed a similar patterns for monomer contents up to 20 wt%, but for 40 wt% of monomer, the fouling patterns were less heterogeneously distributed. In particular, no accumulation of fouling

in the left edge and at the height of the agitator (front side of the baffle) was observed. It looks like, the particles were that soft that any contact resulted in adhesion. In addition the variability of the observations for 40 wt% of monomer may be due to removal of large aggregates from the baffles.

Fortunately, the range 0-20 wt% is the most significant because at industrial scale, most of the semicontinuous emulsion polymerizations are carried out at this range of monomer concentrations. The increase of the wet fouling when the monomer concentration may be in part due to the decrease in the T_g of the monomer swollen polymer and in part due to the lower coverage of the monomer swollen particles by the surfactant. This last effect resulted from the fact that the only surfactant in the system was that of the seed, and as increasing the monomer content, the surface area of the particles increased, and consequently the surfactant coverage decreased. Taking the seed as a reference, the surfactant coverage of the monomer swollen particles is proportional to (1-monomer content)$^{2/3}$. Figure 5.3 shows that in the range of 0-20 wt% of monomer, the relative coverage decreased almost linearly with the monomer content. However, this does not mean that this linearity was related to the almost linear increase in wet fouling (Figure 5.1) because for ionic surfactants the relationship between surface coverage and surface potential is the highly non linear Grahame equation[6] (Eq. 1.3) which predicts that coverage should decrease substantially in order to significantly decrease the surface potential.

$$\sigma_0 = (8 n_0 \varepsilon k_B T)^{1/2} \sinh\left(\frac{z e \Psi_0}{2 k_B T}\right) \qquad (1.3)$$

where σ_0 is the surface charge density, $\Psi_0$the surface potential of the particle *e* and ε are the electron charge and permittivity of the liquid phase; *z* and *n* is the valency and bulk concentration of counter-ions; k_B is the Boltzmann constant, and *T* the absolute temperature.

Figure 5.1 also shows that although with some dispersity in the data, the interfacial fouling seemed to decrease with the monomer content. As the interfacial fouling was due to repeated wetting and drying of the area of the baffles that was near the air-latex interface, a possible reason for this observation is that the presence of monomer in the aqueous phase reduced the rate of evaporation of water allowing rewetting before a solid film was formed.

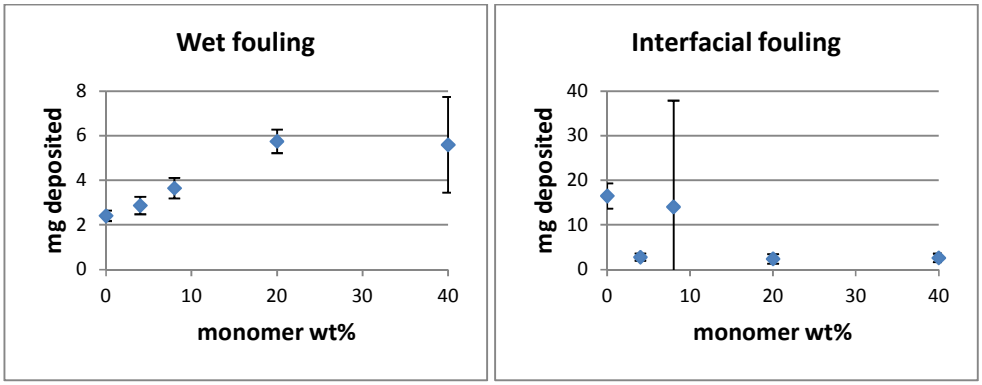

Figure 5. 1. Average values of the wet and interfacial fouling of the four baffles for the different polymer/monomer ratios tested during this work.


a)
b)
c)

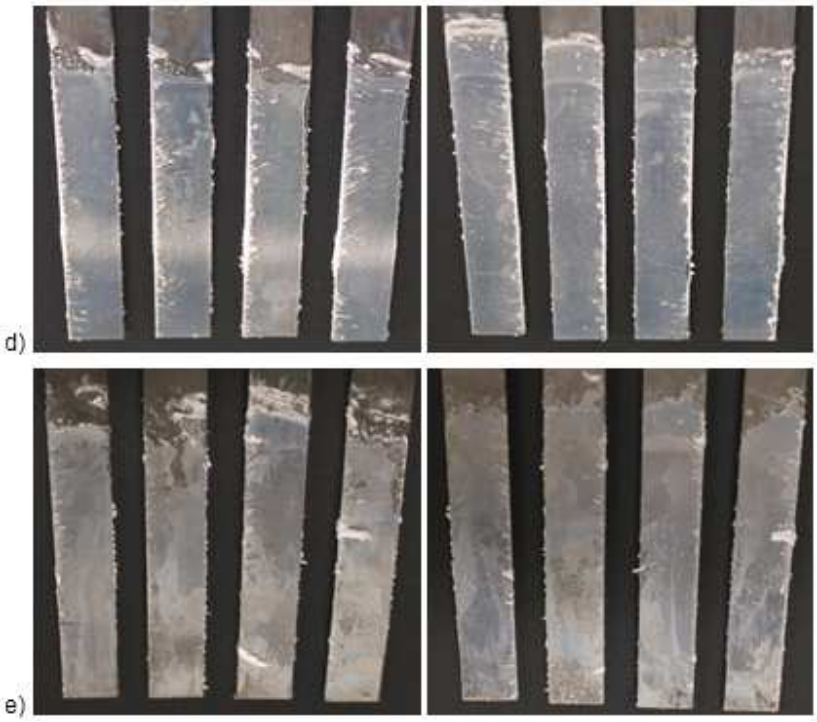

Figure 5. 2. Pictures of the front (left) and back (right pictures) side of the fouled substrates agitated at 400 rpm at 70 °C during 2 hours, corresponding to a) 100/0, b) 96/4, c) 92/8, d) 80/20 and e) 60/40 polymer/monomer ratios.

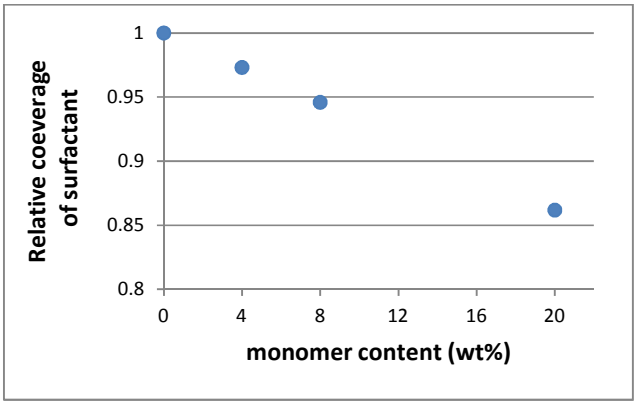

Figure 5. 3. Effect of the monomer content of the swollen particles on the relative surfactant coverage.

5.3.2.Particulate fouling in seeded batch polymerization

Monomer swollen 50/50 batch (1) latex particles were polymerized in batch using potassium persulfate (KPS) as initiator (0.5% weight based on monomers). 96/4, 80/20 and 60/40 polymer /monomer weight ratios were used. The baffles were placed in the reactor which was filled with 650 g of the monomer swollen latex (50 wt% solids), and heated to 70 °C under agitation (400 rpm) and nitrogen purging. Then, the aqueous solution of KPS initiator (KPS was dissolved in 3 grams of deionized water) was added as a shot and the nitrogen tube removed from the dispersion. The system was allowed to react in batch for 2 hours. The reactor was cooled to 25 °C before removing the baffles to measure fouling by gravimetry. The final particle size and coagulum content were measured. The conversion of the monomer(s) was measured

gravimetrically finding that an almost complete conversion was achieved at the end of the process. The final particle size matched with the targeted theoretical values after polymerization. In none of the cases, particle coagulation and/or secondary nucleation were observed.

Figure 5.4 compares the wet fouling measured after the polymerization with that observed in the absence of reaction. It can be seen that for monomer contents of 20 and 40 wt %, fouling tremendously increased during polymerization. This can be observed in the pictures of Figure 5. 5.

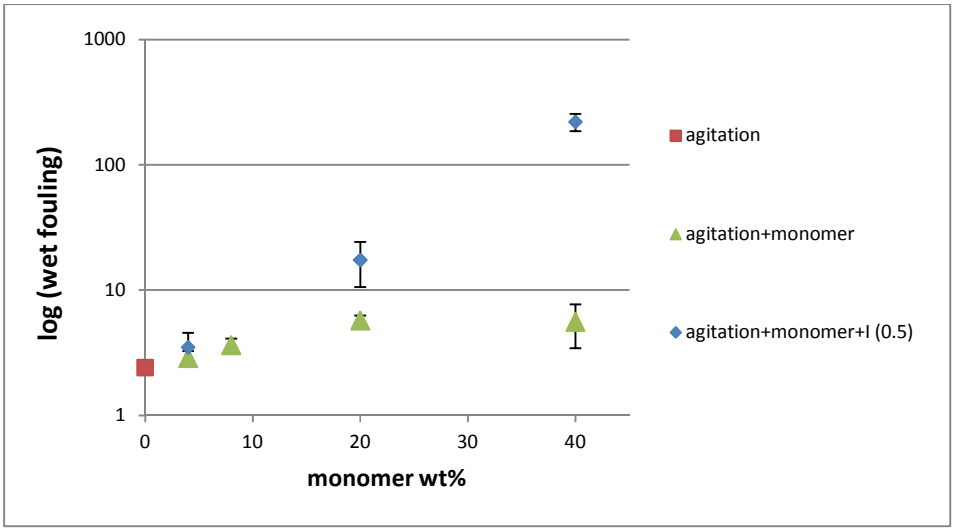

Figure 5. 4. Comparison of the wet fouling measured after polymerization (agitation+monomer+I 0.5 wt%) with that observed without reaction (agitation+monomer).

Figure 5. 5. Fouled substrates for the 96/4, 80/20 and 60/40 ratios under reaction by the addition of 0.5 wt% monomer based KPS.

A possible reason for the fouling increase is that the ionic strength increased when KPS was added. As the amount of KPS added was proportional to the monomer content, the ionic strength also increased with the monomer content, which may explain that the relative effect increased with the monomer content.

In order to shed light on this point, the swollen latex containing 40 wt% of monomer was polymerized with smaller concentrations of KPS. Figure 5.6 shows that the amount of wet fouling slightly decreased when the initiator concentration was reduced from 0.5 wt% to 0.125 wt%, but the effect was very small. The dispersion of the data was due to the random removal of big aggregates from the baffles (Figure 5.7).

The experiment with 20 wt% monomer in Figure 5.4 and the experiment carried out with 0.25 wt% of initiator in Figure 5. 6 were carried out with the same concentration of initiator, but different monomer content. It can be seen that increasing the monomer content from 20 to 40 wt% led to a sevenfold increase in fouling. This suggests that the effect of the monomer content is stronger under reaction conditions.

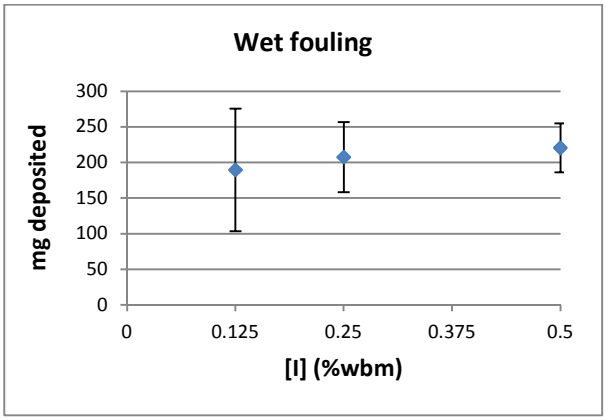

Figure 5. 6. Effect of the KPS concentration on wet fouling for a 40 wt% monomer content.

a) 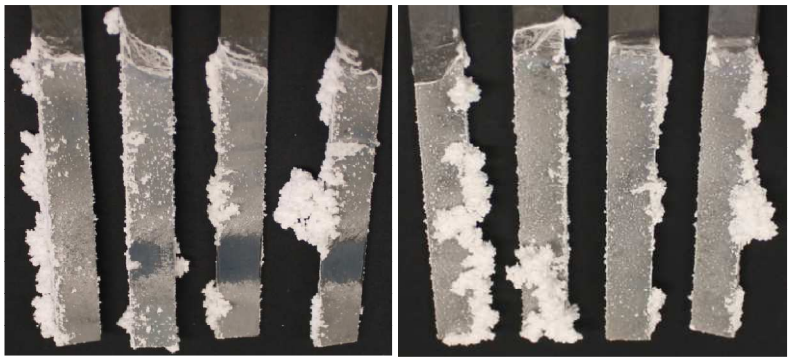

b)

c)

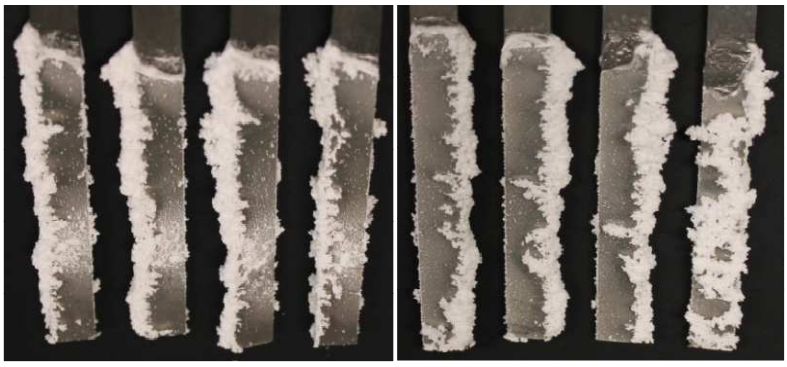

Figure 5. 7. Pictures of the front and back side of the baffles at the end of the polymerization carried out with the 60/40 latex and different concentration of KPS. a) 0.125 %wbm; b) 0.25 %wbm and c) 0.5 %wbm.

In order to investigate the effect of the ionic strength, NaCl was added to the 60/40 latex to reach the same ionic strength than for the case in which 0.125 wt% of KPS was used. Hydroquinone was added to avoid polymerization. Figure 5.8 compares the wet fouling observed in this experiment with those measured in the absence of salt and after

polymerization. It can be seen that the increase in ionic strength caused by adding NaCl led to a severe increase of wet fouling. On the other hand, an even higher relative increase of fouling was provoked by polymerization. Figure 5.9 compares the pictures of the baffles for these experiments.

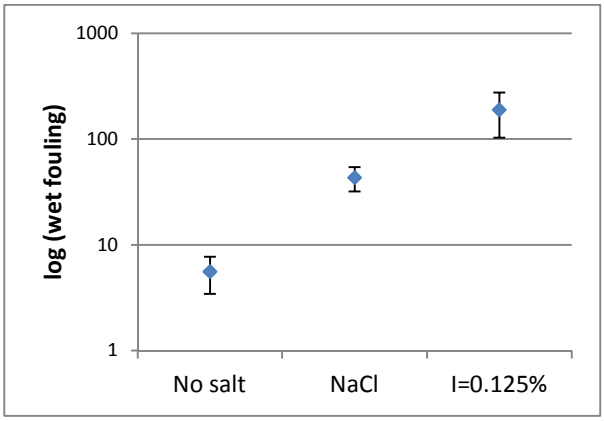

Figure 5. 8. Wet fouling measured with the 60/40 latex,upon adding NaCl and after polymerization with 0.125 % of KPS.

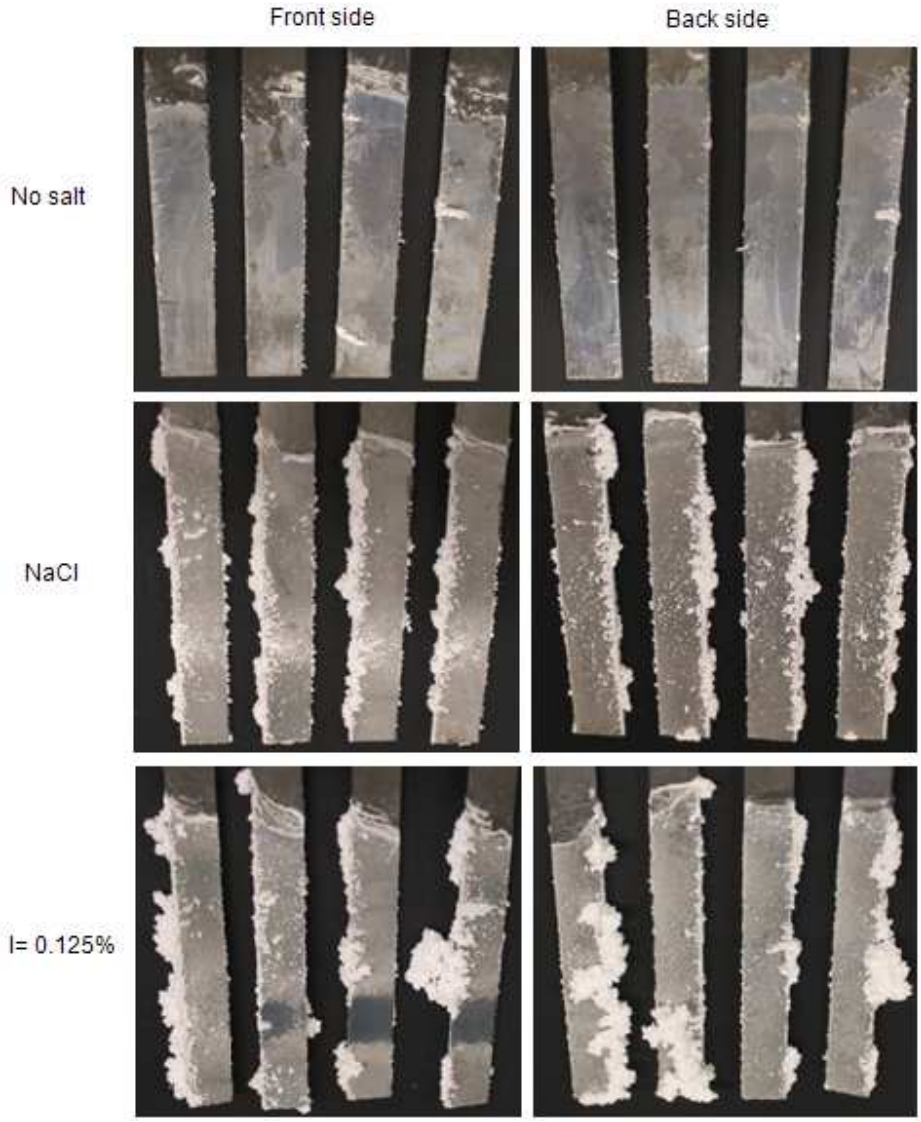

Figure 5. 9. Pictures of the baffles for the 60/40 latex,upon adding NaCl and after polymerization with 0.125 % of KPS.

The results presented above show that during polymerization fouling increased due to both the increase of the ionic strength and the polymerization process itself. In addition, it seems that the effect of the polymerization was higher. In order to further assess the effect of the polymerization, the 50/50 batch (1) latex was swollen with monomer and polymerized using the residual initiator contained in the latex. Figure 5.10 compares the effect of polymerization on wet fouling for 20 and 40 wt% of monomer. It can be seen that the effect was modest for 20 wt% of monomer and stronger for 40 wt%. However, comparison with the wet fouling measured when initiator was added shows that the increase of the fouling provoked by polymerization using a small radical generation rate is relatively modest. The pictures of the baffles are shown in Figure 5.11.

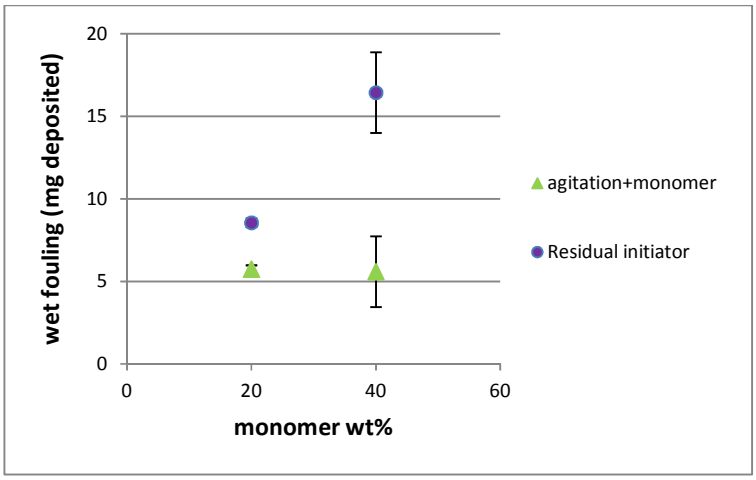

Figure 5. 10. Effect of the polymerization initiated by the residual initiator on the wet fouling.

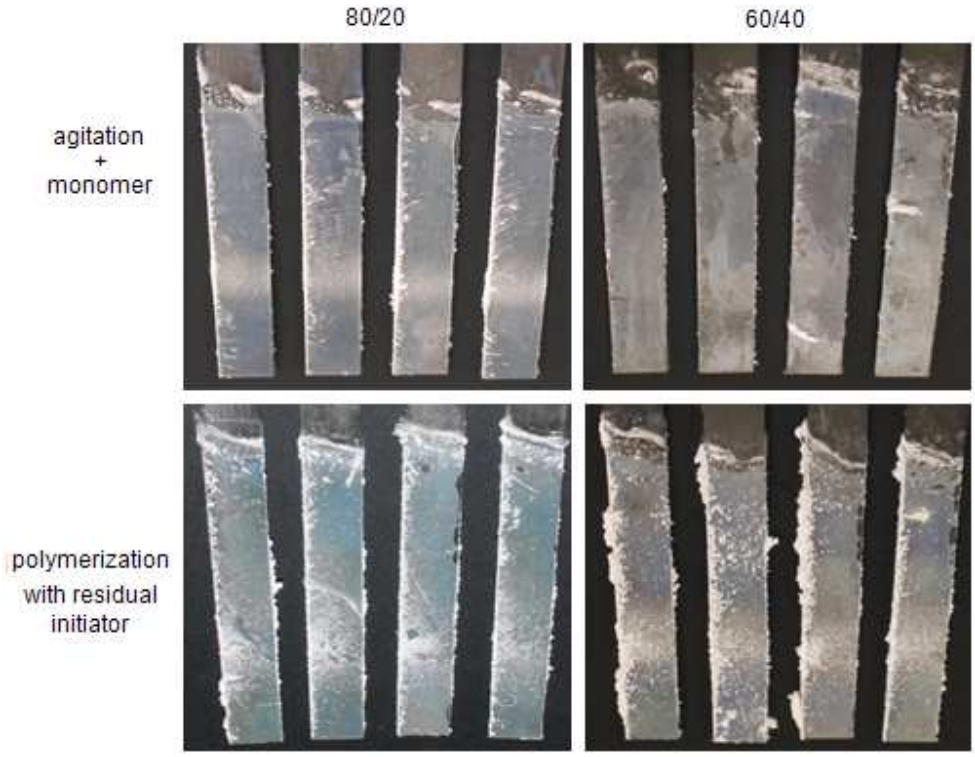

Figure 5. 11. Pictures of the front side of the baffles under agitation without polymerization and after polymerization initiated with the residual initiator.

The increase in fouling observed in the batch seeded polymerizations may be due to the adsorption of the surface active polymer formed in the aqueous phase on the surface of the baffles, followed by absorption of monomer on the polymer film formed and polymerization of this monomer upon arrival of radicals. However, it is difficult to justify with this mechanism the tremendous increase of the amount of fouling for the systems with 20 and 40 wt% of monomer.

A more likely reason is that the secondary nucleation occurred in these experiments. There were several factors that facilitate the occurrence of secondary nucleation: i) a water soluble initiator (KPS) that produces charged inorganic radicals was used; ii) relatively high concentrations of a relatively soluble monomer (MMA) were employed, and iii) the number of seed particles decreased as the monomer concentration increased because the total solids content was kept constant.

The first two factors promote polymerization in the aqueous phase and the third one reduces the capture of radicals by the polymer particles. Under these circumstances, formation of particles by homogeneous nucleation is likely. The newly formed particles suffer a fast increase in surface area (the relative increase in surface area is higher for small particles) and require surfactant to become stable. However, the only surfactant available is in the seed particles and its total amount decreases with the monomer concentration, namely, when it is more needed. The result is that the system becomes unstable and a high amount of fouling is formed.

This mechanism explains the strong increase in fouling observed when the amount of monomer increased, the modest effect of the polymerization when only the residual initiator was used to generate radicals and the slight effect of the initiator concentration for the 40 wt% monomer content.

However, it has to be pointed out that no macroscopic coagulum was observed upon filtering the latex and that the final particle size as measured by DLS agreed quite well with the theoretical one calculated assuming a constant number of particles (Table 5.1). It may be

argued that small particles are difficult to detect by DLS and that only a small fraction of the total polymer was deposit in the baffles, and hence it had almost no effect on the macroscopic measurements, but without further proof, the mechanism outlined above remains a hypothesis.

Particle size distributions were measured by Capillary Hydrodynamic Fractionation chromatography technique (CHDF) for the final latex samples, but the sizes obtained were quite big, likely due to coagulation of the particles as some time elapsed before the measurements.

Table 5. 1. Theoretical and experimental particle sizes measured by DLS in the seeded emulsion polymerizations carried out using 0.5% of KPS.

	dp (nm)	
Monomer	Theoretical	Measured
20%	178	175
40%	196	196

5.4. Conclusions

In this chapter, the effect of the polymerization on fouling formation was studied. In order to decouple the effects of the presence of monomer and that of the polymerization itself, first the formation of fouling in latexes containing a high amount of inhibited monomer (no monomer droplets were present) was investigated. It was found that fouling increased with the amount of monomer due to the combined effect of a decrease of the T_g of the monomer-polymer system and to the lower surfactant coverage that resulted from the addition of monomer to the seed.

In the second part, fouling during batch seeded emulsion polymerization was studied. It was found that polymerization caused a strong increase in wet fouling and this effect increased as the amount of monomer of the system increased. For the highest concentration of monomer used (40 wt%, which was the most unfavorable condition used) it was found that the amount of fouling was very mildly affected by the initiator concentration in the range of 0.125-0.5 wt% (based on monomer). On the other hand, experiments carried out with the same ionic strength in the absence and presence of initiator showed that most of the increase in fouling was due to the initiator. This effect was attributed to the formation of new particles by homogeneous nucleation.

5.5. References

(1) Ballard, N.; Urrutia, J.; Eizagirre, S.; Schäfer, T.; Diaconu, G.; de la Cal, J. C.; Asua, J. M. Surfactant Kinetics and Their Importance in Nucleation Events in (mini)emulsion Polymerization Revealed by Quartz Crystal Microbalance with Dissipation Monitoring. *Langmuir* **2014**, *30*, 9053–9062.

(2) González-Matheus, K.; Leal, G. P.; Tollan, C.; Asua, J. M. High Solids Pickering Miniemulsion Polymerization. *Polymer (Guildf).* **2013**, *54* (23), 6314–6320.

(3) Schoonbrood, H. A. S.; Asua, J. M. Reactive Surfactants in Heterophase Polymerization. 9. Optimum Surfmer Behavior in Emulsion Polymerization. *Macromolecules* **1997**, *30* (20), 6034–6041.

(4) Asua, J. M.; Schoonbrood, H. A. S. Reactive Surfactants in Heterophase Polymerization. *Acta Polym.* **1998**, *49* (12), 671–686.

(5) Gardon, J. L. Emulsion Polymerization. II. Review of Experimental Data in the Context of the Revised Smith-Ewart Theory. *J. Polym. Sci. Part A-1* **1968**, *6*, 643–664.

(6) Grahame, D. C. The Electrical Double Layer and the Theory of Electrocapillarity. *Chem. Rev.* **1947**, *41*, 441–501.

Chapter 6. Conclusions

Emulsion polymerization latexes are thermodynamically unstable and kinetic stability is provided by the use of surfactants. Since the use of surfactant is detrimental for the final latex application, the amount of surfactant used in the industry is limited. Therefore, the process is frequently accompanied by the formation of deposits on the internal surfaces of the polymerization reactor (reactor wall, baffles, impeller). The formation of fouling on the reactor wall reduces heat transfer, lowering production and even affecting product quality. Therefore, fouling must be cleaned periodically, which further reduces productivity. Despite the industrial importance of the fouling, there are still few references to this matter in the technical literature.

Therefore, the main objective of this thesis was to shed some light on the unknown mechanisms that control fouling formation in emulsion polymerization reactors. Emulsion polymerization reactor is a multiphase complex process that involves particle nucleation and coagulation, numerous chemical reactions and mass-transfer of radicals, monomers and surfactants. Because the study of the fundamental mechanisms of fouling in the presence of all these processes is an almost impossible task, in order to achieve this goal, a simpler strategy has been followed in this work, where different effects have being isolated and studied independently.

Firstly, the interaction between polymer particles and solid surfaces was studied under perikinetic conditions (Brownian motion), namely without agitation, monomers and reactions. Secondly, the interaction between polymer particles and solids surfaces was studied under orthokinetic conditions (under agitation) but with the absence of monomer and reactions. Thirdly, the effect of swelling the particles with monomer on fouling was investigated under agitation, but without reaction. Finally, fouling of the reactor during the seeded emulsion polymerization (namely, in the absence of particle nucleation) was investigated.

Acrylic latexes were chosen for this work because they represent the largest and fastest growing type of latexes. Butyl acrylate methyl and methacrylate were used as monomers, and the copolymer composition was varied to include both coatings and adhesives applications. The latexes were stabilized by a mixture of anionic and non-ionic surfactants. Some additional anionic stabilization was provided by sulfate groups from the initiator (KPS). Besides, in some cases 1 wt% of methacrylic acid (MMA) was used for further stabilization. Fouling on stainless steel 316 was studied.

First, fouling formation on stainless steel 316 substrates in the absence of agitation was studied using six latexes of different composition and stability, and the fouling was determined gravimetrically after removing the baffles from the latex, where they were immersed at controlled temperature for a given period of time. It was found that the way in which the non-attached latex was removed from the substrate strongly affected the observed fouling. Even a few seconds of contact with air increased the amount of fouling. This effect was attributed to thermodiffusion, namely the transport of colloids due to differences in temperature. In contact with air a temperature gradient was established between the air-latex interface and the latex-

substrate interface due to water evaporation and convection. For the solids content of the latex, an inverse thermodiffusion (colloids moving from cold to hot areas) is expected and this caused a flow of latex particles towards the substrate, and consequently more fouling. It was found that this problem was overcome by immersing the whole system in deionized water. In this way, a robust and accurate method to measure the fouling under perikinetic conditions was developed.

The particulate fouling without agitation was at least qualitatively well described by the theory that predicts that the rate of fouling is proportional to the number of particles in the system and inversely proportional to the particle-surface repulsive interaction potential. Attractive potentials accelerate fouling. After the reaction, the pH of the latexes was pH=2, due to the effect of the initiator used (KPS). At this pH the stainless steel is positively charged and fouling is favored by electrostatic attraction. The process is fast reaching a limiting amount of fouling that corresponded to a surface partially covered by a monolayer of latex particles. The change in the overall charge of the surface from positive to negative due to the attachment of anionic particles, created an increasing electrostatic repulsion potential that prevented the attachment of more particles. This equilibrium depended on the solids content of the latex, and fouling decreased as solids content decreased.

Fouling was also decreased when the particle-surface repulsive potential was increased making the surface anionic by increasing the pH above the isoelectric point of the stainless steel. Temperature slightly increased fouling, likely due to the lower stability of the non-ionic surfactant. The stability of the latex was a major factor determining fouling, which strongly decreased as latex stability increased. The reason is that for the more stable latexes, the

strong repulsive potential between the particles attached to the substrate and those dispersed basically stops the flow of particles towards the surface of the substrate.

In order to study fouling under orthokinetic conditions (with agitation) a lab reactor with stainless steel removable baffles was built and the fouling on these baffles measured. Two types of fouling were distinguished: fouling formed at the air-latex interface due to continuous wetting-drying processes (interfacial fouling) and fouling formed in the areas that are always submerged in the latex (wet fouling). Because wet fouling is the most significant in large scale reactors the study was centered in this type of fouling. Surface coagulation was observed for agitation rates up to 300 rpm. On the other hand, at 500 rpm a substantial amount of foam was formed. Therefore, the agitation rate was fixed and the study was carried out at 400 rpm.

It was found that the amount of wet fouling increased with time, solids content and temperature, and it decreased as the colloidal stability of the latex increased. For the more stable latexes, fouling increased as the T_g of the polymer was decreased. The flow patterns in the reactor determined the distribution of fouling in the baffles. Combination of computational fluid dynamics and experimental results showed that the observed fouling was the result of the interplay between attachment of polymer particles and removal of the polymer aggregates. In general, the bigger aggregates accumulated in areas where the flow rate was low.

Finally, the effect of the polymerization on fouling formation was studied. In order to decouple the effects of the presence of monomer and that of the polymerization itself, first the formation of fouling in latexes containing a high amount of inhibited monomer (no monomer droplets were present) was investigated. It was found that fouling increased with the amount of

monomer due to the combined effect of a decrease of the T_g of the monomer- polymer system and to the lower surfactant coverage that resulted from the addition of monomer to the seed.

In the second part, fouling during batch seeded emulsion polymerization was studied. It was found that polymerization caused a strong increase in wet fouling and this effect increased as the amount of monomer of the system increased. For the highest concentration of monomer used (40 wt%, which was the most unfavorable condition used) it was found that the amount of fouling was very mildly affected by the initiator concentration in the range of 0.125-0.5 wt% (based on monomer). On the other hand, experiments carried out with the same ionic strength in the absence and presence of initiator showed that most of the increase in fouling was due to the initiator. This effect was attributed to the formation of new particles by homogeneous nucleation.

Part of this Thesis was published or will be published soon.

Publications

Surfactant kinetics and their importance in nucleation events in (mini)emulsion polymerization revealed by quartz crystal microbalance with dissipation monitoring; N. Ballard, J.Urrutia, S. Eizagirre, T. Schäfer, G. Diaconu, De la Cal, J.C., J.M Asua*; Langmuir* 2014, 30, 9053.

In addition, parts of this Thesis were presented in national and international conferences, as well as in some internal Industrial Liason Program (ILP) meetings.

Oral presentations

Particulate fouling in emulsion polymerization reactors; J. Urrutia, J. M. Asua; talk at 2nd Career in Polymers VI 2014 conference, Prague, Czech Republic.

Surfactant kinetics and their importance in nucleation events in heterogeneous polymerizations revealed by quartz crystal microbalance with dissipation monitoring; N. Ballard, J. Urrutia, S. Eizagirre, T.Schäfer, G. Diaconu and J. M. Asua; oral in II Reunión de Jóvenes Investigadores en Coloides e Interfases 2014, Granada, Spain.

Effect of the agitation in the particulate fouling in reactors; J. Urrutia, J. M. Asua; talk at EFCE Working Party on Polymer Reaction Engineering 2012, Hamburg, Germany.

Poster presentations

Fouling in emulsion polymerization reactors; J. Urrutia, J. M. Asua; Frontiers of Polymer Colloids: From Synthesis to Macro-scale and Nano-scale Applications (FPCOL) 2014, Prague, Czech Republic.

Fouling in emulsion polymerization reactors; J. Urrutia, J. M. Asua; 11th Workshop on Polymer Reaction Engineering 2012, Hamburg, Germany.

Resumen y conclusiones

Debido a la escasez de caucho natural el cual estaba controlado por Japón, durante la Segunda Guerra Mundial se desarrolló el proceso de polimerización en emulsión para producir caucho sintético. Actualmente la polimerización en emulsión es el método más empleado industrialmente para polimerizar acetato de vinilo, cloropreno, acrilatos y la copolimerización de butadieno con estireno y acrilonitrilo. También se utiliza para metacrilatos, cloruro de vinilo, acrilamida y algunos etilenos fluorados. Este amplio rango de polímeros encuentra su mercado en multitud de aplicaciones como pinturas, adhesivos, recubrimientos de papel, cemento, aditivos del hormigón, etc.

Además, el éxito que experimento la polimerización en emulsión residió en sus múltiples ventajas frente a otros métodos de polimerización. Entre esas ventajas se encuentra el hecho de poder emplear agua como medio de reacción lo que reduce drásticamente los problemas de contaminación ambiental asociados con el disolvente. Asimismo, que el medio de reacción sea agua implica una baja viscosidad que facilita la agitación durante el proceso, así como la transferencia de masa y también la de calor. Esta última unida a la alta capacidad calorífica del agua permite un mejor control de la temperatura, aunque es bueno señalar que a

pesar que el control de la temperatura es más fácil cuando se utiliza polimerización en emulsión frente a otros métodos, la producción está controlada por la velocidad de disipación del calor. Otra de las múltiples ventajas que ofrece frente a otros métodos de polimerización es que se pueden obtener simultáneamente altas velocidades de reacción y altos pesos moleculares. La eficiencia en la transferencia de masa permite un mejor control de la composición del polímero, pesos moleculares y arquitectura. Dispersiones en base agua de híbridos del tipo polímero-polímero y compuestos polímero-inorgánico no pueden producirse de otra manera.

Los polímeros obtenidos mediante polimerización en emulsión se conocen como látex. Gran parte de los látexes comerciales se sintetizan con un alto contenido en sólidos (sobre el 50% en peso de polímero) y presentan un tamaño de partícula medio cercano a los 120 nm. Esto supone una enorme área superficial que implica que estos polímeros coloidales sean termodinámicamente inestables, aunque el uso de surfactantes (iónicos y no iónicos) les confiere una estabilidad de tipo cinético que les permite mantenerse en estado disperso durante largos periodos de tiempo.

De este modo, cuando dos partículas poliméricas estén lo suficientemente próximas, las fuerzas de atracción de van der Waals entraran en juego, y para prevenir la coagulación una barrera energética es necesaria. Los surfactantes iónicos actúan a través del mecanismo de repulsión iónica o electrostática llevada a cabo por la presencia de cargas eléctricas en la superficie de la partícula. Estas cargas pueden también provenir del iniciador o de los monómeros que contengan grupos funcionales. Los surfactantes no iónicos actúan a través de la repulsión estérica, ya que cuando estos se adsorben en las partículas, el grupo hidrofóbico

se mantiene pegado a la partícula mientras que la parte hidrofílica se extiende en la fase acuosa impidiendo físicamente la aproximación de las partículas.

La repulsión iónica y las fuerzas atractivas de van der Waals se combinan a través de la teoría desarrollada por Derjaguin and Landau and Verwey y Overbeek (teoría DLVO), donde se describe la energía potencial de interacción entre partículas cargadas dispersas en función de su distancia. La barrera de energía frente a la coagulación cuando las partículas se aproximen será mayor cuanto menor sea la fuerza iónica de la fase acuosa y mayor la densidad de carga superficial de las partículas. La fuerza iónica aumenta con la concentración de iones presentes y especialmente cuando esos iones tienen valencia alta.

Desafortunadamente el uso de surfactantes en la polimerización en emulsión está limitado industrialmente debido a los problemas que estos causan en la aplicación (la sensibilidad al agua de los films o un peor brillo o adhesión). Una consecuencia de esta restricción implica que el proceso suele estar acompañado de la formación de depósitos en las superficies internas del reactor de polimerización (paredes, agitador, sondas). El ensuciamiento de las paredes del reactor reduce la transferencia de calor, limita la producción y puede incluso afectar a la calidad del producto si estos depósitos entran a formar parte del producto final. De este modo, los depósitos deben ser limpiados periódicamente lo que reduce aun más la productividad.

A pesar de la importancia a nivel industrial que esto supone, apenas existen referencias sobre el tema en la literatura técnica o académica, por lo que el objetivo principal de esta tesis es clarificar los actualmente desconocidos mecanismos que controlan la formación de

depósitos que ensucian los reactores de polimerización en emulsión. Un reactor de polimerización en emulsión típico consiste en multitud de componentes y fases donde la nucleación, el crecimiento y la estabilización de las partículas de polímero son controladas por los mecanismos de polimerización de radicales libres y se experimentan simultáneamente numerosas reacciones químicas y procesos de transferencia de masa; por lo que un estudio fundamental de los mecanismos se convierte en una tarea prácticamente imposible. La polimerización en emulsión es un proceso heterogéneo de reacción por radicales libres. En una receta típica, los ingredientes principales son el agua, los monómeros (relativamente hidrófobos), surfactante(s) y un iniciador soluble en la fase acuosa (por ejemplo, persulfato de sodio). Inicialmente el monómero se encuentra repartido entre gotas de monómero, dentro de micelas de surfactante y solubilizado en la fase acuosa. Asimismo, el surfactante está localizado estabilizando las gotas de monómero, formando las micelas y parte estará disuelto en la fase acuosa.

El desarrollo del proceso de polimerización en emulsión puede seguirse convencionalmente a través de tres intervalos. Inicialmente está la etapa de nucleación (intervalo I), donde se generan las partículas a causa del crecimiento de los radicales provenientes del iniciador en la fase acuosa, seguido por la entrada de estos en las micelas (nucleación heterogénea) o por la precipitación de los oligómeros de la fase acuosa, los cuales al llegar a un tamaño critico, precipitan (nucleación homogénea o coagulativa). Por lo tanto, en este intervalo, gotas de monómero, micelas de surfactante conteniendo monómero y partículas hinchadas de monómero coexisten en el reactor.

Cuando finaliza el período de nucleación, el número de partículas se mantiene constante y el intervalo II comienza, en el cual las partículas de polímero hinchadas de monómero son el sitio principal de la polimerización. Estas crecen homogéneamente por polimerización del monómero que contenían y la reacción se mantiene por difusión de monómero desde las gotas de monómero. De este modo, las gotas de monómero disminuyen en tamaño mientras que las partículas de polímero crecen durante esta etapa.

El intervalo III comienza cuando las gotas de monómero desaparecen y todo el monómero no reaccionado se considera está dentro de las partículas (el monómero disuelto en la fase acuosa puede ser despreciado para la mayor parte de monómeros) y todas las moléculas de surfactante están adsorbidas en la superficie de las partículas. En este intervalo, la polimerización continúa en las partículas de polímero hinchadas de monómero generadas en el intervalo I y que crecieron durante el intervalo II, hasta que la polimerización es completa y una dispersión de partículas coloidales estable es obtenida (látex).

En resumen, la polimerización en emulsión involucra la propagación de radicales libres con las moléculas de monómero en un gran número de partículas de polímero (10^{16}–10^{18} dm^{-3}) dispersas en agua. Por lo tanto, se siguió una estrategia simplificada en esta tesis, donde los principales posibles efectos han sido aislados y los depósitos del ensuciamiento cuantificados.

Primero, la interacción entre el látex y acero inoxidable fue estudiada bajo condiciones pericinéticas (movimiento Browniano), básicamente en ausencia de agitación, monómero y sin reacción. Después, la interacción entre el látex y acero inoxidable fue estudiada bajo

condiciones ortocinéticas (con agitación),pero en ausencia de agitación, monómero y sin reacción. Finalmente, el ensuciamiento del reactor durante reacción en polimerización sembrada (en ausencia de la etapa de nucleación) fue investigada.

Dentro de los polímeros en emulsión, se eligieron látexes acrílicos por ser el tipo de latex con mayor y más rápido crecimiento. Se usaron butil acrilato y metil metacrilato como monómeros y la composición del copolímero fue variada para que incluyera aplicaciones de recubrimientos y de adhesivos. Los látexes fueron estabilizados con una mezcla de surfactantes anicónicos y no iónicos. Los grupos sulfato provenientes iniciador (KPS) otorgan estabilización adicional. Además, en algunos casos se incorporo un 1% de acido metracrílico (MAA) para obtener látexes más estables para la comparativa del estudio. Como superficie representativa de los reactores de polimerización, se eligió acero inoxidable 316. Se diseñaron montajes adecuados para la medición del ensuciamiento del reactor en condiciones peri y ortocinéticas que se presentaron en el capitulo 2.

Primero, la formación de depósitos en sustratos de acero inoxidable 316 en la ausencia de agitación fue estudiada usando seis látexes acrílicos de distinta composición y estabilidad. El ensuciamiento en placas de acero sumergidas en estos látexes, fue valorado gravimétricamente después de extraer los sustratos del látex del montaje donde fueron puestos en contacto a temperatura controlada por un periodo de tiempo determinado. Se encontró que la manera en que se retiraba la dispersión de látex no depositada, afectaba sustancialmente la cantidad de depósito de ensuciamiento. De este modo, la exposición del sustrato al aire durante unos escasos segundos aumentó la cantidad de depósito medido

después de eliminar el látex húmedo no depositado. Este efecto fue atribuido a la termodifusión que consiste en el transporte de coloides debido a diferencias de temperatura. En contacto con aire, se establecía un gradiente de temperatura entre la interfase aire-látex y la interfase látex-sustrato como consecuencia de la evaporación de agua y de la convección. Para el contenido en sólidos de los látexes estudiados, está reportado el fenómeno de termodifusión inversa (los coloides difunden de zonas frías a zonas calientes) lo que causó un flujo de partículas hacia el sustrato y por lo tanto un mayor ensuciamiento. Este problema se solucionó evitando la exposición al aire sumergiendo todo el sistema en agua desionizada. De esta manera, en esta tesis se ha desarrollado un método sencillo, robusto y preciso para medir el ensuciamiento producido por látexes en condiciones pericinéticas.

El ensuciamiento en condiciones ortocinéticas fue cualitativamente descrito por la teoría que indica que la velocidad de ensuciamiento es proporcional al número de partículas e inversamente proporcional al potencial de interacción repulsivo entre partícula y sustrato. Potenciales atractivos acelerarían el ensuciamiento. Tras la síntesis, el pH del látex principal utilizado en el estudio era 2, debido al efecto del iniciador empleado (KPS) y a ese pH el acero inoxidable presenta una carga superficial positiva y por lo tanto el ensuciamiento está favorecido por la atracción electrostática. El proceso de ensuciamiento alcanzó rápidamente un máximo que corresponde con el depósito parcial de una monocapa de partículas de polímero. Esta deposición de partículas aniónicas supone un cambio en la carga neta superficial del acero inoxidable de positivo a negativo, creando un potencial de repulsión electrostático que evito que más partículas se depositaran. Se observó que este equilibrio

dependía del contenido en sólidos y que la cantidad máxima de depósito era proporcional al contenido en sólidos del látex.

Además, se vio como el ensuciamiento disminuyó cuando se aumentó el potencial de repulsión partícula-sustrato gracias a un aumento en el pH por encima del punto isoléctrico del acero inoxidable que convirtió la superficie del acero en aniónica. El aumento de temperatura incremento ligeramente el ensuciamiento, debido probablemente a una menor estabilidad del surfactante no iónico. Finalmente, la estabilidad del látex fue el factor predominante respecto a la influencia observada en el ensuciamiento, el cual se redujo fuertemente según la estabilidad aumentaba. La razón reside en que para los látexes más estables, el fuerte potencial repulsivo entre las partículas depositadas en el sustrato y aquellas dispersas en el látex, básicamente anula el flujo de más partículas hacia la superficie del sustrato.

En segundo lugar, se estudió ensuciamiento en condiciones ortocinéticas (con agitación) mediante el uso del montaje presentado en el capítulo 2, donde placas de acero inoxidable extraíbles pueden colgarse paralelas a la pared de un reactor de laboratorio. Se distinguieron dos tipos de ensuciamiento. Los depósitos formados en la interfase aire-látex cuyo origen es el continuo mojado y secado de la zona por los cambios en el nivel de la interfase debidos a la agitación (depósito interfacial). Y los depósitos en las aéreas que permanecieron sumergidas en el látex, denominado como depósito húmedo en esta tesis. Ya que el depósito húmedo es el más significativo en reactores a gran escala, el estudio se centró en este tipo de ensuciamiento. Se observó la aparición de coagulo en la superficie (interfase aire-látex) para velocidades de agitación hasta 300 rpm. Por otro lado, a 500 rpm se formó una

cantidad considerable de espuma. Por lo tanto, la velocidad de agitación fue fijada en 400 rpm y el resto de variables fueron estudiadas.

Se encontró que el depósito húmedo aumentó con el tiempo, contenido en sólidos y la temperatura y que disminuyó al aumentar la estabilidad del látex estudiado. Para los látexes más estables, el ensuciamiento aumento según la T_g del polímero disminuía. Finalmente, se vio que los patrones de flujo en el reactor determinan la distribución de agregados de polímero en el depósito húmedo de las placas de acero. La combinación de las simulaciones de flujo realizadas mediante código CFD (Computational Fluid Dynamics) con los resultados experimentales, mostraron que el ensuciamiento del reactor fue el resultado de un compromiso entre la deposición de partículas y la eliminación de agregados de polímero depositados en los sustratos. En general, los agregados más grandes se acumularon en zonas donde la velocidad de flujo era menor.

Para finalizar, se estudió el efecto de la polimerización en la formación de depósitos. Para separar los efectos de la presencia de monómero y de la reacción de polimerización en si misma, primeramente fue investigado el ensuciamiento con látexes que contenían un gran cantidad de monómero inhibido (las proporciones fueron elegidas para que las mezclas no presentaran gotas de monómero). Se encontró que el ensuciamiento aumentó con la concentración de monómero debido a la combinación del efecto de la disminución de la T_g del sistema monómero-polímero y el efecto que implica que las partículas estén menos recubiertas de surfactante como resultado de añadir monómero al látex.

Por último, el ensuciamiento durante la polimerización fue investigado simulando una reacción polimerización en emulsión sembrada mediante un proceso en batch. Se encontró que la polimerización causó un fuerte aumento del depósito húmedo y que ese efecto aumentó según aumentaba la concentración de monómero en el sistema. Para la mayor concentración de monómero utilizada (40% en peso, la cual fue la condición estudiada más desfavorable) se observó que el uso de distintas concentraciones de iniciador en el rango de 0,125 a 0,5% (basado en monómero) afectó solo ligeramente al ensuciamiento. Por otro lado, la comparación de los experimentos llevados a cabo con la misma fuerza iónica en ausencia y presencia de iniciador mostraron que la mayor parte del aumento del ensuciamiento fue debido al iniciador, siendo la causa de este incremento atribuida a la formación de nuevas partículas por nucleación homogénea.

Appendix I. Characterization techniques

I.1. Particle size

The average particle size of the polymeric nanoparticles was measured by dynamic light scattering (DLS) using a Zetasizer Nano ZS apparatus (Malvern Instruments). Samples were prepared by diluting one drop of latex in deionized water in order to avoid multiple scattering. The reported diameters are the z- average of 3 measurements that were analyzed in 12 runs of 30 s each.

I.2. Solids content and monomer conversion

Approximately 2mL of the final latex were placed in a pre-weighed aluminum pan and immediately thereafter a drop of a 1 wt% hydroquinone solution was added to stop the reaction. The pan was dried until constant weight was achieved. The final values are the average of 3 replicates. The solids content (SC) were obtained gravimetrically and is given by:

$$SC = \frac{weight\ of\ the\ solid\ dried\ material}{weight\ of\ the\ latex} \qquad (I.1)$$

The final conversion (*X*) was determined by the following equation,

$$X(t) = \frac{Polymerized\ Monomer}{Total\ Monomer} = \frac{(SC \cdot Latex) - NPS}{MW} \qquad (I.2)$$

Where, *NPS* is the non polymerizable materials (surfactants, buffer and initiators) and *MW* is the amount of organic phase (monomer plus polymer).

I.3. Glass transition temperature

Calorimetric measurements were carried out by means of the differential scanning calorimeter (DSC-Q1000) from TA instruments. The samples were cooled to -40 °C then heated by a heating rate of 10 °C/min until 120 °C and cooled back again at -10 °C/min to -40 °C. Two heating cycles were performed each time. T_g was calculated using TA Instruments Universal Analyzer software, using the midpoint of the step in heat flow.

I.4. Zeta potential

The zeta potential was measured by Phase Analysis Light Scattering (PALS), (Malvern Instruments' Zetasizer Nano.

I.5. Surface tension

The surface tension of the latexes as synthesized and that of the continuous medium of the final latexes dispersions (serums) were determined by a tensiometer (KSV Sigma 70, KSV Instruments Ltd.). The serums were obtained after 4 cycles of centrifugation at 30,000 rpm and 10 °C during 1 hour.

I.6. Latex stability

Salt stability: The latex stability against electrolytes were determined by adding 10 ml of a salt solution to 10 g of latex. After 24 hours, the particle size were measured again by Dynamic Light Scattering, and the amount of coagulum, if any, has been weighed.

Mechanical stability: The test apparatus (Figure 1 a)) consists of a vertical shaft high-speed stirrer capable of maintaining a speed of 14,000 rpm for the duration of the test. The destabilization time is indicated by the seconds passed from the starting of the agitation, to the drop of the meniscus in the interface, the loss of turbulence and change in sound of the stirring action (Figure 1 b)).

a)  b) 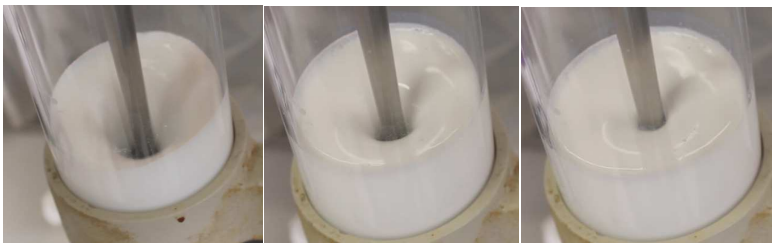

Figure I. a) Mechanical stability test apparatus. b) Destabilization determination scheme.

I.7. Viscosity measurements

The rheological characteristics of the latexes were determined with a AR1500 Rheometer (TA instruments), using a Couette cell geometry (standard recessed end concentric cylinders) with a gap of 4000 µm. The temperature was maintained at 25 °C for all tests. The experiments were conducted with a continuous decrease of shear rate from 1000 to 0.001 s^{-1}.